César José Cardoso Ferreira   Robotic Locomotion combining Central Pattern Generators and Reflexes

UMinho | 2014

Universidade do Minho
Escola de Engenharia

César José Cardoso Ferreira

Robotic Locomotion combining Central Pattern Generators and Reflexes

December 2014

Universidade do Minho
Escola de Engenharia

César José Cardoso Ferreira

Robotic Locomotion combining Central Pattern Generators and Reflexes

Dissertação de Mestrado
Ciclo de Estudos Integrados Conducentes ao Grau de
Mestre em Engenharia Electrónica Industrial e Computadores

Trabalho efetuado sob a orientação da
Professora Doutora Cristina Manuela Peixoto dos Santos

December 2014

DECLARAÇÃO

Nome: César José Cardoso Ferreira

Correio electrónico: cesarferreira1990@gmail.com

Tlm.: 927712219

Número do Bilhete de Identidade: 13765476

Título da dissertação:

Robotic Locomotion combining Central Pattern Generators and Reflexes

Ano de conclusão:2013/2014

Orientador:

Professora Doutora Cristina Manuela Peixoto dos Santos

Designação do Mestrado:

Ciclo de Estudos Integrados Conducentes ao Grau de Mestre em Engenharia Electrónica Industrial e Computadores

Área de Especialização: Automação, Controlo e Robótica

Escola: Escola de Engenharia

Departamento: Departamento de Electrónica Industrial

É AUTORIZADA A REPRODUÇÃO INTEGRAL DESTA DISSERTAÇÃO APENAS PARA EFEITOS DE INVESTIGAÇÃO, MEDIANTE DECLARAÇÃO ESCRITA DO INTERESSADO, QUE A TAL SE COMPROMETE.

Guimarães, ____/____/_______

Assinatura: ____

Acknowledgments

All the work carried during the past year would not be possible without the help, understanding and support from many people.

First and foremost, I would like to express my deepest gratitude to my adviser Prof. Cristina Santos, who allowed me the possibility to integrate the CAR (Control, Automation and Robotics) group of the ALGORITMI center. I am extremely grateful for her dedication, support and constant motivation, providing me an excellent atmosphere to complete my thesis. I am sincerely grateful for her excellent guidance and perseverance, encouraging me to tackle the different problems of this research. The help, constructive criticism and advice that I received were invaluable to the final quality of this work, making suggestions that contributed to overcoming the difficulties that emerged during this journey.

I would like to thank Prof. Lino Costa for the opportunity to learn new topics related with fitness evaluation.

I want to express my gratitude to Prof. Auke Ijspeert, who was always available to help with whatever was needed, provided insighful discussions about the research and presented suggestions that helped me develop this accomplishment.

I am especially thankful to everybody in the lab, for all the friendship and companionship that provided me with an excellent daily environment. A special thanks to João Macedo, who was always available to help me solve computational issues.

I express my warm thank you to my girlfriend Bárbara for her support, dedication and patience during the last year. She assisted me when I was writing this thesis, giving me some insight to stay on track and complete this work successfully.

Finally, I would like to thank my family, my parents and my brother, for their constant support, love and encouragement.

Abstract

Locomotion of quadruped robots has not yet achieved the harmony, flexibility, efficiency and robustness of its biological counterparts. Therefore, the development of bio-inspired controllers seems to be a good and robust way to obtain an efficient and robust robotic locomotion, mimicking their biological counterparts. Taken this matter into consideration, this thesis addresses the development of bio-inspired controllers based on the bio-inspired concepts of Central Pattern Generators (CPGs) and reflexes, implemented in the simulated Oncilla quadruped robot.

Two bio-inspired controllers were developed in order to generate stable and robust locomotion on uneven terrains. Firstly, a reflex controller that has to be capable of generating locomotion in a quadruped robot, based on sensory information that results from the interplay between robot and environment. Secondly, a hybrid controller that combines CPGs and reflexes, thus exploring the advantages of the pure feedforward and feedback approaches. The hybrid controller is more resilient to external perturbations and more robust to noise, thus improving the overall performance.

The results show that the reflex controller is capable of producing stable quadruped locomotion with a regular stepping pattern. Furthermore, it proved to be able to deal with slopes without changing the parameters and with small obstacles, overcoming them successfully. The hybrid controller improved the robot's behavior by increasing its stability, harmony and displacement in the majority of the experiments. Moreover, the stepping patterns become more regular due to the inclusion of the feedforward component in the system. This combination enables to increase robustness to sensor imperfections and to anticipate the robot's motor actions.

This research's main contribution to knowledge is based on the hybrid controller, which presents an innovative approach. CPGs have a different interpretation. They are no longer used to generate oscillatory signals to produce feedforward motor commands, but rather to assist the decoding of sensory information. Since they work as motor actions' predictors, they improve the Oncilla's walking behavior.

Keywords: quadruped locomotion, Central Pattern Generators, reflexes, predictor, feedback, feedforward, sensory information, hybrid controller, reflex controller.

Resumo

A locomoção dos robôs quadrúpedes ainda não atingiu a harmonia, flexibilidade, eficiência e robustez dos seus equivalentes biológicos, por isso, o desenvolvimento de controladores bio inspirados parece ser uma maneira boa e robusta de obter uma locomoção eficiente, imitando os seus equivalentes biológicos. Assim, esta tese aborda o desenvolvimento de controladores bio inspirados baseados em conceitos bio inspirados de Geradores de Padrões Centrais (CPGs) e reflexos, implementados no simulador do robô quadrúpede Oncilla.

Dois controladores bio inspirados foram desenvolvidos com o objetivo de gerar locomoção estável e robusta em terrenos irregulares. Em primeiro lugar, um controlador de reflexos capaz de gerar locomoção num robô quadrúpede, com base em informação sensorial que resulta da interação entre robô e ambiente. Em segundo lugar, um controlador híbrido que combina CPGs e reflexos, explorando, deste modo, as vantagens das abordagens de *feedback* e *feedforward*. O controlador híbrido é mais resiliente a perturbações externas e mais robusto ao ruído, melhorando assim o desempenho geral.

Os resultados mostram que o controlador de reflexos é capaz de produzir uma locomoção quadrúpede estável com um padrão de marcha regular. Para além disso, provou ser capaz de lidar com rampas sem alterar os parâmetros e com pequenos obstáculos, superando-os com sucesso. O controlador híbrido melhorou o comportamento do robô, aumentando a sua estabilidade, harmonia e deslocamento frontal na quase totalidade das experiências. Para além disso, os padrões de marcha tornaram-se mais regulares devido à inclusão da componente de *feedforward* no sistema. Esta combinação permite aumentar a robustez às imperfeições dos sensores e antecipar as ações motoras do robô.

A principal contribuição desta tese para o conhecimento científico está relacionada com o controlador híbrido, que apresenta uma abordagem inovadora. No caso particular dos CPGs, estes não são mais usados para gerar sinais oscilatórios que produzem comandos motores, mas sim para ajudar na descodificação das informações sensoriais. Uma vez que prevêem as ações motoras, os CPGs melhoram a locomoção do robô Oncilla.

Palavras-chave: locomoção quadrúpede, geradores de padrões centrais, reflexos, estimador, *feedback*, *feedforward*, informação sensorial, controlador híbrido, controlador de reflexos.

Contents

1 Introduction **1**

1.1 Motivations, scope and problem statement 1

1.2 Overview of the research 2

1.2.1 Methodological considerations 3

1.2.2 Goals and research questions 5

1.3 Contributions to knowledge 7

1.4 Publications 8

1.5 Thesis outline 9

2 Literature review **11**

2.1 Robot locomotion 11

2.1.1 Reflex based controllers 12

2.1.2 Standard CPG and reflex based controllers 13

2.1.3 CPGs acting as predictors 22

2.2 Summary of the presented studies 24

3 Quadruped locomotion **25**

3.1 Limb movements 25

3.2 Gaits 26

3.3 Oncilla robot 28

4 Biological evidences **31**

4.1 Central Pattern Generators 31

4.2 Reflexes 32

4.3 Combination of CPGs and reflexes 33

4.4 Delays 34

4.5 Biological mechanisms 34
4.5.1 Ground contact 35
4.5.2 Hip position and leg loading 35
4.5.3 Stumbling reflex 37
4.5.4 Vestibulospinal reflex 38
4.5.5 Contralateral coordination 38
4.5.6 Rules for quadruped sensory-driven locomotion 39

5 Bio-Inspired Controllers 41
5.1 Reflex Controller 42
5.1.1 Sensory Inputs 43
5.1.2 Sensory Interneurons 44
5.1.3 Direct Actions 45
5.1.4 Motoneurons 45
5.1.5 Joint Outputs 46
5.1.6 Network Behavior 47
5.1.7 Ipsilateral and Contralateral Coordination 48
5.2 Hybrid Controller 51
5.2.1 CPG model 53
5.2.2 Motoneurons predictor 55
5.2.3 Network Behavior 56

6 Gait analysis 59
6.1 Displacement 59
6.2 Stability 60
6.3 Harmony 61
6.4 Reward 61

7 Simulation results 63
7.1 Reflex controller experiments 64
7.1.1 Flat terrain experiments 65
7.1.2 Ramp experiments 77
7.2 Hybrid controller experiments 81

7.2.1 Synchronization and adaptability of CPGs 82
7.2.2 Internal mapping of the four motoneurons in the CPG 84
7.2.3 Predictor quality 84
7.2.4 Motoneurons replacement 85
7.2.5 Hybrid models: combining feedback and feedforward models . . 87
7.2.6 Comparison between the reflex controller and the hybrid controller 90

8 Conclusions **101**

8.1 Future work 103

List of Figures

2.1 Neural controller implemented in Wadden and Ekeberg (1998). 14

2.2 Quadruped robot - Tekken (Fukuoka et al., 2003). 16

2.3 WSM definition (Fukuoka et al., 2003). 17

2.4 Structure of the neuromuscular locomotor model (Yakovenko et al., 2004). 17

2.5 Leg's control system (Yakovenko et al., 2004). 18

2.6 Quadruped robot - Tekken 2 (Kimura et al., 2007). 19

2.7 Quadruped robot - Oscilex 2 (Owaki et al., 2012). 22

2.8 Hybrid Feedforward/Feedback System (pendulum) (Kuo, 2002). 23

3.1 Illustration of the step cycle. The cycle starts with the foot touching the ground and ends in the same situation. 26

3.2 Bivariate plot adapted from (Hildebrand, 1965; Cartmill et al., 2002). This figure shows a wide range of symmetric gaits used by quadruped animals. Some gaits are identified in the figure: diagonal sequence walks (DS); lateral sequence walks (LS); running pace (RP); running trot (RT); walking pace (WP) and walking trot (WT). 27

3.3 Stepping sequences of two symmetrical gaits (walking trot and lateral sequence walk) and two asymmetrical gaits (bound and gallop), in which the black bars represent the foot contact with the ground. 28

3.4 Oncilla robot (Laboratory, 2014). 28

3.5 Simulated Oncilla robot. 29

5.1 Bio-inspired quadrupedal walking model. The numbers from 1 to 4 represent sensory information provided by four types of sensors. 1 represents the signal of the vestibule; 2 represents the hip joint positions of the four limbs; 3 and 4 represent the touch sensors signals of the foot-pad and dorsum-paw of the four limbs, respectively. μ_i ($i =$ GC, AEP, PEP, DC, Load) represents the sensory interneurons that translate the sensory events based on the limb's sensory information. ζ represents the direct actions that act directly in the specification of the joints' velocities. Ψ_i ($i =$ stance, swing, touchdown, liftoff) are the motoneurons that determine the activation of the motor actions of a step cycle. These are responsible for the generation of the joint movements for the hip or knee, θ_i, $i = h, k$, which interact with the environment, thus closing the loop. 42

5.2 State machine implemented for each limb, in which reflexes trigger the transitions from one state to the next. 43

5.3 Proposed Controller for a single robot's limb. 49

5.4 Proposed Controller for ipsilateral limb coordination. 49

5.5 Proposed controller for contralateral limb coordination. 50

5.6 Bio-inspired quadrupedal walking model. The numbers from 1 to 4 represent sensory information provided by four types of sensors. 1 represents the signal of the vestibule; 2 represents the hip joint positions of the four limbs; 3 and 4 represent the touch sensors signals of the foot-pad and dorsum-paw of the four limbs, respectively. μ_{j} (j = GC, AEP, PEP, DC, Load) represents the sensory interneurons that translate the sensory events based on the limb's sensory information. ζ represents the direct actions that act directly in the specification of the joints' velocities. $\Psi_{\mathrm{i,RC}}$ (i = stance, swing, touchdown, liftoff) are the motoneurons of the reflex controller (RC). $\mathrm{CPG_i}$ (i = Fore Left, Fore Right, Hind Left, Hind Right) are the four CPGs of the model, one for each leg. $\Psi_{\mathrm{i,CPG}}$ (i = stance, swing, touchdown, liftoff) are the predicted motoneurons of the CPGs. The combination of both motoneurons determines the activation of the four motor actions of a step cycle, generating the joint movements for the hip or knee, $\theta_{\mathrm{h}}, \theta_{\mathrm{k}}$, which interact with the environment, thus closing the loop. 52

5.7 Three situations for the oscillator given by eq. 5.15 according to index $\frac{\omega}{\sigma \mathrm{GRF}}$. Top: Phase ($\phi$) of the CPG. Bottom: GRF value. 55

5.8 Proposed hybrid controller for a single robot's limb. 58

7.1 Simulated Oncilla quadruped robot. 63

7.2 Quadruped walking simulation using the reflex network - in flat terrain. . 65

7.3 Hind left limb's hip joint movement (θ_{h}), swing and stance motoneurons (Ψ_{swing} and Ψ_{stance}) and sensory interneurons (μ_{AEP} and μ_{GC}). For the hip angle, the dashed orange line represents the reference hip value and the blue solid line the produced joint angle. For the motoneurons (Ψ_{swing} and Ψ_{stance}), the dashed orange line represents the stance motoneuron and the solid blue line the swing motoneuron. 67

7.4 Hind left limb's knee joint movement (θ_k), touchdown and liftoff motoneurons ($\Psi_{\text{touchdown}}$ and Ψ_{liftoff}) and sensory interneurons (μ_{AEP}, μ_{PEP} and μ_{Load}). For the knee angle, the dashed orange line represents the reference knee value and the blue solid line the produced joint angle. For the motoneurons ($\Psi_{\text{touchdown}}$ and Ψ_{liftoff}), the dashed orange line represents the touchdown neuron and the solid blue line the liftoff neuron. 68

7.5 Oncilla stepping sequence in flat terrain. 70

7.6 Stumbling reflex operation in the fore left leg. 73

7.7 Stumbling reflex operation in the hind left leg. 74

7.8 Trajectory details of the robot overcoming an obstacle in fore limb followed by an obstacle in hind limb. Left column depicts fore left leg. Right column the hind left leg. Top panels: hip movement (θ_h). Middle panels: knee movement (θ_k). Bottom panels: sensory interneuron (μ_{DC}). For the hip and knee joints movements, the dashed orange lines represent the joints references and the solid blue lines represent the performed joint angle. . . 75

7.9 Similar legend to Figure 7.8 but when the stumbling reflex is turned OFF. 76

7.10 Similar legend to Figure 7.8 when the stumbling reflex is turned ON, but both noise and delays were added. 76

7.11 Schematic of the ramps used in the experiments. 77

7.12 Body roll and pitch angles in ramp experiment, when no noise was considered. Top panel: pitch angles. Bottom panel: Roll angles. The blue solid lines represent the variables with the vestibulospinal reflex turned ON, and the dashed orange lines represent the variables with the vestibulospinal reflex turned OFF. 79

7.13 Body roll and pitch angles in the ramp experiment, when noise was considered at the sensors and actuators level. Legends were built similarly to the ones of figure 7.12. 80

7.14 CPG activity (solid blue line) and sensory interneuron of ground contact (GC) (dashed orange line), for each limb. The step cycle is defined by the sensory interneuron of GC (μ_{GC}). 83

7.15 Internal mapping of motoneuron activity to the CPG phase. The blue line represents the CPG phase. In each panel, the orange area shows the activity of the corresponding motoneuron, and the gray area represents the remaining predicted motoneurons. 85

7.16 Maximum CPG prediction for each motoneuron. 86

7.17 Gait analysis of the eleven models, tested in six different situations. The blue, orange and gray bars represent the *harm*, *stab* and *disp* components, respectively. The green and gray lines represent the rewards of the models and reflex controller, respectively. 89

7.18 Hind left limb's hip and knee joint movement (θ_h and θ_k, respectively), final motoneuron activity ($\overline{\Psi}$) and reflex network motoneurons (Ψ) of swing, stance, touchdown and liftoff. For the hip and knee angles (θ_h and θ_k, respectively), the dashed orange lines represent the hip and knee signals of the reflex controller and the solid blue lines the produced joints angle of the hybrid controller. The final motoneurons ($\overline{\Psi}$) are represented with solid blue lines and the reflex network motoneurons (Ψ) with dashed orange lines. 91

7.19 Oncilla stepping sequences in flat terrain without noise and delays. 97

7.20 Oncilla stepping sequences in flat terrain with noise of 5%. 98

7.21 Oncilla stepping sequences in flat terrain when a 12 ms delay is considered. 99

7.22 Oncilla stepping sequences in flat terrain when both noise of 5% and a delay of 12 ms are considered. 100

List of Tables

2.1 Transitions between states governed by sensory signals (Ekeberg and Pearson, 2005). 13

2.2 Reflexes/responses implemented in Fukuoka et al. (2003). 17

2.3 Reflexes/responses implemented in Kimura et al. (2007). 19

2.4 Postural responses implemented in Sousa et al. (2010). 21

7.1 Sensory thresholds, attractors values and joint output parameters. 65

7.2 Locomotion data from the experiments in flat terrain. 69

7.3 Locomotion data from the experiments in ramp. 78

7.4 Sensory thresholds, attractors values, joint output parameters and CPG parameters. 82

7.5 Step cycle period of the reflex controller ($T_{\text{step cycle,RC}}$) and the CPG ($T_{\text{step cycle,CPG}}$). 84

7.6 Correlations between predicted motoneurons (Ψ_{CPG}) and reflex motoneurons (Ψ_{RC}). 86

7.7 Eleven hybrid models. 87

7.8 Three best hybrid models and the corresponding rewards. 90

7.9 Locomotion data from the experiments in flat terrain without noise and delays. 92

7.10 Locomotion data from the experiments in flat terrain with noise. 93

7.11 Locomotion data from the experiments in flat terrain with delays. 95

7.12 Locomotion data from the experiments in flat terrain with noise and delays. 96

Acronyms

CAR Control, Automation and Robotics

CPG Central Pattern Generator

NPG Neural Phase Generator

AEP Anterior Extreme Position

PEP Posterior Extreme Position

GC Ground Contact

WSM Wide Stability Margin

MOSS Motor Output Shape Stage

PFCM Propulsive Force Control Module

GRF Ground Reaction Force

CNS Central Nervous System

EMG Electromyography

GTOs Golgi Tendon Organs

AMARSi Adaptive Modular Architecture for Rich Motor Skills

DC Dorsum Contact

BPA Body Pitch Angle

RC Reflex Controller

RQ Research Question

Chapter 1

Introduction

This thesis presents the work developed during the past year in the Control, Automation and Robotics (CAR) group of the ALGORITMI Center from University of Minho.

This work addresses the field of the quadruped locomotion generation through the implementation of bio-inspired concepts. The ultimate goal of this work is the development of a new controller capable of generating robotic locomotion based on Central Pattern Generators (CPGs) and reflexes, more resilient to external disturbances and more robust to noise coming from imperfect sensors and actuators. The underlying idea is that one could combine feedback and feedforward signals. In this context, the CPG's mechanism would provide for an internal model of the controlled mechanical oscillations during locomotion.

The projected controllers were implemented in the simulated Oncilla quadruped robot, with position controlled hips and retractable passive compliant knees.

1.1 Motivations, scope and problem statement

Legged animals present an efficient and harmonious locomotion, capable of walking and running on unstructured terrains, with obstacles, holes and slopes. Animal's ability to deal with real world situations have always fascinated researchers, compelling them to understand what natural mechanisms are responsible for the generation of simple movements like walking and running, but also more complex and intelligent motions. The development of bio-inspired controllers seems to be a good and robust way to obtain an efficient and robust robotic locomotion, mimicking their biological equivalents. The technological advancements allowed the evolution of legged robots, including quadruped locomotion, which this thesis addresses.

Despite current and intensive research, locomotion of quadruped robots has not yet achieved the harmony, flexibility, efficiency and robustness of its biological equivalents, and, therefore, its development seems to be crucial. The generation of locomotion on unpredictable terrains is a big challenge, one that traditional methodologies were not yet able to successfully solve, and the biological evidences recorded over the years give us sufficient bases and supports to start the development of bio-inspired robots, reinforcing this thesis' interest and viable use, with the application of the most important biological mechanisms of quadruped animals.

It is known that locomotion in animals is generated at the spinal cord by a combination of CPGs and reflexes. CPGs can be simply defined as biological neural networks capable of producing rhythmic patterns in absence of sensory information. On the other hand, reflexes are events triggered by sensory signals. How exactly this combination is made in animals is still unknown, however, this innovative thesis proposes a network which combines both identities, contributing with research to this enigmatic field. The proposed closed-loop control strategy proposes to introduce CPGs, modeled by nonlinear oscillators, as gait modulators on top of a reflex-based model.

The development of bio-inspired locomotion can serve as a basis or inspiration for a relevant field: rehabilitation. Particularly, the knowledge obtained with bio-inspired locomotion can be crucial in the progress of prostheses and orthoses, making them capable of generating limb movements closest to humans exhibiting the same level of flexibility.

1.2 Overview of the research

The integrated use of CPGs and reflexes provide for improved performance considering robustness and sensibility to disturbances, as well as speed-adaptive capability. On one hand, the combination of CPGs and reflexes can bring greater responsiveness of the robot to all types of disturbances through the reflexes. On the other hand, due to the presence of CPGs, the robot can have a supervisor able to predict every movement and, thus, be able to correct disabilities found during locomotion, such as system noise and sensory feedback failure. This approach is sustained by the existent and ever growing consensus that both intrinsic and sensory feedback signals play a crucial role in controlling the act of locomotion (Gossard et al., 2011). It is also largely supported and inspired by biological evidence, in which it is believed that the CPG provides for an internal model of the controlled mechanical oscillations during locomotion, *i.e.*, it contains the input-output relationship (internal model) of the motor behavior it controls. Additionally, there is also biological evidence that there is a two-way interaction between the CPGs and the body, such that the CPGs actively process sensory inputs, and mechanical factors contribute to entrainment of the CPGs (Grillner et al., 1981; Cohen, 1992). In such case, CPGs could instead be interpreted as generators of oscillatory signals as a means to decode sensory information, instead of producing motor commands in a feedforward manner.

Some projects were carried comprising CPGs and reflexes (Kimura et al., 2007; Wadden and Ekeberg, 1998; Maufroy et al., 2008; Ekeberg and Pearson, 2005; Klein and Lewis, 2012). In all these studies, CPGs are the central mechanism responsible for direct motor generation, and reflexes had the function of regulating/modifying the CPG's activity. In our approach, CPGs have an alternative role, serving as predictors of motor actions, providing an internal model of the limbs movements. Therefore, CPGs are capable of filtering the errors from sensory information, producing a more robust locomotion, at the same time being very adaptable to the real world, since the controller has a reflex network that generates motor actions through the robot's interaction with the environment.

All aspects previously expressed show the relevance of this field, presenting an innovative character, contributing to the scientific community with advancements able to help answer some important questions. The major questions that arise, in this case, are how reflexes are combined with CPGs and what is the role that each part performs in the locomotor system. Main innovation comes from the hypothesis of using CPGs as feedback predictors, following an idea from Kuo (2002), in which the CPG component is derived from the feedback pathways, and then modulate their timing, amplitude and duration.

1.2.1 Methodological considerations

In order to combine both feedforward and feedback strategies, firstly, both strategies have to be developed independently. Therefore, two bio-inspired controllers capable of generating stable and robust locomotion on uneven terrains were developed. Primarily, a reflex controller that has to be capable of generating locomotion in a quadruped robot, based on sensory information that results from the interplay between robot and environment. Secondarily, a hybrid controller that should combine CPGs and reflexes, making the controller more resilient to external perturbations and more robust to noise, thus, with an improved overall performance.

The correct implementation of these controllers comprise several concepts and steps. Firstly, it is required to formalize the components of the reflex network and verify their mathematical formulation and behavior. The reflex network is based on neural networks. These will be simulated in Matlab, allowing their better understanding, interpretation and tuning. CPGs can be modeled using different nonlinear dynamical systems, such as phase oscillators and/or Landau Stuart oscillators. Herein, phase oscillators will be explored to model the required CPGs. These oscillators provide for independency, considering their amplitude and, thus, are simple to deal with, while presenting the required characteristics for CPG modeling. CPGs will be mathematical formulated and analyzed, and then simulated in Matlab for correct tuning. Finally, the integration of CPGs and reflexes will be addressed. In order to achieve this, different types of designs will be formulated, tested, tuned and implemented.

The controllers will be deployed in the simulated Oncilla robot, a small quadruped robot developed on an European project (AMARSi: Adaptive Modular Architecture for Rich Motor Skills). Learning and understanding the Webots simulator is an important task, since the AMARSi consortium developed a Webots-based simulation of the Oncilla robot that runs under Linux operating system. The implementation of controllers in the Oncilla robot required several skills at programming level, being implemented using the C++ programming language.

Experiments will be delineated in order to enhance the desired characteristics of the proposed controllers. In order to evaluate the controllers' performance, a gait analysis will be developed, which facilitates the calculation of the required gait characteristics. Firstly, no noise will be included in any simulation and the obtained gait patterns will be evaluated and classified. The addition of noise will enable to verify the network robustness and ascertain about the interest of the addition of the CPGs later on. The system will also be tested and evaluated considering perturbations and its ability to deal with them without falling, and by disturbing as little as possible the gait. In such case, it is expected that the reflex network performs better. Experiments will also address the possible benefits that the CPG inclusion brings to the model. In order to verify this, the thesis focuses on studying the relative importance of the different feedback/feedforward pathways. The thesis also addresses the controller's ability to exhibit a biologically-consistent trend of increasing/decreasing gait cycle network for increasing/decreasing walking slope without changing controller parameters. Emphasis will be given to the analysis of each feedback pathway and its combination with the feedforward predictor, as well as to the increase in robustness.

Physics based simulations will be done in the Webots simulator. Simulations will be performed from normal/level walking to slope climbing/descending and distances of stumble.

1.2.2 Goals and research questions

The ultimate goal is the implementation of a controller that combines two relevant biological concepts: CPGs and reflexes. The final controller implemented in this thesis is innovative because it addresses the integration of two biological systems, something that is not yet understood how is done correctly by the animals' biological system. To achieve this final goal, new ideas related with biological concepts in quadrupeds have to be learned, several goals will be achieved and research questions will be answered. Specifically, it is important to notice that engineering evidence favours feedback alone, especially if combined with natural dynamics, without the need for a centrally generated command (Raibert et al., 1986). Thus, it is important to understand what possible advantage is taken in biological systems from this combination, and in which way this could be applied to the robotics domain and, in particular, to the quadruped locomotion domain.

Thereby, it is necessary to achieve the following goals:

Goal 1: The first step is to conduct an extensive survey on the state of the art related with the biological evidences of reflexes in quadrupeds, and by specifically unveiling the ones which are more important and/or relevant to achieve an efficient locomotion. This goal will provide the biological basis to develop a reflex network able to generate locomotion in a quadruped robot.

Goal 2: Hereinafter, an extensive research will take place, about the bio-inspired controllers implemented in quadruped robots, allowing a better understanding of the advantages and disadvantages of the current state of the art.

Goal 3: The development of a reflex network is the next step. This sensory driven controller has to be capable of generating locomotion in a quadruped robot, based only on the interactions of the robot with the environment, being the sensory information crucial in the robot's movement. It is assumed that the final trajectories are not previously known, and should result from the interplay between motor actions and sensory information. The goal is to accomplish a parsimonious controller, resorting to the necessary number of reflexes to produce a successful walking behavior. This controller should be able to generate quadruped robot locomotion, capable of walking in irregular and unexpected terrains. It is important to stress that a preliminary version of a reflex controller was developed previously by another student (Ferreira et al., 2014b), but it presented some shortcomings. This thesis builds up on this controller and tries to improve it, by enabling the robot to overcome obstacles, going up and down ramps while minimizing the risk of falling, and most importantly, to make the robot's stepping sequence more regular. This implied a research through the biological reflexes that could make sense and bring advantages in their inclusion onto the reflex driven quadruped locomotion controller. Therefore, a mapping relating the known reflexes from biology and the addressed robot enabled to setup the required reflexes and rules that could provide for a regular, patterned locomotion, more resilient to perturbations. Besides, the validation of the proposed controller is to be done, through systematic and carefully designed simulations, as well as the evaluation of the produced gait, through a gait evaluation analysis.

Goal 4: After the successful development and validation of the reflex network, a new controller has to be implemented, comprising and combining the two biological concepts: CPGs and reflexes. Firstly, it is required to formalize the CPGs which will be modeled by phase oscillators. This implies to mathematical formulate and analyze the CPGs. Then these will be simulated in Matlab and tuned. Finally, will be tackled the integration of CPGs and reflexes. In order to achieve this, different types of designs will be formulated, tested, tuned and implemented. In the overall, this combination will be achieved by having the oscillator acting as an internal model of limb motion which predicts the state of the limb, and having the CPG entrained by a feedback sensory signal, acting as an error signal, which will accelerate/deaccelerate the CPG. CPGs are combined with reflexes simply through a proportional term that controls the relative importance of the CPGs vs. the motoneuron activity they predict. Additionally, in order to study the relative importance of the different motoneurons/feedforward pathways, a variety of models combining CPGs and motoneurons is proposed. This is different from the actual state of the art, though see Dzeladini et al. (2014) for related work in bipeds. Comparatively to Dzeladini et al. (2014) work, the main differences and advantages of our work are the absence of phase reset mechanism and the oscillator tries to adapt in an online fashion. Besides, the proposed CPG will act at the motor level instead of acting at the sensory feedback level.

The following research questions (RQ) are expected to be answered:

RQ1: What are the most important reflexes in a quadruped robot that may enhance the generated locomotion in terms of regular gait?

RQ2: Is it possible to design a reflex network capable of generating stable, regular and robust quadruped locomotion?

RQ3: How can we measure the performance of a quadruped gait?

RQ4: Since we address a real problem that includes delays and noise, how can we achieve a system that is robust to such disturbances?

RQ5: In order to add a feedforward component to the system, how can we predict the robot's motor actions?

1.3 Contributions to knowledge

This thesis provides two bio-inspired controllers capable of producing regular locomotor patterns, which can be seen as two tools that are capable of helping in the study of quadruped locomotion. The main contributions of this work are:

- A sensory-driven controller resorting to the minimum number of reflexes to produce a successful walking behavior. This tool is designed for a quadruped robot and can be used to understand what are the most relevant reflexes in quadruped animals, that should be mimicked in legged quadruped robots. This includes the ability to deal with stumbling in objects and also climbing and descending slopes.

- An innovative hybrid controller that combines concepts of CPGs and reflexes. This tool showed a way of combining the two bio-inspired concepts and proved that the CPGs could have an alternative role in locomotion. Specifically, CPGs are used as predictors of the motor actions that would be generated by reflexes, and therefore, they are capable of compensating for both disturbances and sensor noise. This way, we apply CPGs with a different interpretation, since they are no longer used to generate oscillatory signals to produce feedforward motor commands, but rather to assist the decoding of sensory information.

1.4 Publications

The developed work during the past year allowed the publication of four conference papers and the submission of two journal articles.

Journal articles

- César Ferreira and Cristina P. Santos, *A Sensory-Driven Controller for Quadruped Locomotion*, International Journal of Applied Mathematics and Computer Science (submitted).

- César Ferreira and Cristina P. Santos, *Combining Central Pattern Generators and Reflexes*, Neurocomputing (submitted).

Conference papers

- César Ferreira, Cristina P. Santos and Auke Ijspeert, *Quadruped Sensory-Driven Locomotion*, International Conference on Mathematical Methods, Computational Techniques and Intelligent Systems (MAMECTIS ’14), Lisbon, Portugal, October 30th - November 1st, 2014.

- César Ferreira, Vítor Matos, Cristina P. Santos and Auke Ijspeert, *Quadrupedal Locomotion based in a Purely Reflex Controller*, ICINCO 2014 - 11th International Conference on Informatics in Control, Automation and Robotics, Vienna, Austria, September 1st - 3rd, 2014.
- César Ferreira, Pedro Silva João André, Cristina P. Santos and Lino Costa, *Genetic Programming applied to Biped Locomotion Control with Sensory Information*, ICINCO 2014 - 11th International Conference on Informatics in Control, Automation and Robotics, Vienna, Austria, September 1st - 3rd, 2014.
- César Ferreira, Vítor Matos, Cristina P. Santos and Auke Ijspeert, *Sensory-driven Purely Reflex Controller for Quadruped Locomotion*, Dynamic Walking 2014, Zurich, Switzerland, June 10th - 13th, 2014.

1.5 Thesis outline

This document is organized as follows. In chapter 2 is announced a literature review of the most important projects developed in the past years, using bio-inspired concepts of Central Pattern Generators and reflexes. Chapter 3 presents the robot used in the project, as well as several aspects related with quadruped animals providing a better understanding of the following chapters. Chapter 4 shows the most important biological evidences applied in the controllers of this thesis. Chapter 5 presents the bio-inspired controllers developed during the past year, explaining in detail all the aspects involved on the networks’ design and their functioning. The tool used to evaluate the robot’s gait during the experiments is exposed in chapter 6. The simulation results of the two implemented controllers are announced in chapter 7. Finally, in chapter 8, are presented the conclusions and the future work.

Chapter 2

Literature review

In animals, the control of locomotion is adaptable to various situations they face every day, allowing them to move on unpredictable terrains. They have a system capable of providing simple movements like walking and running, but also more complex motions. Although the exact way of how this system is controlled is still unknown, it is generally accepted that locomotion in animals is generated at the spinal cord level by a combination of CPGs and reflexes (Geyer and Herr, 2010; Kimura et al., 2007).

Robotic quadruped locomotion on irregular and unknown terrains is still a problem to solve, so if a robot is expected to move in irregular terrains, it needs "motor intelligence" (Cruse et al., 1998) to be capable of adapting its moves according to unexpected situations. It has been shown that CPGs and feedback pathways are highly integrated for locomotion generation. For instance, it has been demonstrated (Rossignol et al., 2006) that sensory events can adjust the duration of the rhythmic activity, stimulation of sensory afferents can elicit locomotion and the generation of locomotion is adapted accordingly to sensory information.

2.1 Robot locomotion

Over the past fifty years, engineering has presented good solutions to describe locomotion. It can be produced without muscle contractions, and can be defined as an oscillatory behavior resulting from the animal's interaction with the environment (Gossard et al., 2011). Therefore, stable locomotion can be achieved by simple mechanical models consisting of a mass bouncing on weightless limbs (Alexander et al., 1976), in which the dynamics of these models resembles an inverted pendulum. (Cavagna et al., 1976, 1977).

When an animal runs, the muscles and ligaments store energy, which is subsequently used during the stance phase (Gossard et al., 2011). This behavior can be described by a mass-spring system, which can be defined as a pendulum with a spring element between the point of ground contact and the center of mass.

The mechanical models or passive walkers presented above can serve as templates for the description of locomotion, but they can not predict the locomotor frequency and energy expenditure in overground walking. Therefore, it is necessary to complement passive walkers with muscles' models and sensory feedback (Gossard et al., 2011).

On the other hand, biological evidences proved that feedback pathways and CPGs act jointly in the generation of locomotion (Kuo, 2002) and, therefore, the question arose of what would be the advantages of combining these two concepts. During the last years, robotic locomotion has been achieved by the application of simple sensory driven reflexes rules, both in simulations and in robotic platforms (Geyer and Herr, 2010; Cruse et al., 1998), and also comprising CPGs and reflexes, as shown in Wadden and Ekeberg (1998), Kimura et al. (2007) and Maufroy et al. (2008).

Hereinafter, we present the literature review of the most important works made in the past years, that aimed to create bio-inspired controllers capable of mimicking the locomotion of their biological equivalents. Firstly, we present the most important reflex based controllers, followed by the standard CPG and reflex based controllers and, finally, the controllers that use CPGs as predictors.

2.1.1 Reflex based controllers

Cruse et al. (1998) projected a bio-inspired controller of a hexapod robot that generates locomotion based on sensory events. They developed a system which can be used as a scientific tool to study insect locomotion, more specifically hexapods. In this work, the authors consider that each leg has two step phases: stance and swing. The implemented controller outputs the joint velocities and was constituted by three distinct parts: stance net, swing net and selector net. The stance net controls the leg's movement when it is in stance phase, and the swing net when it is in swing phase, while the selector net determines if the swing or stance net controls the motor's output. To make the transition between phases, they used two reflexes, the Anterior Extreme Position (AEP) and Posterior Extreme Position (PEP), reflexes also used in other works (Wadden and Ekeberg, 1998; Maufroy et al., 2008). In this contribution, AEP had the function of initiating the transition from swing to stance phase, and PEP's function works contrariwise (from stance to swing phase).

Ekeberg and Pearson (2005) developed a computer model of the cat's hind legs used to study mechanisms regulating stance to swing transition. This study aimed to investigate the role of two sensory signals in the regulation of this transition: unloading of the ankle extensors and hip angle. Each leg muscle's activation was controlled in a sequence of four states: liftoff, swing, touchdown and stance. There can only be one state activated at once, and the transition between them was governed by sensory information related to the leg, presented in table 2.1. Authors concluded that the unloading of the ankle extensor was capable of stabilizing the alternating gait and mechanically couple the two hind legs, leading the model to stable alternating stepping of the legs.

Table 2.1: Transitions between states governed by sensory signals (Ekeberg and Pearson, 2005).

Phase transition	**Trigger**
Liftoff to swing	Ground release
Swing to touchdown	Hip and knee angle
Touchdown to stance	Ground contact
Stance to liftoff	Unloading of the leg and hip angle

Hartmut Geyer and Hugh Herr presented a human locomotion model controlled by muscle reflexes exploiting the principles of legged mechanics (Geyer and Herr, 2010). Each one of the legs had two possible step phases: stance and swing, and each had separate reflexes, which were activated accordingly to the current step phase, based on contact sensing. In order to generate locomotion, these reflexes specify muscle activation, stabilizing into a walking gait, due to its dynamic interaction with the ground. The model was capable of dealing with ground disturbances and slopes without parameter interventions.

2.1.2 Standard CPG and reflex based controllers

In the earliest studies with reflexes, Wadden and Ekeberg (1998) presented a neuronal model of a single leg that combines properties of mechanical and neuronal systems as the first step in the process of creating a quadruped robot. The neural controller, depicted in figure 2.1, was constituted by four distinct parts: Higher Level Control, Neural Phase Generator (NPG), Fast Feedback Pathways and Mechanical System. The Higher Level Control

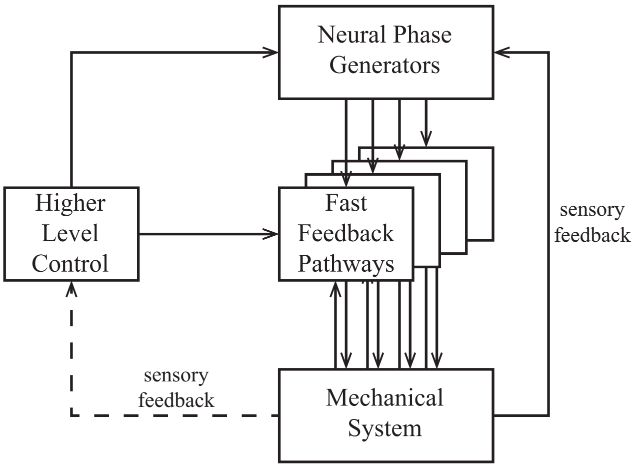

Figure 2.1: Neural controller implemented in Wadden and Ekeberg (1998).

is used to initiate and choose the leg's movements and make the necessary adjustments based on sensory information through the Fast Feedback Pathways. The Neural Phase Generator (NPG) has an internal representation of the stepping, providing a consistent description of the leg's state, allowing the NPG to filter the inconsistencies from the sensory inputs. The NPG is implemented using neurons as leaky integrators. The Fast Feedback Pathways are set by the NPGs, so only the necessary actions for a particular phase of the step cycle are performed. The Mechanical System produces the leg's movement and receives afferent information from limbs and environment. The authors divided the step cycle in four phases (swing, propulsion, liftoff and touchdown), and each of them activated the respective excitatory and inhibitory interneurons that activate the extensor and flexor muscles. According to them, the basic stepping movements can be generated without sensory information, but the movements are different when sensory feedback is used. Therefore, they proposed some reflexes that can improve the leg's movements, since they influence directly the transition in the activity of the NPG:

- AEP - the closer the hip joint comes to the AEP, the quickest is the transition from swing to touchdown phase;
- PEP - the closer the hip joint comes to the PEP, the quickest is the transition from propulsion to liftoff phase;
- Ground Contact (GC):

    (a) if the leg is in touchdown phase, the ground contact shortens the transfer time from this phase to the propulsion phase;
    (b) if the leg is in liftoff phase, the ground contact shortens the transfer time from this phase to the swing phase;

- Stretch Reflex - it is a muscle contraction in response to stretching within the muscle, to prevent tearing. Therefore, the reflex regulates an overly stretched muscle.

Two years following, Kimura et al. (2000) presented their first attempt to build a quadruped robot capable of walking dynamically on uneven terrains, using bio-inspired nervous system models based on concepts of CPGs and reflexes. They build a quadruped robot named Patrush, which had three joints (hip, knee and ankle) for each one of the legs. To perform stable walking in a environment with bumps and ramps, they needed to add three reflexes to the controller:

- Stretch Reflex - used to prevent the robot's body from rising by an excess of reaction force from the ground, when the robot's leg lands on a bump, and helps keeping the body posture flat when the robot climbs a slope.

- Vestibulospinal Reflex - used to maintain the posture of the body flat when the robot descends a slope, extending the forelegs and bending the hindlegs.

- Flexor Reflex - when the leg is in the swing phase, the flexor reflex is used to prevent the leg from stumbling in small obstacles.

In this work, they defined three essential rules for a successful robot locomotion on irregular terrains:

(a) In the previous period of the swing phase, the leg should not be prevented from moving forward;

(b) The leg should be landed safely on the ground in the final period of the swing phase;

(c) At the landing moment, the angular velocity of the supporting legs around the contact points should be kept constant.

These rules are satisfied using the three implemented reflexes mentioned above. The rule (a) is satisfied with the flexor reflex and with a vision system. The rule (b) is satisfied with the implemented stretch reflex, and the rule (c) is satisfied with the implementation of the vestibulospinal reflex. This robot was able to climb a long slope and overcome a step of 3 cm in height.

Fukuoka et al. (2003) presented a new quadruped robot called Tekken, depicted in figure 2.2, that was capable of walking with medium speed on uneven terrains. This work represents the progress of the authors' work in the development of a quadruped robot able to move in the most varied terrains. Tekken was designed to solve mechanical problems in the Patrush robot used in the past study (Kimura et al., 2000). It has four joints for each leg: a hip pitch joint, a hip yaw joint, a knee pitch joint and a passive ankle pitch joint to prevent the swinging leg from stumbling on an obstacle. The interactions between CPGs and reflexes are very important to achieve dynamic locomotion in irregular terrains. In this work, the reflexes or sensory information have the role of modifying the CPG's activity, *i.e.*, they change the period of the active step phase. Based on these ideas, the authors presented a neural system based on bio-inspired concepts of CPGs, reflexes and responses, as in the past study (Kimura et al., 2000). The responses are used to make a rapid modulation of the CPG phase and the reflexes to make a rapid and direct adjustment of the joint torque. The reflexes and responses implemented by the authors are presented in table 2.2. In this contribution, they implemented a stability evaluation method, defined as the Wide Stability Margin (WSM). It is depicted in figure 2.3 and was referred as "the shortest distance from the projected point of the center of gravity to the edges of the polygon constructed by the projected points of the legs independent of their stance or swing phases". The Tekken robot was capable of walking over a step 4 cm in height, walking up and down a slope of 10 degrees, and walking over a series of obstacles 2 cm in height, thus showing the

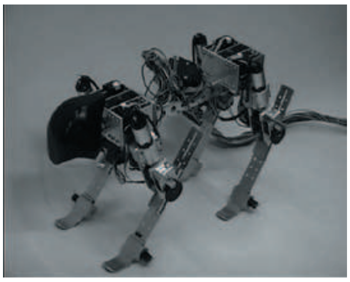

Figure 2.2: Quadruped robot - Tekken (Fukuoka et al., 2003).

Table 2.2: Reflexes/responses implemented in Fukuoka et al. (2003).

Reflex/response	**Trigger**	**Step phase**	**Description**
Flexor reflex	Collision with obstacle	Swing	Flexion of the leg to prevent the leg from stumbling in obstacles
Vestibulospinal reflex	Body pitch	Stance	Shortens or extents the legs to compensate an excessive body pitch angle
Tonic response	Body roll	Stance and swing	Shortens or extents the legs to compensate an excessive body roll angle

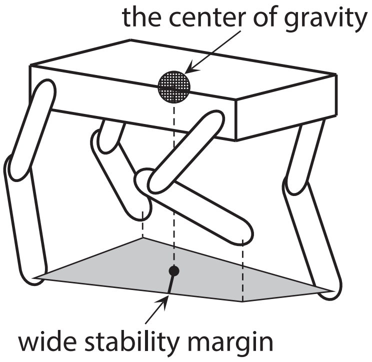

Figure 2.3: WSM definition (Fukuoka et al., 2003).

adaptability of its locomotion.

Yakovenko et al. (2004) presented a modeling study to estimate the stretch reflex influence in locomotion. In previous works, researchers thought that stretch reflex did not have an important role in the load compensation in mammals, however, they changed their minds. The authors developed a planar locomotor model of two hind limbs connected to a horizontal trunk supported at the front by a frictionless wheel, depicted in figure 2.4, which was designed to approximately mimic a cat. Each leg was constituted by four segments

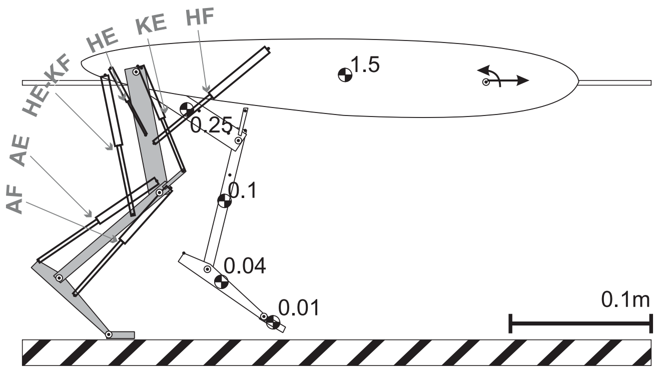

Figure 2.4: Structure of the neuromuscular locomotor model (Yakovenko et al., 2004).

(thigh, shank, foot and toes), that were driven by six musculotendon actuators simulating the muscles feedback. The organization of the leg's control system is depicted in figure 2.5, which can be solely dependent on CPGs or can also have the stretch reflex component. If the stretch reflexes were presented, the neural activation model for each leg would be defined by the equation 2.1, that simulates feedback from spindle Ia and tendon organ Ib afferents.

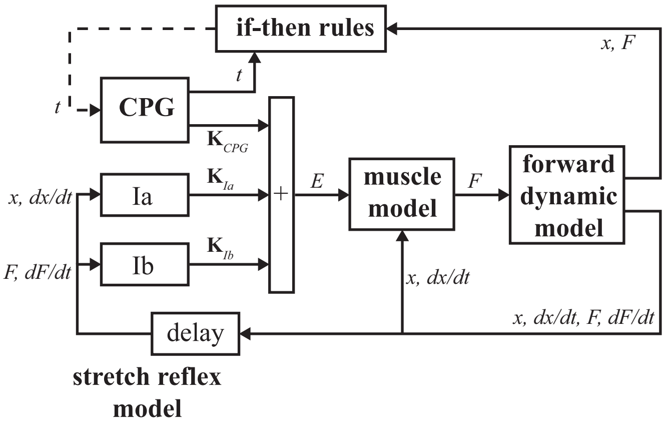

Figure 2.5: Leg's control system (Yakovenko et al., 2004).

$$u_l = CPG_l + f_{Ia} + f_{Ib} \tag{2.1}$$

This sensory feedback can have two roles: stiffness control of individual muscles and higher-level control of balance, stability and coordination (Yakovenko et al., 2004). With this in mind, the researchers weighed the CPG with 70% (without enough activation to generate stable locomotion) of the total neural activation and the reflexes with 30%, allowing a stable locomotion of the model. The reflex component increased the muscular stiffness, allowing the load compensation, so, if this component was removed, the model locomotion would not be possible. If the researchers weighed the CPG with 100% of the total neural activation (enough activation to generate stable locomotion), the stretch reflexes would just make a small increase in locomotion speed. This study shows that the stretch reflex contributes significantly to the load compensation and to improve the model's stabilization.

One more quadruped robot, named Tekken 2, depicted in figure 2.6, was presented by Kimura et al. (2007). As in previous works (Kimura et al., 2000; Fukuoka et al., 2003), this robot would be capable of walking in irregular terrains, but this time, the robot was able to move in an unknown outdoor environment. The implemented neural system has

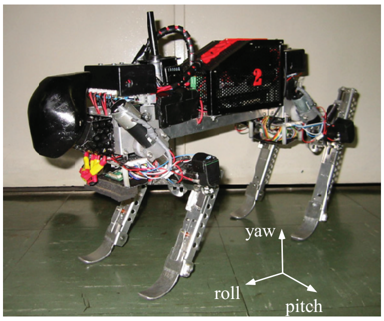

Figure 2.6: Quadruped robot - Tekken 2 (Kimura et al., 2007).

the same basis of the controller implemented in the previous study (Fukuoka et al., 2003), consisting of CPGs, reflexes and responses. To achieve dynamic locomotion, correcting the stepping motions in case of disturbances, they maintain the reflexes previously implemented (Fukuoka et al., 2003) and added new ones. The proposed reflexes are presented in table 2.3. In this study, the researchers showed that the combination of reflexes/responses with CPGs allows the locomotion on several irregular terrains, such as: slopes of 14 degrees at maximum in pitch inclination, 6 degrees at maximum in roll inclination, pebbles with a diameter of 30 mm at most, and scattered fallen leaves. Despite these results, the

Table 2.3: Reflexes/responses implemented in Kimura et al. (2007).

Reflex/response	**Trigger**	**Step phase**	**Description**
Flexor reflex	Collision with obstacle	Swing	Flexion of the leg to prevent the leg from stumbling in obstacles
Vestibulospinal reflex	Body pitch	Stance	Shortens or extents the legs to compensate an excessive body pitch angle
Tonic response	Body roll	Stance and swing	Shortens or extents the legs to compensate an excessive body roll angle
Stepping reflex	Forward speed	Swing	Adjustment of the touchdown angle of a swinging leg
Sideways stepping	Body roll	Swing	Angle adjustment of the hip yaw joint, proportional to body roll
Corrective stepping	Loss of ground contact	Swing	At the end of the swing, makes the leg land at the more forward position if it doesn't touch the ground as expected
Crossed flexor	Ground contact of contralateral leg	Swing	Higher swing in contralateral leg due to excessive yield

authors claim that additional reflexes/responses should be required to have locomotion on more complicated terrains, as well as using vision at the higher level.

Based on Ekeberg works (Wadden and Ekeberg, 1998; Ekeberg and Pearson, 2005), Maufroy et al. (2008) presented a simulation model of the two hind legs of a quadruped robot, which also has a bio-inspired controller based on CPGs and sensory events. Each leg of the model was constituted by three segments (thigh, shank and foot), linked by three articulations (hip, knee and ankle) actuated by seven muscles. The authors pursued the following two goals:

- The simulated model should be able to achieve high locomotion, capable of autonomous gait transitions according to changing speed;
- Adaptive locomotion in irregular terrains.

The leg's controller was constituted by the Neural Phase Generator (NPG), the Motor Output Shape Stage (MOSS) and the Propulsive Force Control Module (PFCM). In Ekeberg's work (Wadden and Ekeberg, 1998), the NPG was constituted by four parts (swing, touchdown, stance and liftoff), responsible for the rhythm generation, but, in this work, it was only made with two modules: the Extensor and the Flexor modules. The locomotion cycle was also divided in four parts, four synergies (swing, touchdown, stance and liftoff), but in this case, this division is in the MOSS level. This level was responsible for the generation of the muscle activation, allowing the implementation of the synergies aforementioned. Finally, the PFCM was responsible for the stepping frequency adjustment and locomotion speed, accordingly to an input from the upper neural system - tonic input. As in Ekeberg previous work (Ekeberg and Pearson, 2005), the controller relies on sensory information related to the hip angle, AEP and PEP, as well as leg loading, to regulate the transitions between the NPG modules and, according to the authors, this last one is considered the main sensory information that a controller for legged locomotion should rely on. As in Yakovenko work (Yakovenko et al., 2004), the contributions of the CPGs and sensory feedback are summed, thus obtaining the levels of muscle activation for the muscular systems.

An important requirement to achieve adaptive locomotion on irregular terrains is the postural stability (Sousa et al., 2010). Based on this idea, the authors proposed a posture control system which generated movements for posture correction based on sensory feedback and CPGs. Table 2.4 presents the several postural responses triggered by sensory inputs implemented by them. Some of the implemented postural responses had the same function as the implemented reflexes/responses in other works. The Roll and Pitch Compensation were implemented in moving robots in Fukuoka et al. (2003) and Kimura et al. (2007) referred to them as tonic response and vestibulospinal reflex, respectively. The Touch Control had the same function of the corrective stepping in Kimura et al. (2007). The Center of Mass Adjustment adjust the hip swing and hip flap joints to keep the robot stable, while the Load Distribution distributes the weight of the body equally over the four legs and the Leg Disperser had the function of preventing the collision of the fore and hind knees.

Table 2.4: Postural responses implemented in Sousa et al. (2010).

Postural response	**Trigger**
Roll Compensation	Body roll
Pitch Compensation	Body pitch
Center of Mass Adjustment	Encoders and body angle
Load Distribution	Joints load
Touch Control	Foot touch
Leg Disperser	Leg encoders

Recently, Klein and Lewis (2012) presented a neural controller implemented with CPGs and reflexes, employed in a bipedal robot that models the human muscular architecture, using muscles on straps and bifunctional muscles. The neural network had four CPGs, which controlled hip flexion and extension, while additional reflex signals modified the individual joints behavior. The controller receives sensory information related to the hip angle, AEP and PEP, as well as ground contact and load sensor. The hips' motion, controlled by CPGs, influenced the time of ground contact, while the rhythm of the CPGs was influenced by sensory feedback. On the other hand, the CPGs regulated the immediate reflexes which governed knees and ankles. The reflexes implemented in this work are phase dependent, *i.e.*, their activity was restricted to certain portions of the step cycle.

In the same year, Owaki et al. (2012) presented a study to understand the interlimb coordination mechanism capable of generating locomotor patterns. To achieve this purpose, they built a simple quadruped robot named Oscillex 2, illustrated in figure 2.7, and proposed a controller with four CPGs with local force feedback in each leg. The quadruped robot had a leg structure without knee and ankle, allowing the authors to ignore the intralimb coordination in each leg. The interlimb coordination should rely on the physical leg's interaction with the environment, so they exploited the sensory information related to the force in each leg to achieve the correct locomotor patterns. Each leg was controlled by a phase oscillator (basic element of each CPG):

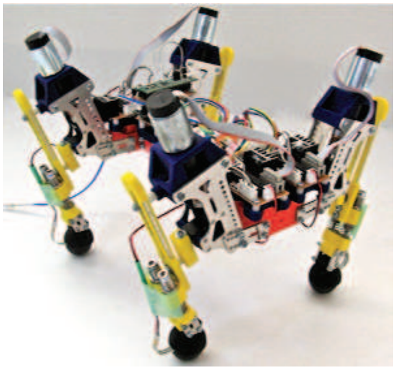

Figure 2.7: Quadruped robot - Oscilex 2 (Owaki et al., 2012).

$$\dot{\phi}_i = \omega + f_i \tag{2.2}$$

where ϕ_i was the phase introduced in the CPG's oscillator for each leg, ω was the intrinsic angular velocity and f_i was the local sensory feedback component. The equation 2.3 shows the representation of this last component, *i.e.*, the force sensor in each foot:

$$f_i = -\sigma N_i cos(\phi_i) \tag{2.3}$$

where σ was the magnitude of the feedback to the corresponding oscillator and the N_i was the Ground Reaction Force (GRF) acting on the corresponding leg. The model presented in this study was capable of exhibiting stable locomotion, the control of parameter ω allowed the transition between walk and trot gaits and the locomotion was achieved without any neural connection between the CPGs, due to the local sensory feedback, allowing each leg to recognize the positional relationship of all others.

2.1.3 CPGs acting as predictors

Arthur D. Kuo used a simple pendulum to study the combination of the feedforward (CPG) and feedback components in locomotion, which can be reached basically in three ways: with a feedforward component, with a feedback component, or with the combination of both (Kuo, 2002). In the first case, the generated movement would be very susceptible to unexpected disturbances, and on the second case, the movement would be very sensitive to sensory noise. Regarding the two components, feedforward and feedback, biological evidences show that they are somehow connected, providing a better locomotion (Kuo, 2002). This way, the author proposed a Hybrid Feedforward/Feedback System, depicted in figure 2.8, which exploits the advantages of combining the two components. The CPG in the system should produce a prediction of the pendulum's movements that, in turn, drives the feedback system. The sensors included in the system (stretch receptors) signal perturbations and the resulting error sends a feedback to the oscillator, which will change the pendulum's movements. In this contribution, the author demonstrates that a correct combination of the two components results in a better performance than either the feedback or feedforward approaches alone.

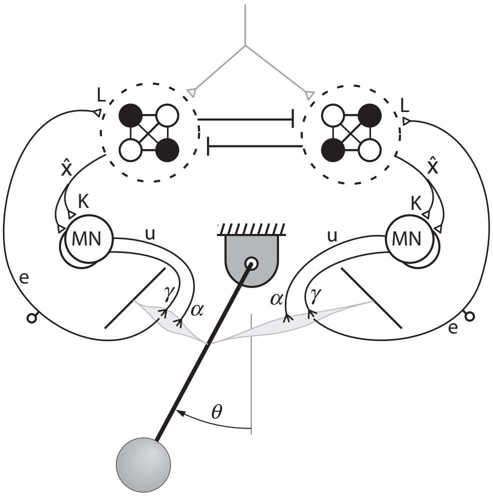

Figure 2.8: Hybrid Feedforward/Feedback System (pendulum) (Kuo, 2002).

Recently, Dzeladini et al. (2014) presented an extension of the neuromuscular model of human locomotion developed by Geyer and Herr (2010). They hypothesized that the addition of a CPG to the model would improve the controller in terms of gait speed control. They introduced CPGs as a feedforward component, in which CPGs should be able to reproduce feedback signals generated by a stable walking gait of the model presented by Geyer and Herr (2010). The authors used "morphed non-linear phase oscillators" to modulate the CPGs. These oscillators have the capability of generating limit cycles of arbitrary shapes. This work showed that the addition of a feedforward model on top of a reflex based controller is relevant, since the controller was capable of controlling the robot's velocity, as opposed to a purely reflex based system.

2.2 Summary of the presented studies

Most of the presented works are implemented in simulation, using models of musculoskeletal fore and hind legs, with some solutions producing muscle activations, others joint velocities, or torques to be applied at the joints, calculated from the musculoskeletal models.

From an engineering perspective, a stable and efficient locomotion is better achieved with feedback, since feedback signals can compensate for unexpected disturbances, as opposed to pure feedforward controllers (Kuo, 2002). Thereby, these works presented some sensory events that seem to be crucial to trigger locomotor actions (reflex based walking) or regulate the rhythm activity of CPGs. In common is the use of the hip joint angle regulating the timing of the stance and swing phases, signals indicating ground contact from foot sensors, promoting transitions of the step phases, and leg load used to inhibit the transition from the stance to the swing phase. Furthermore, the studies of Kuo (2002) and Dzeladini et al. (2014) suggest that one can achieve greater flexibility when combining CPGs and reflexes in a non-standard way. In this case, CPGs' function would be to predict the motor actions based on sensory information's track record.

Chapter 3

Quadruped locomotion

This chapter is presented aiming to provide to the reader a better understanding of the following chapters. Several principles and characteristics of quadruped locomotion are introduced, enabling a better analysis of the results presented in this thesis.

In the real world, animals adapt the limbs' movements accordingly to the situations they face every day, such as changes in terrain and desired walking velocity. Quadruped animals, like cats and horses, use their four limbs in the generation of locomotion patterns, supporting the body during it and generating the adequate propulsive force, propelling the animal forward.

3.1 Limb movements

The movement of each limb in the locomotion process is crucial for the effective generation of locomotor patterns. When an animal walks, each of its limbs respect a cycle, in which the foot is placed on the ground performing a propulsive movement that pushes the body forward, followed by the liftoff of the foot from the ground and placement in a more advanced position, preparing the limb for the next cycle (Cartmill et al., 2002).

The step cycle, or stride, depicted in figure 3.1, is a complete cycle of limb movements, *i.e.*, it is the cycle from one event (e.g. ground contact) of a particular foot to the next same event of the same foot (Alexander, 1984). The necessary time to complete the step cycle is the step cycle duration or stride period (Cartmill et al., 2002).

The step cycle can be divided into four distinct phases (Maufroy et al., 2008; Wadden and Ekeberg, 1998): stance, liftoff, swing and touchdown. The stance phase starts when the foot touches the ground and assures that a necessary force is generated to support

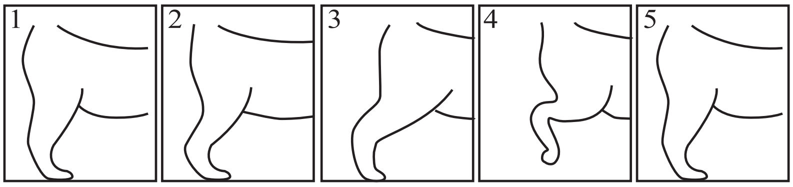

Figure 3.1: Illustration of the step cycle. The cycle starts with the foot touching the ground and ends in the same situation.

and propel the animal's body forward. Subsequently, the liftoff is started, ensuring the unloading of the leg by initiating the knee flexion, lifting the foot from the ground. During the next phase, the swing, the leg is brought forward like a pendulum, guarantying that the leg is in the correct position for the next phase. Finally, in the touchdown phase, the leg is placed in an appropriate position for landing, thus allowing the cycle to restart.

Another two concepts related with limb movements emerge: duty factor and diagonality. The duty factor (β) is the period of time during which the foot is on the ground (T_{st}), expressed as a fraction of the stride period ($T_{\text{st}} + T_{\text{sw}}$) (Cartmill et al., 2002; Alexander, 1984), calculated as follows:

$$\beta = \frac{T_{\text{st}}}{T_{\text{st}} + T_{\text{sw}}} \tag{3.1}$$

The diagonality (D) can be defined as the percentage of stride period by which the fore footfall follows the ipsilateral hind footfall (Cartmill et al., 2002). These two concepts presented by Hildebrand (1965) are very important in the characterization of gaits.

3.2 Gaits

A quadruped gait is a cyclic manner of moving the legs in terrestrial locomotion (Hildebrand, 1965). Gaits are grouped into two major categories: symmetrical and asymmetrical.

In symmetrical gaits, the footfall of the left and right foot of each pair is evenly spaced in time, presenting the same duty factor (Hildebrand, 1965; Alexander, 1984). In quadrupeds, the most common gaits are symmetrical gaits, including the pace, walk and trot. This category of gaits is often described in terms of the two dimensions of Hildebrand (Hildebrand, 1965): duty factor (β) and diagonality (D). In the figure 3.2 is presented the bivariate plot of diagonality against duty factor, showing a wide range of symmetric gaits exhibited by quadrupedal animals. As shown in figure 3.2, the duty factor dimension defines if the gait is a walking ($\beta > 50\%$) or running ($\beta < 50\%$) gait. If the duty factor (β)

exceeds fifty percent, each of the animal's feet is in contact with the ground most of the time, and at least two feet are always on the ground. If the duty factor (β) is less than fifty percent, then the right and left limb swing phases must overlap in time, and the animal will present periods of flight during a stride. Regarding the diagonality, the figure 3.2 shows that this dimension defines if the gait is a diagonal or lateral sequence gait.

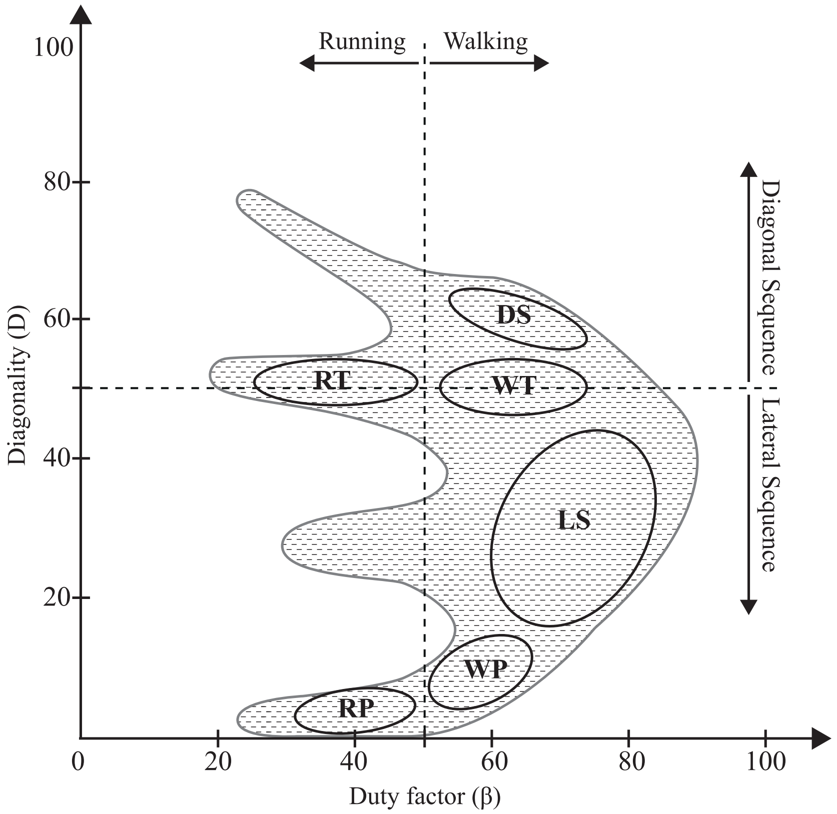

Figure 3.2: Bivariate plot adapted from (Hildebrand, 1965; Cartmill et al., 2002). This figure shows a wide range of symmetric gaits used by quadruped animals. Some gaits are identified in the figure: diagonal sequence walks (DS); lateral sequence walks (LS); running pace (RP); running trot (RT); walking pace (WP) and walking trot (WT).

In asymmetrical gaits (e.g. gallop and bound), the footfalls of a pair of feet are unevenly spaced in time, *i.e.*, the pair of feet do not exhibit strict alternation between the limbs (Hildebrand, 1977).

The figure 3.3 presents the stepping sequence of two symmetric gaits (lateral sequence walk and walking trot) and two asymmetrical gaits (gallop and bound).

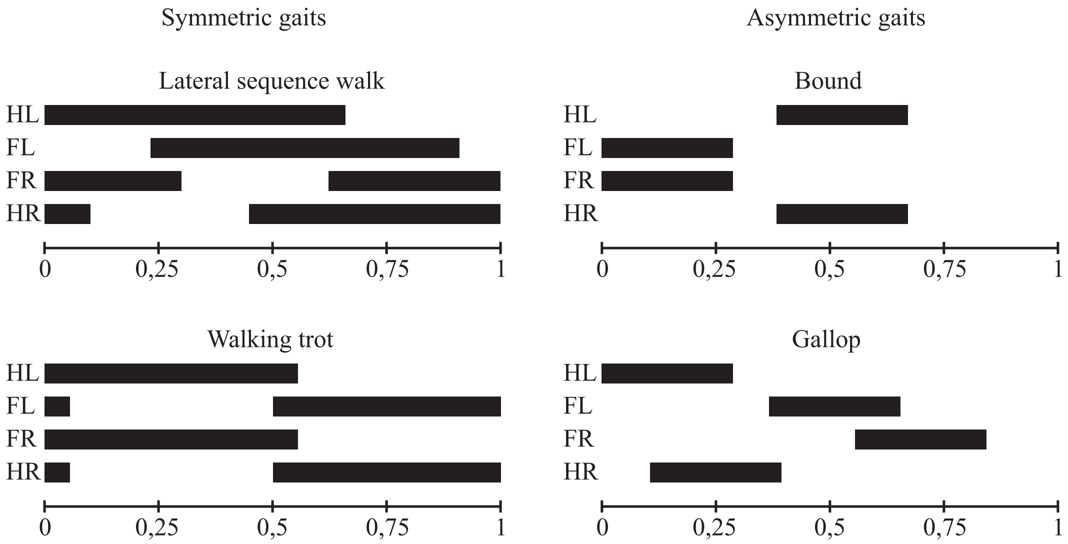

Figure 3.3: Stepping sequences of two symmetrical gaits (walking trot and lateral sequence walk) and two asymmetrical gaits (bound and gallop), in which the black bars represent the foot contact with the ground.

3.3 Oncilla robot

Oncilla, depicted in figure 3.4, is an open-source, open-hardware quadruped robot based on the design of Cheetah-cub robot and developed on an European Project (AMARSi: Adaptive Modular Architecture for Rich Motor Skills) improving biological richness of robotic motor skills (Laboratory, 2014). The robot was developed with pantograph and three-segment leg design, providing passive compliant behavior to the cable driven retractable knees. It has twelve degrees-of-freedom, three on each leg: hip-swing, hip-flap

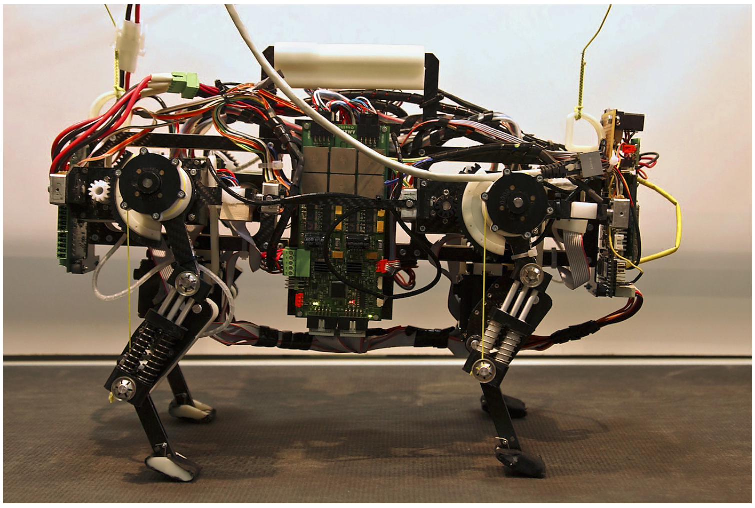

Figure 3.4: Oncilla robot (Laboratory, 2014).

and knee. The robot has compliant knees and the hip joints are position controlled.

The figure 3.5 shows the simulated Oncilla quadruped robot, developed for the Webots (Michel, 2004) robotic simulator. Webots is a simulation environment that allows the development of complex robots, enabling the setup of several object parameters, such as shape, color, texture, mass and friction. The simulator provides a wide range of simulated actuators and sensors and allows simulation in physically realistic worlds.

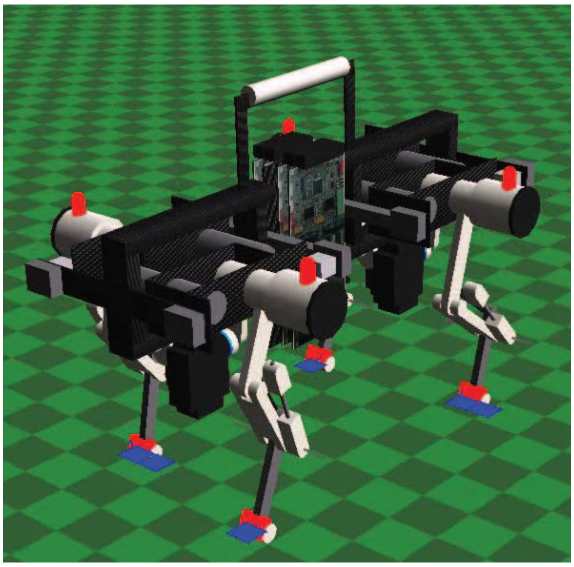

Figure 3.5: Simulated Oncilla robot.

All the work developed in this thesis was implemented in the simulated Oncilla quadruped robot, which reflects most of the real world features, from internal robot characteristics to its interaction with the environment. Therefore, all the results obtained in simulation are possible to be obtained with the real robot.

Chapter 4

Biological evidences

In the real world, animals have the ability to deal with uncertain situations and react quickly to changes in the environment, serving as inspiration in the development of controllers capable of providing stable locomotion. Many robotic researchers (Pfeifer et al., 2007) agree that bio-inspired concepts should be used to develop robots for the real world, thus presenting similar properties to their biological counterparts, such as adaptability, robustness, versatility and agility.

Understanding how simple movements like walking and running are controlled seems to be a big challenge for scientists. It is known that the Central Nervous System (CNS) is capable of controlling which joint has to be moved and in what moment (Duysens and Van de Crommert, 1998). The limb movement is achieved through muscle activation (Duysens and Van de Crommert, 1998) and the animal's locomotion constantly adapts to the environment, dealing with several perturbations in the real world. The smooth progression of the animal's lower limb movements is achieved by the combination of two major components: reflexes and Central Pattern Generators (CPGs), which are neural networks capable of repeating particular actions over and over again.

4.1 Central Pattern Generators

CPGs are neural networks of the CNS capable of producing rhythmic locomotor patterns in the absence of inputs from higher brain centers and peripheral sensory feedback (Ijspeert, 2008; Rybak et al., 2006). They are needed for rhythmic activities such as walking, running, breathing, chewing, digesting, flying and swimming (Duysens and Van de Crommert, 1998; Ijspeert, 2008), and present several important properties for the generation of locomotion: intrinsic rhythmic behavior, limit cycle stability, smooth online trajectory modulation by parameters change, low computational cost, easy feedback integration, robustness and entrainment phenomena when coupled to mechanical systems. The concept of CPG for animal locomotion is generally attributed to Brown (1911). He defended that the rhythms were centrally generated by neural networks that don't require sensory input. Brown showed that cats with transected spinal cord and cut dorsal roots still produce rhythmic activity, proving the existence of CPGs in the cat's spinal cord. Another important study that proved the existence of CPGs in cats was made by Grillner and Zangger (1979), in which it was proven that a central network of neurons produced rhytmic patterns similar to intact animals locomotion after suppression of all afferent signals. Duysens and Van de Crommert (1998) assumed that cats have at least one CPG for each limb. Other studies were done to prove the existence of CPGs in living beings, for instance, research on invertebrates (Marder et al., 2005) and on vertebrates animals (Kiehn, 2006). Bässler (1986) proposed that CPGs could have different functions. He states that the sensors signal can define the step phases transitions and the CPG may only function as a filter. Kuo (2002) presented a similar idea. He argued that the CPGs can have the function of predicting the limbs' movements, which, in turn, drives the feedback systems.

4.2 Reflexes

CPGs are not the only way to implement rhythmic locomotion patterns, since it can be implemented using discontinuous bi-stable systems such as reflex chains (Daun-Gruhn and Büschges, 2011). Charles S. Sherrington (Burke, 2007) defended that rhythms are the result of a chain of reflexes, in which sensory signals play an important role in triggering transitions between different step phases. Reflexes are events triggered in response to sensory signals, *i.e.*, the excitatory sensory signals are capable of producing an appropriate output (Bässler, 1986). Some reflexes are responsible for reacting quickly to unexpected perturbations, such as stumbling reflex, crossed reflex, lateral stepping and leg extension reflex. This kind of systems are triggered externally by sensory inputs and are capable of producing stable locomotion, like in the work presented by Cruse et al. (1998).

4.3 Combination of CPGs and reflexes

A crucial subject in the locomotion generation is the combination of CPGs and reflexes. It is generally accepted that locomotion in animals is generated at the spinal cord level by a combination of CPGs and reflexes (Rossignol et al., 2006). Studies have presented the idea that the reflex networks are integrated in the CPG network (McCrea, 2001), providing the capability of adapting and correcting the walking behavior accordingly to changes in environment. This coupling is also evident in the fact that reflexes are phase dependent, *i.e.*, they trigger different actions depending on the step phase within the locomotor cycle (Ijspeert, 2008; Cohen and Boothe, 1999). In this context, reflexes have a crucial role, presenting several functions and actions in the locomotor cycle. They define some muscle activations (Duysens and Van de Crommert, 1998), regulate the excitability of motoneurons (McCrea, 2001), contribute for the selection of locomotor patterns, define the timing of extensor and flexor phases and can modulate the CPG output neuronal activity (Pearson et al., 2006; Verdaasdonk et al., 2007; Orlovsky et al., 1999). Furthermore, reflexes can correct non-linear limb mechanics (McCrea, 2001). Even though locomotion generation is a centrally generated process, reflexes and sensory feedback play an important role in the adaptation and correction of legged locomotion (Pearson, 2004). In this study, the author presents his doubts related with locomotion being primarily generated by CPGs modulated by sensory feedback. This explanation may be too simplistic, since the cat's motor pattern is substantially altered after deafferentation. There are neural networks in the spinal cord capable of generating motor patterns without sensory feedback, but the CPGs may have a different function and the reflexes can be responsible for the primarily establishment of motor patterns. The author's statements are supported in cats, since it is the sensory information that regulates the transitions between the stance and swing phases. According to the author, the challenge is to establish how the combination of the reflexes and Central Pattern Generators is accomplished.

How CPGs and reflexes are exactly combined is still an unanswered question. This thesis addresses this innovative thematic, in which it is suggested a network that presents a proposal for the combination of the Central Pattern Generators and reflexes, hoping to contribute to the continuous research in this specific field. In chapter 5 is presented the bio-inspired controllers developed throughout the thesis.

4.4 Delays

An important biological evidence is responsiveness, the time that an animal takes to sense and react. Sensorimotor control is greatly affected by this factor (More et al., 2010), affecting the terrestrial mammals in different ways, due to their wide range of sizes. Responsiveness comprises many sources of delay and is proportional to axonal conduction velocity and to axon diameter (More et al., 2010). In the study made by More et al. (2010), the authors done tests in six shrew and one Asian elephant, obtaining the correspondent conduction velocity. The conduction velocity of the elephant was greater than that of the shrew, but did not change to the extent required to maintain sensorimotor responsiveness. For that reason, the CNS should have an internal model capable of predicting the best future motor response, compensating the internal delays existing in animals (More et al., 2010). The delays are greater in larger animals, therefore, they are more dependent on the predictability of the CNS to maintain sensorimotor performance.

4.5 Biological mechanisms

This section presents some biological studies made in animals with the purpose of understanding the internal organization of the systems that generate locomotion. Some of these studies inspired the creation of biologically inspired controllers capable of generating locomotion in robots. This way, these studies served as basis to the creation of the controllers implemented on the Oncilla robot.

Locomotion generation is largely dependent on reflexes: animals react to specific stimulus by generating particular movements. In fact, Charles S. Sherrington (Burke, 2007), defended that reflexes were the main neuronal mechanism capable of promoting locomotion. According to the author, locomotor patterns can be the result of a chain of reflexes triggered and governed by external sensorial events, producing the final rhythmic locomotor activity. Brown (1911) refuted Charles S. Sherrington opinion with experiments conducted in a decerebrated cat. According to Brown, locomotion was generated by a central mechanism, but, without sensory feedback, in an uneven terrain, the animal's progression would be inefficient. In an ideal situation, the central mechanism would be capable of driving the animal with precision. The author defended that the proprioceptive mechanism (sensory feedback) would have the function of regulating the locomotion generated by the central mechanism. Both authors agreed that sensory signals were crucial for the generation of stable and robust locomotion, and therefore, it is necessary to have a deep knowledge in the major biological evidences that contributes to the generation of locomotion in animals, specifically in quadrupeds.

Hereinafter are presented several existing mechanisms in the biological systems of the animals, necessary to generate stable quadruped locomotion. These mechanisms are sensory events used by the animals to adapt its locomotion and to make the correct transitions between the step phases, providing an effective locomotion in the most diverse terrains.

4.5.1 Ground contact

Duysens and Pearson (1976) presented a study to understand the role of sensory signals coming from the pad and plantar surface of the foot in the quadruped locomotion. Experiments done in sixteen decerebrated cats showed that extensor reflexes elicited from the skin participated in locomotion. The experiments were performed with all the animals supported over a treadmill and electromyographic activity was recorded. To clearly understand the ground contact mechanism function, the authors electrically stimulated the pad and plantar surface of the foot. When the electrical stimuli (trains of rectangular pulses) were applied during the stance phase, the extensor activity of the walking cat was enhanced and prolonged, causing a prolongation of this phase and delaying the onset of the following swing phase.

The observations presented in this study support the effective contribution of ground contact in the quadruped locomotion, enhancing and promoting the stance phase.

4.5.2 Hip position and leg loading

Some studies were performed showing the importance of the hip position and the leg loading in locomotion. Grillner and Rossignol (1978) explored the hip position importance in the determination of the stance phase duration and the swing phase initiation. They made experiments in nine chronic spinal cats, using the hind legs to walk on a treadmill. Electromyography (EMG) signals were recorded during the experiments. The researchers, during the cat walk, slowly pulled the leg back, checking to see when the liftoff-reaction occurs, and they noticed that this reaction always occurred at the same hip angle. The results also showed that the liftoff-reaction was initiated at a similar hip angle both during normal locomotion and during the passive extension of the limb. Furthermore, the authors also showed that the extension of ankle and knee did not initiate the liftoff-reaction, unlike the situation in which the hip was brought back. The experiment proved that the hip position is crucial for the initiation of the swing phase, specifically, the posterior extreme position (PEP) proved to be an important sensory signal directly related with the stance to swing transition.

Another relevant study made by McVea et al. (2005) shows that sensory signals related with the hip position play an important role in initiating the swing to stance transition. The experiments were made with decerebrated walking cats on a treadmill. As in the study presented above, when the transition from swing to stance occurs, the hip angle was similar during normal and assisted locomotion. This study showed that signals related to hip position, more specifically the anterior extreme position (AEP), are important in the initiation of the stance phase, even though the authors state that there are more sensory signals involved in this transition. Similar to the previous work, results of this study showed that the extension of ankle did not regulate the transition from stance to swing phase.

An important review made by Pearson (1995) presented the involvement of the group Ib afferents from Golgi Tendon Organs (GTOs). These afferents are located in series with the muscle fibers, transmitting information related with the exerted force at the muscle. They have an important function in cats' locomotion: regulating the duration of the stance phase, *i.e.*, the decrease in muscle Ib afferents from GTOs signalize the unloading of the limb, and consequently enables the initiation of the swing phase.

Hiebert et al. (1995) conducted experiments in cats to test their behavior when they fail the ground contact (foot in hole) at the end of swing phase. When this occurs, the limb is rapidly lifted and replaced, attempting to seek support. The authors test the hypothesis that the factor related to the inititation of this corrective response is the absence of signals from the group Ib afferents from GTOs in the extensor muscles. They made experiments in seven decerebrated adult cats on a treadmill with a hole in the left side, into which the left limb would periodically step. The researchers stimulated the extensor group I afferents, simulating leg loading, when the cat's foot enter the hole, and consequently the corrective response was inhibited. This result showed that the leg loading is essential to define the beginning of the limb flexion movements in cats.

Pearson (2008) presented an important review showing that there are two sensory signals that controls the transition from stance to swing phase: afferents activated by hip position and group Ib afferents from GTOs in the ankle extensor muscles. The function of the GTOs from the ankle extensor muscles is to prevent the initiation of the swing phase while the leg is loaded, *i.e.*, the stimulation of the group Ib afferents will inhibit the transition from stance to swing phase. On the other hand, the author states that the signals from the hip position have a significant contribution to the stance to swing transition. Once again, this review shows the relevance of the hip position (PEP) in the swing phase initiation, and the importance of the unloading of the leg near the end of the stance phase, allowing the leg to enter the swing phase.

4.5.3 Stumbling reflex

The stumbling reflex is evoked when the dorsum of a cat's paw strikes an obstacle during the swing phase of the step cycle, producing an enhanced flexion (Forssberg et al., 1977). The paw is lifted from the ground in the attempt of clear the obstacle and prevent tripping (Quevedo et al., 2005). Forssberg et al. (1977) presented a study in cats with spinal lesions, showing that this reflex could be organized at the level of the lumbar spinal cord. The authors applied electrical stimuli in the paw dorsum, that induced a flexion response, showing that this reflex is crucial to overcome obstacles. Other studies performed in intact cats showed that the stumbling reflex is evoked during the early swing phase of locomotion (Prochazka et al., 1978; Forssberg, 1979).

A more recent work (Quevedo et al., 2005) proved the efficiency of the stumbling reflex. They made tests in twenty eight purpose-bred cats, by the application of stimuli in the superficial peroneal nerve. The study's observations shows the stumbling reflex being evoked by the superficial peroneal nerve stimulation during the swing phase in decerebrate cats. In fact, the authors showed the sequence of activations during the process of avoiding an obstacle. When the reflex is activated, it starts with a knee flexion and ankle extensor to remove the paw from further contact with the obstacle. After these two activations, they observed a period of ankle flexion, allowing the foot to have a correct placement. The authors also proved that the effects of the peroneal nerve stimulation had the same pattern in decerebrate and in intact cats.

The observations presented in these studies showed the importance of a mechanism capable of making the locomotion more robust, avoiding obstacles, and able to adapt to the different environment situations.

4.5.4 Vestibulospinal reflex

In vertebrates, the vestibular system is a biological sensor responsible for maintenance of the body's balance, located in the inner ears on both sides of the head (Kaushik et al., 2007). Brustein and Rossignol (1998) presented a study that proves the importance of the vestibular pathways in the posture control. In particular, they made experiments in eight adult cats that were trained to walk on a treadmill with different inclinations (maximum of 10º). The cats were submitted to the ventral-ventrolateral spinal lesion, preventing the carrying of vestibular pathways by the spinal cord. After the observations, the authors stated that the cats suffer from postural deficits, particularly, during locomotion on an inclined treadmill. This study shows the relevance of the vestibulospinal reflex in locomotion, helping the body to compensate an excessive inclination in pitch plane (Fukuoka et al., 2003).

When the vestibule of the head detects an excessive pitch inclination, the downward-inclined leg is extended and the upward-inclined leg is flexed. This reflex improves the animal's locomotion regarding climbing or going down ramps, keeping the posture of the body flat, preventing the center of gravity from being pulled backward (going up a ramp) or forward (going down a ramp), increasing the animal's stability.

4.5.5 Contralateral coordination

In order to achieve a successful locomotion, the contralateral leg should be coordinated with the ipsilateral leg. Grillner and Rossignol (1978) (study presented previously in subsection 4.5.2) recorded some conclusions related with contralateral coordination. Specifically, they observed that the hip angle is not the only factor responsible for the swing phase initiation. When the leg was brought backwards, it was coordinated with the step phase in the contralateral leg. They noticed that when the hip angle was attained (PEP), the swing phase initiation was delayed if the contralateral leg was not in stance phase, *i.e.*, if the contralateral leg was not in position to support the body weight.

Other studies have found that the step phase of the contralateral leg influenced the initiation of the swing phase. In "foot in hole" experiments on intact (Gorassini et al., 1994) and spinal cats (Hiebert et al., 1994), the leg corrective response, when the cat's limb enters the hole, was not initiated if the contralateral leg was in swing phase. The leg waits for the contralateral leg to enter the stance phase, making sure that this leg was supporting the body weight, preventing the animal from falling.

4.5.6 Rules for quadruped sensory-driven locomotion

Bio-inspired rules were defined for the success of quadruped locomotion. These rules are based on previously animal's studies that verified the importance of several mechanisms and sensory events, allowing them to perform a more efficient and robust locomotion in real world. These mechanisms are resultant from the animal's interaction with the environment, as follows:

(a) The hip position is key factor in the transition between the stance and swing phases (Grillner and Rossignol, 1978; McVea et al., 2005; Pearson, 2008);

(b) During the stance phase, the stimulation of the footpad promotes/enhances this phase (Duysens and Pearson, 1976);

(c) The unloading of the leg is a necessary condition for swing phase initiation (Pearson, 2008; Hiebert et al., 1995; Pearson, 1995);

(d) When the vestibule in the head detects an excessive body pitch angle, the downward-inclined leg is extended and the upward-inclined leg is flexed in order to maintain balance (Kimura et al., 2007; Kaushik et al., 2007; Brustein and Rossignol, 1998);

(e) During the swing phase, if the paw dorsum touches an obstacle, an enhanced flexion is produced in order to overcome the obstacle (Forssberg et al., 1977; Quevedo et al., 2005; Prochazka et al., 1978; Forssberg, 1979);

(f) The leg's swing phase is initiated when the contralateral leg is in stance phase (Grillner and Rossignol, 1978; Gorassini et al., 1994; Hiebert et al., 1994).

Chapter 5

Bio-Inspired Controllers

This chapter presents the core of the thesis, and describes the two bio-inspired controllers developed during the past year. The design of the controllers is based on the previous chapter, in which the main biological mechanisms responsible for the generation of locomotion were presented.

The reflex network was the first controller developed for the Oncilla quadruped robot, using neural networks. It is capable of producing quadruped locomotion on irregular terrains, based on the interactions of the robot with the environment, therefore, the generated trajectories are a result from the interplay between the motor actions and the sensory information. The work builds on a previous controller developed within the team (Ferreira et al., 2014b) which was lacking some relevant feedback pathways. The walking behavior is an emergent realization of motor actions reflecting the general rules encoded in reflexes, improving robustness to unexpected disturbances and a more periodic final stepping sequence comparatively to the previous one (Ferreira et al., 2014b).

The hybrid controller comprises the extension of the reflex network through the addition of CPGs, modeled by a dynamical system presented by Owaki et al. (2012). This is an abstract model of biological CPGs in which these are represented as dynamical systems exhibiting limit cycle behavior. It is a usually employed strategy to test hypothesis on the role of biological CPGs (Ijspeert, 2008). In this controller a feedforward component in each limb, modeled by CPGs, was added to the system, compensating for both disturbances and sensor performance, and thus improving the walking behavior. The CPGs present a rhythmic internal model which drives the reflex network, serving as predictors of the expected motor actions resultant from the reflex network. Thereby, the four CPGs are constantly supervising the locomotor cycle, correcting the shortcomings of the purely sensory-driven controller previously designed. An innovative aspect of the work herein proposed is that CPGs are acting as predictors of the motoneurons and not as predictors of the sensory information as in Dzeladini work. This could be used in the mean time, to explore the use of primitives or motor synergies to simplify the control problem. Additionally, also contrarily of Dezladini work (Dzeladini et al., 2014), the CPGs are entrained by the load signal at runtime, and there is never no artificial synchronization such as a reset introduced to the system.

5.1 Reflex Controller

The proposed sensory-driven controller, depicted in figure 5.1, refers to a bio-inspired quadrupedal walking model. This model uses feedback rules connecting multimodal sensory information to a set of sensory interneurons (μ), and motoneurons (Ψ), to achieve the effective joints velocities. Sensory information is also connected to a set of direct actions (ζ,) which in turn can act directly in the specifications of the joints' velocities.

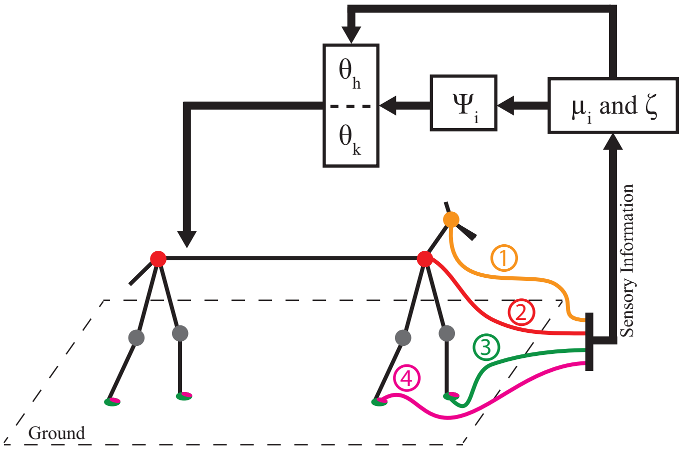

Figure 5.1: Bio-inspired quadrupedal walking model. The numbers from 1 to 4 represent sensory information provided by four types of sensors. 1 represents the signal of the vestibule; 2 represents the hip joint positions of the four limbs; 3 and 4 represent the touch sensors signals of the foot-pad and dorsum-paw of the four limbs, respectively. μ_i ($i =$ GC, AEP, PEP, DC, Load) represents the sensory interneurons that translate the sensory events based on the limb's sensory information. ζ represents the direct actions that act directly in the specification of the joints' velocities. Ψ_i ($i =$ stance, swing, touchdown, liftoff) are the motoneurons that determine the activation of the motor actions of a step cycle. These are responsible for the generation of the joint movements for the hip or knee, θ_i, $i = h, k$, which interact with the environment, thus closing the loop.

Four sets of feedback rules switched according to a state machine (Fig. 5.2),are specified as follows. A set generates the **stance** phase control, propelling the robot forward, by acting on the hip. Another set of rules controls the **swing** phase, bringing the leg forward by acting on the hip. The other two sets control **touchdown** and **liftoff** phases by extending (increasing the leg length to support the foot on the ground once in the rostral position) and flexing the knee (reducing the leg length by lifting the foot from the ground), respectively.

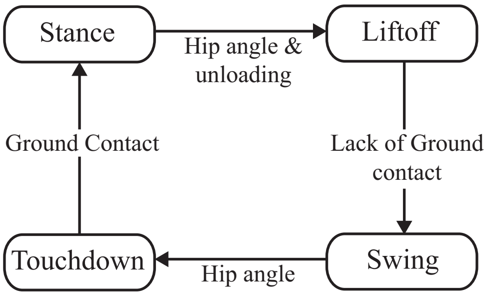

Figure 5.2: State machine implemented for each limb, in which reflexes trigger the transitions from one state to the next.

These motor actions or states are not mutually exclusive in time, for example, the swing action could be executed just after lift-off has started. Together these four motor actions constitute a step cycle.

Physiologically, a joint-based CPG is incorrect though some roots could be found in Grillner's review in 80's (Grillner and Wallen, 1985). The alternative is to consider the muscle organization and then superimpose it on the joint controller for the robot. However, our perspective is an engineering one and abstractions are done such that the proposed models are well suited for robots while keeping the models as simple as possible. The inclusion of such a musculoskeletal organization could be done in the future to prepare the extension of the model and would bring no functional differences, if carefully parameterized.

The sensors to joints mapping are separate in two biologically relevant stages: sensory interneurons (μ) and motoneurons (Ψ).

Hereinafter, each component of the model is described in detail.

5.1.1 Sensory Inputs

The sensory inputs to the reflex network translate the robot interactions with the environment. There are four different types of sensors:

- touch sensor of foot-pad to detect ground contact and to detect when the limb is supporting the body weight;
- touch sensor of the dorsum paw to detect obstacles;
- joint encoder to calculate the joint position to be able to detect the anterior extreme position (AEP) and posterior extreme position (PEP);
- the vestibule to measure the body pitch angle (BPA).

5.1.2 Sensory Interneurons

Sensors signals stimulate a set of sensory interneurons (μ), translating sensory events based on the limb's sensory information. Sensory events are detected through the sensory interneurons of each limb, μ_{GC}, μ_{AEP}, μ_{PEP}, μ_{DC}, μ_{Load} implemented as logistic functions, activated ($= 1$) when the sensory values cross a defined threshold. μ_{GC} (sensory interneuron of Ground Contact) becomes active when the touch sensor of the foot-pad exceeds the threshold $F_{\text{threshold}}$. μ_{AEP} (sensory interneuron of AEP) becomes active if hip exceeds the AEP angle Θ_{AEP}. μ_{PEP} (sensory interneuron of PEP) becomes active if hip exceeds the PEP angle Θ_{PEP}. μ_{DC} (sensory interneuron of dorsum contact) becomes active when the touch sensor of the dorsum paw exceeds the threshold $F_{\text{threshold}_{\text{DC}}}$. μ_{Load} (sensory interneuron of limb loading) becomes active when the touch sensor of the foot-pad exceeds the threshold $F_{\text{threshold}_{\text{Load}}}$. These interneurons are implemented with sigmoid functions, allowing the sensory interneurons of each limb to become active when the sensory value exceeds a certain threshold:

$$\mu_{\text{AEP}} = \frac{1}{1+\exp^{-b(\theta_{\text{h}}-\Theta_{\text{AEP}})}} \tag{5.1}$$

$$\mu_{\text{PEP}} = \frac{1}{1+\exp^{b(\theta_{\text{h}}-\Theta_{\text{PEP}})}} \tag{5.2}$$

$$\mu_{\text{GC}} = \frac{1}{1+\exp^{b(F_{\text{threshold}}-F_{\text{touch}})}} \tag{5.3}$$

$$\mu_{\text{DC}} = \frac{1}{1+\exp^{b(F_{\text{threshold}_{\text{DC}}}-F_{\text{touch}_{\text{DC}}})}} \tag{5.4}$$

$$\mu_{\text{Load}} = \frac{1}{1+\exp^{b(F_{\text{threshold}_{\text{Load}}}-F_{\text{touch}})}} \tag{5.5}$$

where Θ_{AEP}, Θ_{PEP}, $F_{\text{threshold}}$, $F_{\text{threshold}_{\text{DC}}}$ and $F_{\text{threshold}_{\text{Load}}}$ are the specified threshold values; θ_h is the measured hip joint angle, F_{touch} and $F_{\text{touch}_{\text{DC}}}$ are the sensor readings.

5.1.3 Direct Actions

Direct actions refers to a set of reflexes that are not connected to motoneurons but rather act fast and directly in the specification of the velocity of the robot joints. In this work these are the stumbling reflex (ζ_{StH} and ζ_{StK}) and the vestibulospinal reflex (ζ_{VR}). When the dorsum paw touches an obstacle, the stumbling reflex is activated acting in the hip and knee joints of the limb that tripped, allowing the robot limb to overcome small obstacles. The vestibulospinal reflex is activated when the vestibule detects an excessive body pitch angle, helping the robot to maintain its posture, through a fast action in the knees of the four legs.

These reflexes are phase dependent since they are only active during a specific motor action: the stumbling reflex is active when the limb is in the swing phase, and the vestibulospinal reflex is active when the limb is in the stance phase.

Their implementation brings the joints to a specific position, using attractors that pull towards the desired joint positions, allowing a rapid response from the robot:

$$\zeta_{\mathrm{StH}} = -w_{\mathrm{St}}\lambda_{\mathrm{St}}\sin(\theta_{\mathrm{h}} - \Theta_{\mathrm{StH}}) \tag{5.6}$$

$$\zeta_{\mathrm{StK}} = -w_{\mathrm{St}}\lambda_{\mathrm{St}}\sin(\theta_{\mathrm{k}} - \Theta_{\mathrm{StK}}) \tag{5.7}$$

$$\zeta_{\mathrm{VR}} = -w_{\mathrm{VR}}\lambda_{\mathrm{VR}}\sin(\theta_{\mathrm{k}} - \delta_{\mathrm{VR,j}}) \tag{5.8}$$

where w_{St} and w_{VR} are the strength of the connection: $w \in [0,1]$; λ_{St} and λ_{VR} represent the attractors strength; θ_{h} and θ_{k} are the measured hip and knee joint angle, respectively; Θ_{StH} and Θ_{StK} are the attracting hip and knee joint positions, respectively; $\delta_{\mathrm{VR,j}}$ is an attracting knee position given by: $\delta_{\mathrm{VR,j}} = \theta_{\mathrm{k}} \pm \mathrm{BPA}$, where j represents the limb type (fore or hind).

5.1.4 Motoneurons

Motoneurons are based on a non-spiking neuron model, representing a population of functionally similar neurons and outputting a mean firing frequency. These neurons are simple leaky integrators. The excitatory (ξ_{+j}) and inhibitory (ξ_{-j}) synaptic inputs are calculated from first-order differential equations adapted from Wadden and Ekeberg (1998), as follows:

$$\dot{\xi}_{+j} = \frac{1}{\tau}\left(\sum_{i\in\Upsilon_+} \mu_i w_i - \xi_{+j}\right) \tag{5.9}$$

$$\dot{\xi}_{-j} = \frac{1}{\tau}\left(\sum_{i\in\Upsilon_-} \mu_i w_i - \xi_{-j}\right) \tag{5.10}$$

where j represents the motoneuron (stance, swing, touchdown, liftoff) acting on a limb; τ is the time constant; Υ_+ and Υ_- are the sets of excitatory and inhibitory synapses; w_i is the strength of synapse: $w \in [0,1]$ and μ_i is the output value from the corresponding presynaptic sensory interneuron. The neuron activation of the motoneurons is given by :

$$\Psi_j = \begin{cases} 1 - \exp((\Theta - \xi_{+j})\Gamma) - \xi_{-j} & \text{, if positive} \\ 0 & \text{, otherwise} \end{cases} \tag{5.11}$$

The output of the neuron model reflects a mean firing rate, between 0 and 1, and is characterized by its time constant, the gain Γ and the activation threshold Θ.

5.1.5 Joint Outputs

The position controlled joints track the position as integrated from the reflex system output in joint velocity, $\dot{\theta}_\text{i}$, where $i = h,k$ for hip and knee joints, respectively.

For the hip joint: a) by specifying a negative velocity for the hip joint, the leg produces the motion of propulsion, reflecting the hip action in the **stance**; b) a positive velocity for the hip joint transfers the leg to the front, reflecting what happens in the **swing**.

For the Knee joint: a) A positive velocity in the knee flexes the leg and decreases the leg length, achieving **liftoff**; b) a negative velocity in the knee releases the spring, extending the leg, achieving **touchdown**.

The motor actions are implemented by assigning fixed rates of change, activated by discrete motoneuron from a reflexive network dependent on sensory information. Despite the joint output generator being in the form of velocity the desired output is the joint position, which is obtained through integration.

A single limb is controlled by four motoneurons, which determine the activation of the four motor actions of the robot step cycle. Two motor actions are assigned to the hip joint, each governed by one neuron, Ψ_swing and Ψ_stance. The other two motor actions are governed by Ψ_liftoff and $\Psi_\text{touchdown}$ neurons and are assigned to the knee joint. The velocity joint output is directly dependent on the neuronal activity of the motoneurons, ($\Psi \in [0,1]$), as follows:

$$\begin{aligned}
\dot{\theta}_{\mathrm{h}} &= -(\alpha_{\mathrm{h}}\Psi_{\mathrm{stance}} - \gamma_{\mathrm{h}}\Psi_{\mathrm{swing}}) + \zeta_{\mathrm{StH}} && (5.12)\\
\dot{\theta}_{\mathrm{k}} &= -(\alpha_{\mathrm{k}}\Psi_{\mathrm{touchdown}} - \gamma_{\mathrm{k}}\Psi_{\mathrm{liftoff}}) \\
&+ g_{\mathrm{lim}}(\theta_{\mathrm{k}} - \Theta_{\mathrm{k,max}}) \exp^{-\frac{(\theta_{\mathrm{k}}-\Theta_{\mathrm{k,max}})^2}{2\sigma^2}} \\
&+ g_{\mathrm{lim}}(\theta_{\mathrm{k}} - \Theta_{\mathrm{k,min}}) \exp^{-\frac{(\theta_{\mathrm{k}}-\Theta_{\mathrm{k,min}})^2}{2\sigma^2}} \\
&+ \zeta_{\mathrm{VR}} + \zeta_{\mathrm{StK}} && (5.13)
\end{aligned}$$

α and γ are the fixed rates of change for hip and knee joints, respectively. To limit the range of activity on the knee, due to its limited range of action, two joint repellers are included. Parameters g_{lim} and σ define the strength and width of these repellers, respectively. The values of $\Theta_{\mathrm{k,max}}$ and $\Theta_{\mathrm{k,min}}$ are the maximum and minimum knee joint limits, respectively. They are used to prevent knee joint overextension. Three direct actions, ζ, directly influence the desired joint positions: ζ_{StH} entrains directly the hip joint velocity; ζ_{StK} and ζ_{VR} entrain directly the knee joint velocity, as given by eqs 5.6, 5.7 and 5.8.

5.1.6 Network Behavior

Based on the description of the biological rules and the six sensory events, the following behaviors are encoded in the reflex network as excitatory and inhibitory connections and direct actions on the robot joints (*i* stands for one limb). Note the relationships between the network behaviors presented below and the biological rules of section 4.5.6.

- Hip reaching AEP elicits the touchdown action on the knee, exciting the touchdown neuron, extending the knee: $\Upsilon_{+,\mathrm{touchdown},i} \supset \{(\mu_{\mathrm{AEP},i})\}$ and $w_{\mathrm{AEP,touchdown},i} = 1$ - rule a);

- Hip reaching AEP inhibits the continuation of hip protraction: $\Upsilon_{-,\mathrm{swing},i} \supset \{(\mu_{\mathrm{AEP},i})\}$ and $w_{\mathrm{AEP,swing},i} = 1$ - rule a);

- Load in the limb is low enough and hip reaching PEP elicits liftoff, making the knee flex: $\Upsilon_{+,\mathrm{liftoff},i} \supset \left\{(\mu_{\mathrm{Load},i} \cap \mu_{\mathrm{PEP},i})\right\}$ and $w_{\mathrm{PEP,liftoff},i} = 1$, $w_{\mathrm{Load,liftoff},i} = 1$ - rule c) and a), respectively;

- Ground contact elicits and reinforces the stance, propelling the robot forward: $\Upsilon_{+,\text{stance},i} \supset \{(\mu_{\text{GC},i})\}$ and $w_{\text{GC},\text{stance},i} = 1$ - rule b);
- Lack of ground contact excites the swing neuron: $\Upsilon_{+,\text{swing},i} \supset \{(1-\mu_{\text{GC},i})\}$ and $w_{\text{GC},\text{swing},i} = 1$ - rule c);
- Dorsum paw contact promotes an enhanced leg flexion to overcome the obstacle, by triggering the stumbling reflex, leading the hip and knee joints to a specific position - rule e);
- The variations of the body pitch angle are compensated by the vestibulospinal reflex, leading the knee joint to a specific position, dependent on the pitch angle, increasing the robot's stability - rule d).

This simple reflex network for a single limb, depicted in figure 5.3 is enough to produce stepping motions in a single limb.

5.1.7 Ipsilateral and Contralateral Coordination

Ipsilateral limb coordination is necessary to prevent the execution of the swing motor actions in ipsilateral limbs, as in a pace gait, and impose some phase relationship in ipsilateral limbs to achieve walk or trot gaits. Ipsilateral coordination (blue dashed connection in fig. 5.4) can be achieved by applying an inhibitory connection when a strict alternation of ipsilateral limbs is desired: Lack of ground contact in the ipsilateral limb (*o*), inhibits the initiation of the liftoff (in limb *i*): $\Upsilon_{-,\text{liftoff},i} \supset \{(1-\mu_{\text{GC},o})\}$ and $w_{\text{GC},\text{liftoff},o} = 1$.

Although independent limb reflex networks produce alternated stepping in a girdle, the addition of an inhibitory contralateral connection imposes strict alternation of step phases, preventing the execution of simultaneous swing motor actions on contralateral limbs. This connection has a relationship with the biological rule (f) of section 4.5.6.

The inhibitory contralateral connection (blue dashed connection in fig. 5.5) comes from the contralateral ground contact sensory interneuron, μ_{GC}, to the liftoff motor action in the knee: Lack of ground contact in the contralateral limb (*j*), inhibits the initiation of the liftoff (in limb *i*): $\Upsilon_{-,\text{liftoff},i} \supset \left\{(1-\mu_{\text{GC},j})\right\}$ and $w_{\text{GC},\text{liftoff},j} = 1$.

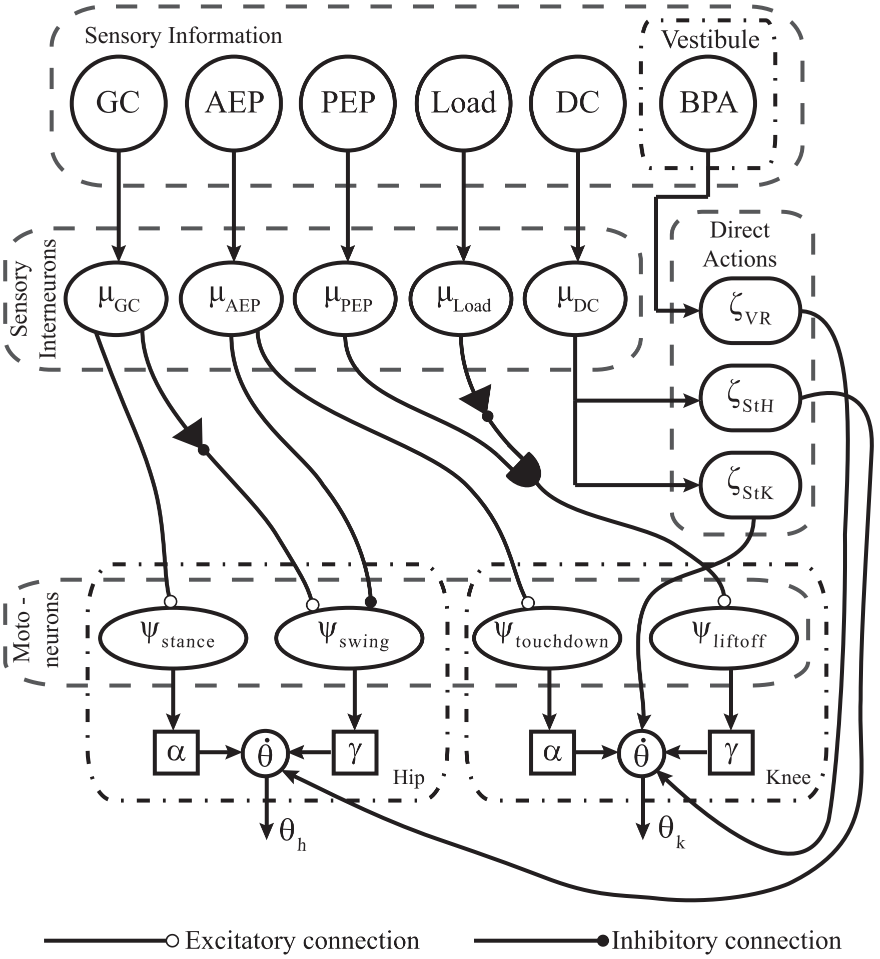
Sensory Information
Vestibule
GC
AEP
PEP
Load
DC
BPA
Sensory Interneurons
μ_{GC}
μ_{AEP}
μ_{PEP}
μ_{Load}
μ_{DC}
Direct Actions
ζ_{VR}
ζ_{StH}
ζ_{StK}
Moto - neurons
ψ_{stance}
ψ_{swing}
$\psi_{touchdown}$
$\psi_{liftoff}$
α
$\dot{\theta}$
γ
Hip
Knee
θ_h
θ_k
Excitatory connection
Inhibitory connection

Figure 5.3: Proposed Controller for a single robot's limb.

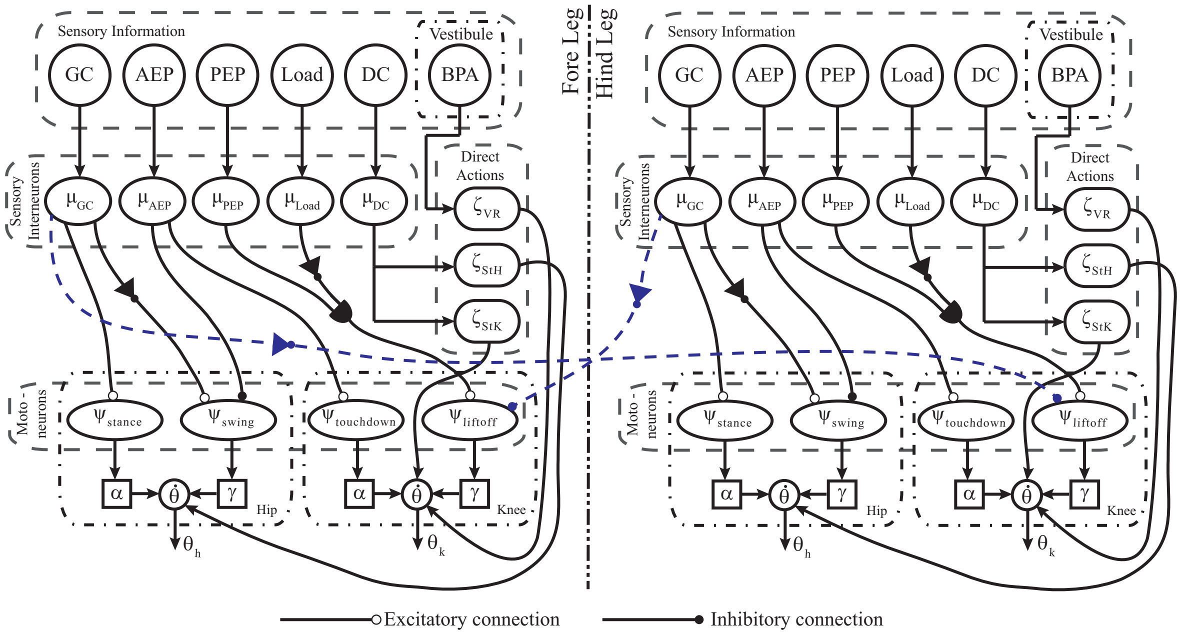
Sensory Information
Vestibule
GC
AEP
PEP
Load
DC
BPA
Sensory Interneurons
μ_{GC}
μ_{AEP}
μ_{PEP}
μ_{Load}
μ_{DC}
Direct Actions
ζ_{VR}
ζ_{StH}
ζ_{StK}
Moto - neurons
ψ_{stance}
ψ_{swing}
$\psi_{touchdown}$
$\psi_{liftoff}$
α
$\dot{\theta}$
γ
Hip
Knee
θ_h
θ_k
Fore Leg
Hind Leg
Excitatory connection
Inhibitory connection

Figure 5.4: Proposed Controller for ipsilateral limb coordination.

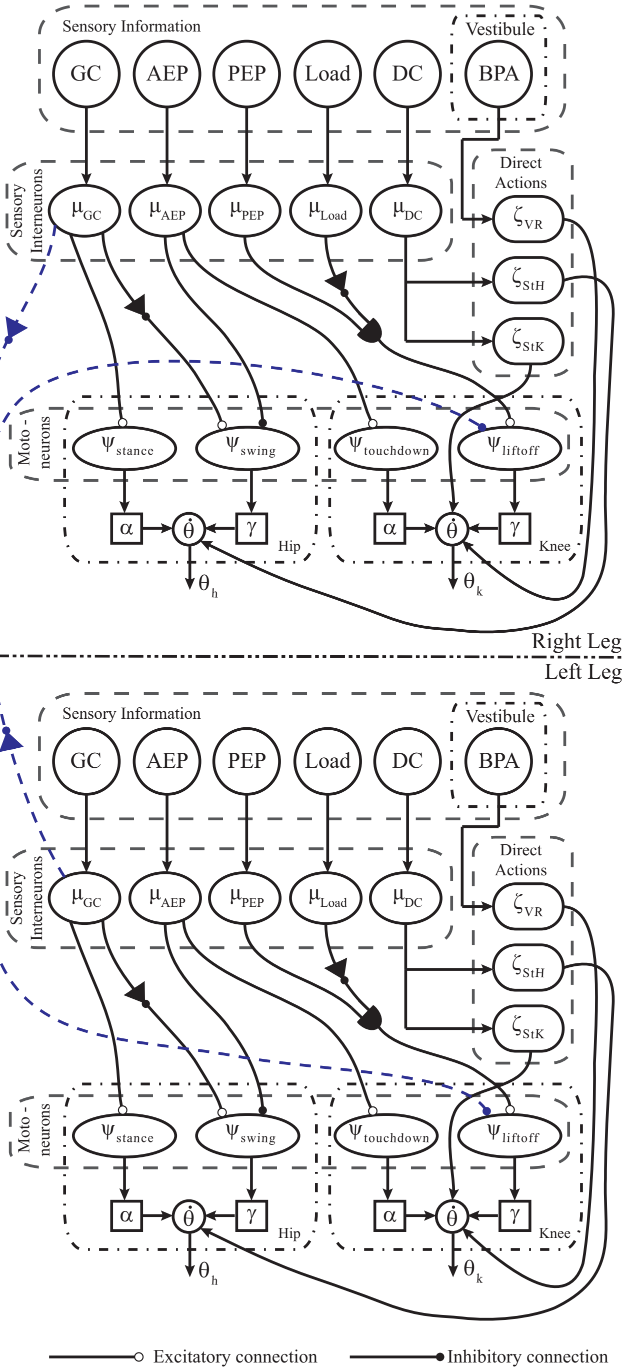
Sensory Information
GC
AEP
PEP
Load
DC
Vestibule
BPA
Sensory Interneurons
μ_{GC}
μ_{AEP}
μ_{PEP}
μ_{Load}
μ_{DC}
Direct Actions
ζ_{VR}
ζ_{StH}
ζ_{StK}
Moto - neurons
ψ_{stance}
ψ_{swing}
$\psi_{touchdown}$
$\psi_{liftoff}$
α
$\dot{\theta}$
γ
Hip
Knee
θ_h
θ_k
Right Leg
Left Leg
Sensory Information
GC
AEP
PEP
Load
DC
Vestibule
BPA
Sensory Interneurons
μ_{GC}
μ_{AEP}
μ_{PEP}
μ_{Load}
μ_{DC}
Direct Actions
ζ_{VR}
ζ_{StH}
ζ_{StK}
Moto - neurons
ψ_{stance}
ψ_{swing}
$\psi_{touchdown}$
$\psi_{liftoff}$
α
$\dot{\theta}$
γ
Hip
Knee
θ_h
θ_k
Excitatory connection
Inhibitory connection

Figure 5.5: Proposed controller for contralateral limb coordination.

5.2 Hybrid Controller

The hybrid controller, depicted in figure 5.6, refers to a bio-inspired quadrupedal walking model, which can be divided into two components: the feedback (reflex) and the feedforward (CPG) components.

The feedback component, previously described in section 5.1, uses feedback rules connecting multimodal sensory information to a set of sensory interneurons (μ) and motoneurons (Ψ_{RC}). Sensory information is also connected to a set of direct actions (ζ), which, in turn, can act directly in the specifications of the joints' velocities.

The feedforward component, entrained by sensory information, uses CPGs to predict the state of the limb and thus reproduce any motoneuron's signal (Ψ_{CPG}) generated by a stable walking gait of this hybrid controller. CPGs' prediction of motoneurons activity (Ψ_{CPG}) and the motoneurons' neuronal activity (Ψ_{RC}) are linearly combined to produce the effective motoneuron' activity ($\overline{\Psi}$), thus controlling the relative importance of motoneurons vs. CPGs.

The interaction of the internal model provided by the CPG and a feedback control that uses the predicted state provides for the emergence of a CPG behavior.

The original aim of this controller is to improve the Oncilla's walking behavior achieved with the reflex network by making the locomotion more resilient to external perturbations and more robust to noise and delays and, thus, with an improved performance in the overall.

Following an idea from Kuo (2002), the CPG component acts as a regulator or supervisor of the locomotor reflex network's motor actions. The CPG acting as a feedforward component presents a rhythmic internal model which drives the reflex controller, predicting sensorimotor processes. Thereby, the hybrid controller has an entity that supervises the feedback component, trying to correct the shortcomings of the purely sensory driven controller. Also, the CPG is entrained by load sensory information to synchronize with the robot's step cycle according to a feedback mechanism (Owaki et al., 2012).

This CPG prediction of the state of the limb is used to build an internal mapping of the four motor actions that constitute a step cycle (stance, swing, touchdown and liftoff), and, therefore, it should be capable of reproducing the motoneurons activity generated by a stable walking gait of the reflex network. This mapping relates the CPG-phase to the

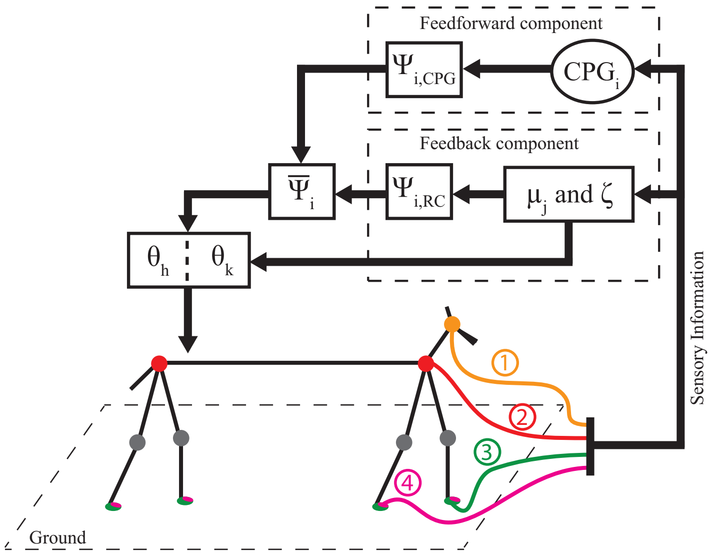

Figure 5.6: Bio-inspired quadrupedal walking model. The numbers from 1 to 4 represent sensory information provided by four types of sensors. 1 represents the signal of the vestibule; 2 represents the hip joint positions of the four limbs; 3 and 4 represent the touch sensors signals of the foot-pad and dorsum-paw of the four limbs, respectively. μ_{j} (j = GC, AEP, PEP, DC, Load) represents the sensory interneurons that translate the sensory events based on the limb's sensory information. ζ represents the direct actions that act directly in the specification of the joints' velocities. $\Psi_{\mathrm{i,RC}}$ (i = stance, swing, touchdown, liftoff) are the motoneurons of the reflex controller (RC). $\mathrm{CPG_i}$ (i = Fore Left, Fore Right, Hind Left, Hind Right) are the four CPGs of the model, one for each leg. $\Psi_{\mathrm{i,CPG}}$ (i = stance, swing, touchdown, liftoff) are the predicted motoneurons of the CPGs. The combination of both motoneurons determines the activation of the four motor actions of a step cycle, generating the joint movements for the hip or knee, $\theta_{\mathrm{h}}, \theta_{\mathrm{k}}$, which interact with the environment, thus closing the loop.

motoneuron activity and, thus, the corresponding motor action the robot should be in.

The motor actions executed by the Oncilla robot result of a direct combination of the feedforward and feedback components, using a proportional term to control the relative importance of the CPG vs. the feedback it predicts. Thus, the motoneurons activity is now obtained by a direct combination of feedforward and feedback components, using a proportional term to control the relative importance of the two group of signals. The predicted motor actions from the CPG (Ψ_{CPG}) are compared with the motoneurons of the reflex component (Ψ_{RC}), correcting erratic motor actions that can be generated by the purely sensory-driven controller. The final motoneurons activity is calculated as follows:

$$\overline{\Psi}_{\mathrm{j}} = \varphi \Psi_{\mathrm{j,RC}} + (1-\varphi)\,\Psi_{\mathrm{j,CPG}} = \Psi_{\mathrm{j,CPG}} + \varphi\left(\Psi_{\mathrm{j,RC}} - \Psi_{\mathrm{j,CPG}}\right) \tag{5.14}$$

where j represents the step phase (stance, swing, touchdown, liftoff); $\overline{\Psi}_{\mathrm{j}}$, $\Psi_{\mathrm{j,CPG}}$ and $\Psi_{\mathrm{j,RC}}$

are the final motoneuron activity, predicted motoneuron activity and motoneuron activity from the reflex component, respectively; $\varphi \in [0,1]$ controls the relative importance of the motoneurons vs. their CPG prediction. If $\varphi = 0$, then the motoneuron activity is solely feedforward-driven, whereas if $\varphi = 1$, then the motoneuron activity is exclusively sensory-driven.

Note that $\Psi_{\mathrm{j,CPG}}$ provide for a model of the corresponding $\Psi_{\mathrm{j,RC}}$ motoneurons, which are a simple linear combination of the underlying feedback pathways. The final right term emphasizes the role of the predictive term plus a corrective error given by the difference between the pure feedback term and the predicted one.

The final motoneurons activity ($\overline{\Psi}$) is used similarly to the reflex controller 5.1.5 to achieve the effective joints' velocities.

In overall, this controller can be divided into three biological relevant stages: feedforward (CPG) component, feedback (reflex) component and final motoneuron activity ($\overline{\Psi}$). The ipsilateral and contralateral coordination is implemented similarly to the reflex controller presented in section 5.1. The sensory inputs are also similar, except for the touch sensors of each foot-pad that also provide information about the Ground Reaction Force (GRF), which will be used in the CPG component. Hereinafter, each stage of the model is described in detail, except for the feedback (reflex) component, which has already been detailed in section 5.1.

5.2.1 CPG model

The biological CPG model is implemented through a phase oscillator. This oscillator provides for a phase signal $\phi \in [0,2\pi]$ (rad). It is considered that a stride corresponds to a cycle. However, this phase signal has to be synchronized with the environment in order to ensure that CPGs stay synchronized with the cycle gait. Thus, it is required to couple the CPG with the environment. Herein, it is employed a strategy similar to the one used by Owaki et al. (2012) and Andre et al. (2014). For each limb is assigned a phase oscillator as follows:

$$\dot{\phi} = \omega + f \tag{5.15}$$

where $\phi \in [0,2\pi]$ (rad) is the CPG phase of each limb, ω is the intrinsic angular velocity of the oscillator and f is the local sensory feedback mechanism. The local sensory feedback

(f) is given by the force sensor in each foot:

$$f = -\sigma \mathrm{GRF} \cos(\phi) \tag{5.16}$$

where σ is the magnitude of the feedback to the oscillator and GRF is the value read by the foot sensor acting on the corresponding limb.

The phase oscillator generates a periodic time varying signal, which is parameterized according to the step cycle period of the reflex network. The feedback mechanism (f) that entrains the CPG plays an important role in the coupling of the CPG with the gait phases, ensuring that the CPG stays synchronized with the step cycle and, thus, with the reflex network. If the period of the reflex network step cycle is not constant, then the feedback mechanism entrains the oscillator phase (ϕ), accelerating or decelerating the evolution of the CPG phase (ϕ). The limb oscillator should accelerate when the limb is not supporting load ($\mathrm{GRF} = 0$), introducing a phase advance in the oscillator; and should decelerate when the limb is supporting load ($\mathrm{GRF} > 0$), introducing a phase delay in the oscillator. If there is a GRF value, this means that the limb is still supporting load and, therefore, the phase should be delayed to maintain the robot's stability, waiting for the opposite leg to touch the ground before the swing phase initiation. Further, note that the mechanism provides for a quantitative feedback in the sense that phase adjustment depends on the value of the GRF signal. This results in an attempt of the system to synchronize with the feedback load signal and, thus providing for a synchronization between the CPGs and the gait cycle they are estimating and will act. Thereby, this coupling scheme attempts to couple the CPG phase with the feedback component's step cycle, making a correct prediction of the expectable limb's motor actions.

The phase oscillator has to be correctly tuned. The CPG can present an oscillatory or excitatory behavior (Owaki et al., 2012), depending on the value of the index $\frac{\omega}{\sigma \mathrm{GRF}}$. When $\frac{w}{\sigma \mathrm{GRF}} > 1$, the CPG presents an oscillatory behavior, and the solution evolves as a periodic time signal. When $\frac{w}{\sigma \mathrm{GRF}} < 1$, the CPG presents an excitatory behavior, converging to a stable equilibrium point. Besides, the oscillator should have a frequency ω initially set to an estimate of the reflex's walking gait. In the future, this estimate could be automated.

Figure 5.7 shows a simulation of the CPG phase evolution over time, with $\omega = 2\pi$ rad/s (a period of 1 s) and $\sigma = 0.4$. The simulation shows three different situations:

(1) when $\mathrm{GRF} = 0$, $t = 0...2.5$ s, the CPG has no active feedback mechanism. The phase

evolves normally from 0 to 2π rad;

(2) when GRF $= 20$, $t = 2.5...5$ s, the condition $\frac{w}{\sigma \mathrm{GRF}}$ is lower than one and, therefore, the CPG presents an excitatory behavior and its solution converges to a stable equilibrium point;

(3) when GRF $= 10$, $t = 5...8.5$ s, the condition $\frac{w}{\sigma \mathrm{GRF}}$ is higher than one and, therefore, the CPG presents an oscillatory behavior which solution is affected by the GRF value. The feedback mechanism causes a delay in the CPG phase, since the wave period increased, in comparison to situation (1).

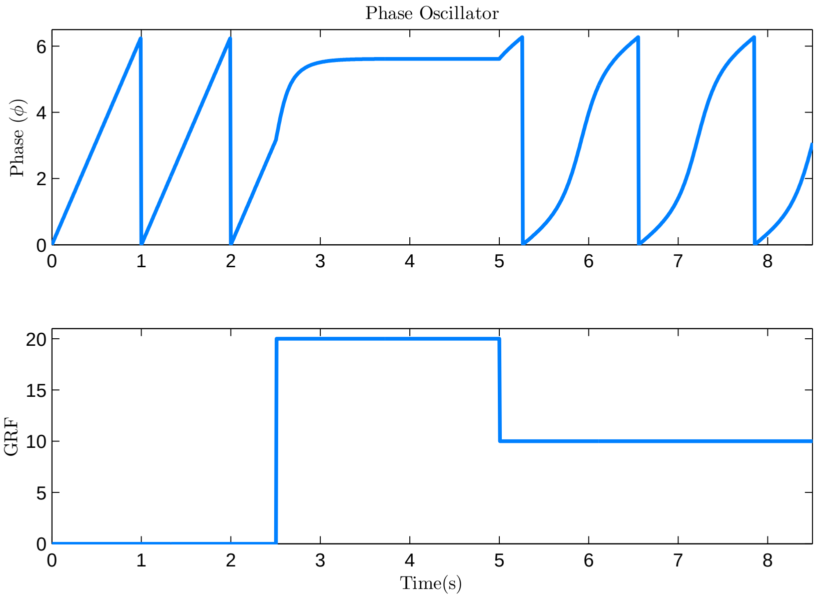

Figure 5.7: Three situations for the oscillator given by eq. 5.15 according to index $\frac{\omega}{\sigma \mathrm{GRF}}$. Top: Phase ($\phi$) of the CPG. Bottom: GRF value.

5.2.2 Motoneurons predictor

The motoneurons predictor (Ψ_{CPG}) implements an internal model of the expected motoneurons' outputs generated by reflex circuits. This mapping is built based on the hypothesis that CPGs can be viewed as motoneuron output predictors. Thus, the four motor actions that define the step cycle are mapped to one period of the phase oscillator, *i.e*, the different values of the CPG phase are related to the gait phases on which each motor action should be activated. Thereby, the CPG's activity should be capable of reproducing the motoneurons' activity generated by a stable walking gait of the reflex network. This is defined as follows:

$$\forall \ \ 0 < \phi < 2\pi \ \ \exists \ \ \Psi_{\mathrm{j,CPG}} = \Psi_{\mathrm{j,RC}} \tag{5.17}$$

where j represents the motor action stance, swing, touchdown and liftoff; $\Psi_{\mathrm{j,CPG}}$ and $\Psi_{\mathrm{j,RC}}$ are the CPG predicted motoneuron' activity and motoneuron' activity from the reflex component, respectively.

5.2.3 Network Behavior

Based on the description of the feedforward signals from the CPG and the feedback signals from the reflex circuits, the following behaviors are encoded in the hybrid network as a combination of the predicted motoneurons with the excitatory and inhibitory connections of the reflex network and direct actions on the robot joints (i stands for one limb).

- The predicted touchdown motoneuron ($\Psi_{\mathrm{touchdown,CPG}}$) combined with the touchdown neuron ($\Psi_{\mathrm{touchdown,RC}}$) elicited by hip reaching AEP, extends the knee: $\Psi_{\mathrm{touchdown,CPG,i}} \cap (\Upsilon_{+,\mathrm{touchdown},i} \supset \{(\mu_{\mathrm{AEP},i})\})$ and $w_{\mathrm{AEP,touchdown},i} = 1$;
- The predicted swing motoneuron ($\Psi_{\mathrm{swing,CPG}}$) combined with the hip reaching AEP, stops the continuation of hip protraction: $\Psi_{\mathrm{swing,CPG,i}} \cap (\Upsilon_{-,\mathrm{swing},i} \supset \{(\mu_{\mathrm{AEP},i})\})$ and $w_{\mathrm{AEP,swing},i} = 1$;
- The predicted liftoff motoneuron ($\Psi_{\mathrm{liftoff,CPG}}$) combined with the liftoff neuron ($\Psi_{\mathrm{liftoff,RC}}$) elicited by lack of load in the limb and the hip reaching PEP, makes the knee flex: $\Psi_{\mathrm{liftoff,CPG,i}} \cap (\Upsilon_{+,\mathrm{liftoff},i} \supset \left\{(\mu_{\mathrm{Load},i} \cap \mu_{\mathrm{PEP},i})\right\})$ and $w_{\mathrm{PEP,liftoff},i} = 1$, $w_{\mathrm{Load,liftoff},i} = 1$;
- The predicted stance motoneuron ($\Psi_{\mathrm{stance,CPG}}$) combined with the stance neuron ($\Psi_{\mathrm{stance,RC}}$) elicited and reinforced by ground contact, propels the robot forward: $\Psi_{\mathrm{stance,CPG,i}} \cap (\Upsilon_{+,\mathrm{stance},i} \supset \{(\mu_{\mathrm{GC},i})\})$ and $w_{\mathrm{GC,stance},i} = 1$;
- The predicted swing motoneuron ($\Psi_{\mathrm{swing,CPG}}$) combined with the swing neuron ($\Psi_{\mathrm{swing,RC}}$) excited by lack of ground contact, transfers the leg to the front : $\Psi_{\mathrm{swing,CPG,i}} \cap (\Upsilon_{+,\mathrm{swing},i} \supset \{(1 - \mu_{\mathrm{GC},i})\})$ and $w_{\mathrm{GC,swing},i} = 1$;
- Dorsum paw contact promotes an enhanced leg flexion to overcome the obstacle, by triggering the stumbling reflex, leading the hip and knee joints to a specific position;

- The variations of the body pitch angle are compensated by the vestibulospinal reflex, leading the knee joint to a specific position, dependent on the pitch angle, increasing the robot's stability.

This simple hybrid network depicted in figure 5.8 is enough to produce stepping motions in a single limb, which joins the advantages of both pure feedforward and feedback approaches when both unexpected disturbances and imperfect sensory information are presented. The system is expected to be more resilient to perturbations, exploring the performance advantages of the pure feedback controller. The system is also expected to be more robust to noise in face of imperfect sensory information, exploring the performance advantages of the pure feedforward system. In the overall, we have an internal model acting as a CPG, which is capable of generating rhythmic behavior in the form of locomotion. This model is then tuned with sensory feedback through the reflex controller that uses the predicted state.

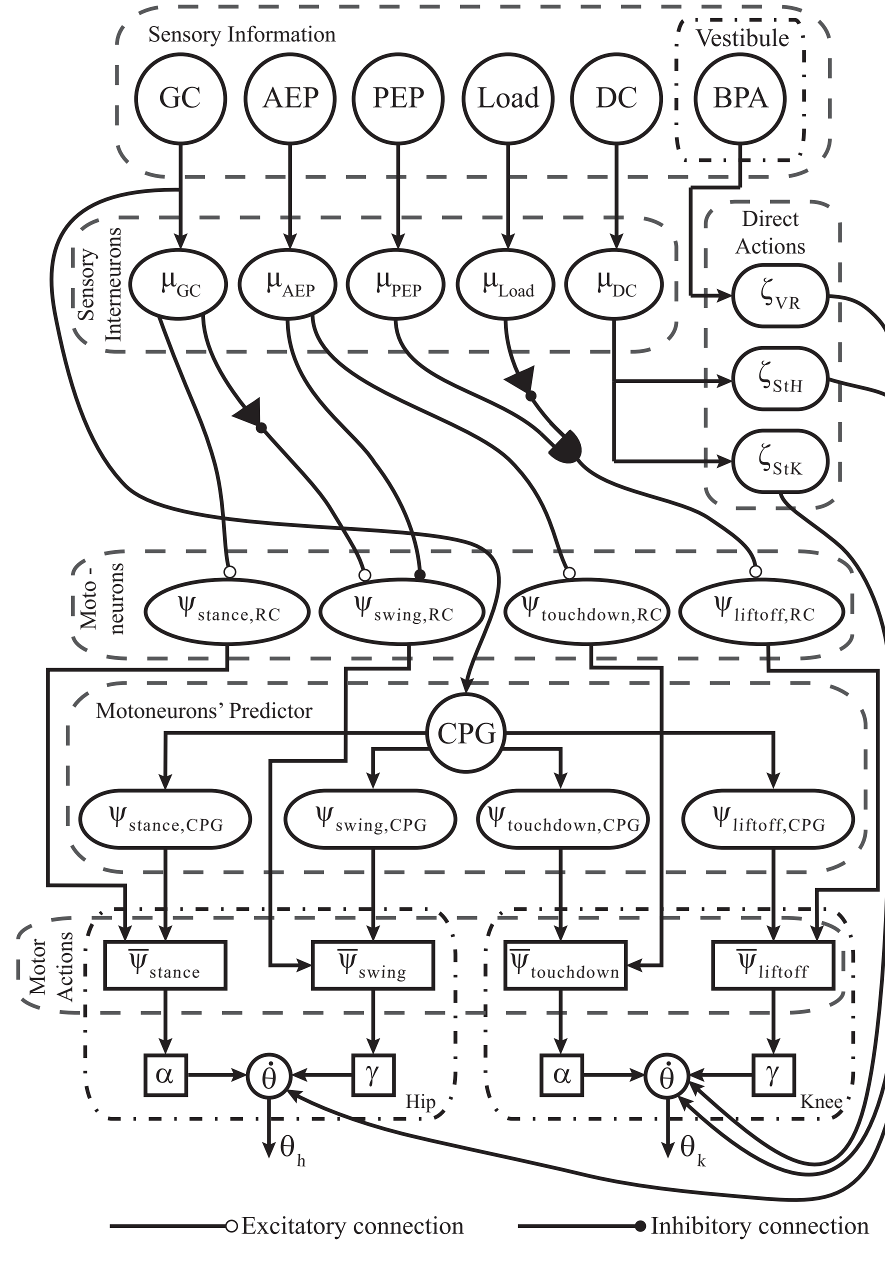
Sensory Information
Vestibule
GC
AEP
PEP
Load
DC
BPA
Sensory Interneurons
μGC
μAEP
μPEP
μLoad
μDC
Direct Actions
ζVR
ζStH
ζStK
Moto - neurons
Ψstance,RC
Ψswing,RC
Ψtouchdown,RC
Ψliftoff,RC
Motoneurons' Predictor
CPG
Ψstance,CPG
Ψswing,CPG
Ψtouchdown,CPG
Ψliftoff,CPG
Motor Actions
Ψ̄stance
Ψ̄swing
Ψ̄touchdown
Ψ̄liftoff
α
θ̇
γ
Hip
α
θ̇
γ
Knee
θh
θk
Excitatory connection
Inhibitory connection

Figure 5.8: Proposed hybrid controller for a single robot's limb.

Chapter 6

Gait analysis

The bio-inspired architectures presented in the previous chapter are capable of producing stable and robust locomotion in the Oncilla robot. In order to evaluate the gait performance of this robot, we implement a function that comprises three components, based on a previous team work (Teixeira et al., 2014). Thereby, we evaluate the robot's frontal displacement (*disp*), the gait's harmony (*harm*) and the robot's stability (*stab*). The reward function results from the combination of the three components, allowing a correct assessment of the resultant locomotion.

Hereinafter, we describe how each component is obtained.

6.1 Displacement

The frontal displacement of the robot achieved in a fixed interval is evaluated using the equation 6.1. This equation penalizes the excessive traveled distance, the lateral displacement and the low frontal displacement. Thereby, we find out which are the experiments that have the largest frontal displacement.

$$disp = \frac{|\Delta z|^2 \Delta z}{\Delta s ||\Delta r|| T_{\text{exp}} V_{\text{max}}} \tag{6.1}$$

where Δz, $||\Delta r||$ and Δs are the frontal displacement, total displacement and traveled distance, respectively. The *disp* equation is normalized by dividing it by the experiment time (T_{exp}) and by the robot's maximum velocity (V_{max}), both previously defined.

6.2 Stability

We installed an accelerometer and a gyroscope in the simulated Oncilla robot. These sensors provide information related with accelerations (Acc) and angular velocities (Ang) in all three axes. The DC component is removed from both signals during the experiment.

According to Iosa et al. (2011, 2012), higher decelerations (Acc_{min}) and rotational oscillations (Ang_{PP}) decrease the locomotion's stability. The values of Acc's minimum peak (Acc_{min}) and Ang's peak-to-peak (Ang_{PP}) characterize the locomotion's stability and should be low. Thereby, these stability metrics are calculated as follows:

$$Acc_{\text{min}} = |\min(Acc)| \tag{6.2}$$

$$Ang_{\text{PP}} = \max(Ang) - \min(Ang) \tag{6.3}$$

To calculate the stability component, two intermediate values have to be computed using Acc_{min} and Ang_{PP}:

$$a_{\text{min}} = \max(Acc_{\text{min}}) \tag{6.4}$$

$$PP_{\text{min}} = \max(Ang_{\text{PP}}) \tag{6.5}$$

The stability is evaluated during the time of the experiment. This time is divided into several cycles or periods (N_{periods}) and, therefore, the equations depicted previously are computed independently for each cycle, *i.e.*, metrics are calculated taking into account the sensory information of each period: $A_{\text{min}} \subset \{a_{\text{min},1}; a_{\text{min},2}; ...; a_{\text{min},\text{N}_{\text{periods}}}\}$ and $PP \subset \{PP_{\text{min},1}; PP_{\text{min},2}; ...; PP_{\text{min},\text{N}_{\text{periods}}}\}$.

Thus, at the end of the experiment, the final metrics to calculate the robot's stability were selected as the worst ones calculated in the several cycles of the experiment, *i.e.*, the maximum of the stability metrics:

$$A_{\text{min}_{\text{final}}} = \max(A_{\text{min}}) \tag{6.6}$$

$$PP_{\text{final}} = \max(PP) \tag{6.7}$$

The robot's stability is calculated using the final metrics ($A_{\text{min}_{\text{final}}}$ and PP_{final}), as follows:

$$stab = \frac{\exp^{-0.1A_{\text{min}_{\text{final}}}} + \exp^{-0.1PP_{\text{final}}}}{2} \tag{6.8}$$

6.3 Harmony

The gait's harmony is dependent on the stability metrics (Acc_{min} and Ang_{PP}). Thereby, the Ratio Indexes of both Acc_{min} and Ang_{PP} can be calculated as follows:

$$RI_{a_{\text{min}}} = \frac{\min(Acc_{\text{min}})}{\max(Acc_{\text{min}})} \tag{6.9}$$

$$RI_{PP_{\text{min}}} = \frac{\min(Ang_{\text{PP}})}{\max(Ang_{\text{PP}})} \tag{6.10}$$

As in the stability case, the values of $RI_{a_{\text{min}}}$ and $RI_{PP_{\text{min}}}$ are computed independently for each cycle, *i.e.*, metrics are calculated taking into account the sensory information of each period: $RI_{\text{A}} \subset \{RI_{a_{\text{min},1}}; RI_{a_{\text{min},2}}; \ldots; RI_{a_{\text{min},\text{N}_{\text{periods}}}}\}$ and $RI_{\text{PP}} \subset \{RI_{PP_{\text{min},1}}; RI_{PP_{\text{min},2}}; \ldots; RI_{PP_{\text{min},\text{N}_{\text{periods}}}}\}$.

At the end of the experiment, the final metrics to calculate the robot's harmony were selected as the worst ones calculated in the several cycles of the experiment, *i.e.*, the minimum of the harmony metrics:

$$RI_{A_{\text{final}}} = \min(RI_{\text{A}}) \tag{6.11}$$

$$RI_{PP_{\text{final}}} = \min(RI_{\text{PP}}) \tag{6.12}$$

The robot's harmony is calculated using the final metrics ($RI_{A_{\text{final}}}$ and $RI_{PP_{\text{final}}}$), as follows:

$$harm = \frac{RI_{A_{\text{final}}} + RI_{PP_{\text{final}}}}{2} \tag{6.13}$$

6.4 Reward

The reward value is computed as a weighted-sum of the three components previously described ($disp$, $stab$ and $harm$):

$$reward = w_{\text{disp}} disp + w_{\text{stab}} stab + w_{\text{harm}} harm \tag{6.14}$$

where w_{disp}, w_{stab} and w_{harm} control the relative importance of each component. For an appropriate normalization, the condition $w_{\text{disp}} + w_{\text{stab}} + w_{\text{harm}} = 1$ must be respected.

Chapter 7

Simulation results

This chapter describes the more relevant Webots (Michel, 2004) simulations made on the compliant quadruped robot Oncilla, presented in figure 7.1. The Oncilla is a small quadruped robot, with pantograph, three-segment leg design, providing passive compliant behavior to the cable driven retractable knees. It has 12 degrees-of-freedom, three on each leg: hip-swing, hip-flap and knee. The robot has compliant knees and the hip joints are position controlled.

The simulation results are divided into two major groups: the experiments related with the reflex controller, and related with the hybrid controller, *i.e.*, CPG and reflex based controller. Pertaining videos of all the experiments are available at http://asbg.dei.uminho.pt/node/402.

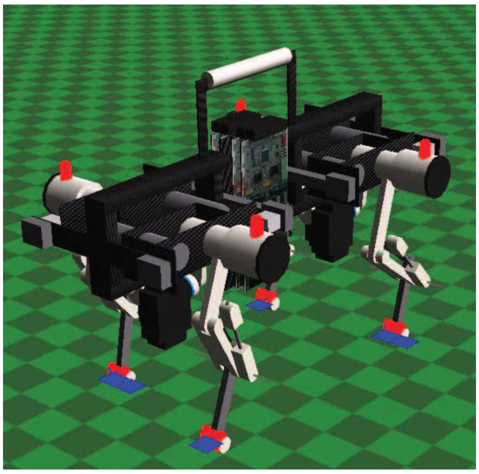

Figure 7.1: Simulated Oncilla quadruped robot.

7.1 Reflex controller experiments

Two experimental scenarios were considered: a flat terrain and a ramp. The robot is expected to locomote in these two scenarios.

The first setup is intended to accomplish the full quadruped walking on straight, flat terrain. We start by comparing our earlier work (Ferreira et al., 2014a) with the reflex network proposed in this thesis (figure 5.3), in which the limb loading information plays an important role. Specifically, in our earlier work, when no load information is included (Ferreira et al., 2014a), all the load components are removed from the network, *i.e.*, the load's sensory information and the sensory interneuron of load (μ_{load}) are removed from the reflex network presented in this thesis (figure 5.3). We verify the proposed network robustness by adding noise to the sensors and actuators, and adding delays to create a more biologically relevant model. It is also expected that the robot is capable of walking on irregular terrains, therefore we have included the stumbling reflex. These experiments evaluate the performance of this reflex in dealing with small obstacles, by verifying if the robot is able to overcome them.

The second setup is intended to verify the ability of the robot to deal with other perturbations, namely to climb up and down a ramp with a maximum inclination of 10%. In this experiments, we analyze the vestibulospinal reflex importance, namely if it is capable of improving the robot's locomotion when climbing up and down a ramp, comparing results with an experiment in which the vestibulospinal reflex is turned-off. The role of this reflex is to flex or extend the knees of the legs, trying to keep the posture of the body flat, preventing the center of gravity from being pulled backward (climbing up a ramp) or forward (going down a ramp). System robustness in climbing up and down is also evaluated by adding noise to the system.

As far as startup conditions are concerned, the joint positions are established such that the contralateral limbs are at the AEP and PEP positions, and initial neuron activities are set to the respective step phase. Table 7.1 shows the set of parameters used for these experiments, setting the sensory thresholds necessary for the sensory interneurons, the attractors to a specific hip and knee joint positions and the joint output parameters. The reflex network is parameterized empirically based on the authors know-how and on other works (Wadden and Ekeberg, 1998; Maufroy et al., 2008; Ekeberg and Pearson, 2005).

Table 7.1: Sensory thresholds, attractors values and joint output parameters.

Parameters	Limbs	
	Fore	Hind
Θ_{AEP}	8	10
Θ_{PEP}	5	5
$F_{\text{threshold}}$	1	1
$F_{\text{threshold}_{\text{DC}}}$	10	10
$F_{\text{threshold}_{\text{Load}}}$	8	8
Θ_{StH}	-7	-10
Θ_{StK}	42	40
α_h	45	45
γ_h	400	400
α_k	300	300
γ_k	500	500

Simulations show that the robot is able to move in a flat terrain and to go up and down a ramp, with a controller only based on the robot interactions with the environment.

7.1.1 Flat terrain experiments

In this simulation the robot uses both fore and hind girdles, thus accomplishing stepping motions of the legs while propelling the robot forward and maintaining its balance (fig. 7.2).

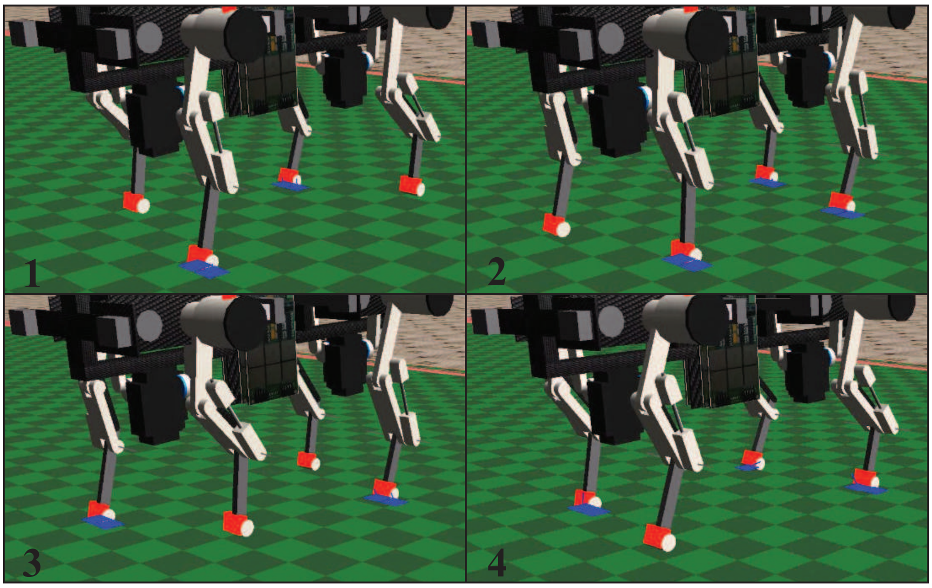

Figure 7.2: Quadruped walking simulation using the reflex network - in flat terrain.

For a better comparison between the different controllers and experiments in flat terrain, locomotion characteristics usually considered in gait analysis were calculated, namely the swing time (T_{sw}), the stance time (T_{st}), the duty factor (β) and the robot's velocity (v)). Additionally, are also calculated the chosen three indicators of gait performance (*disp*, *harm* and *stab*). In order to easily distinguish amongst the different experiments, these are identified as follows:

- Experiment A - actual reflex network;
- Experiment B - reflex network presented in previous work (Ferreira et al., 2014a) (without load information);
- Experiment C - reflex network presented in previous work (Ferreira et al., 2014a), with noise and delays;
- Experiment D - actual reflex network with noise;
- Experiment E - actual reflex network with delays;
- Experiment F - actual reflex network with noise and delays;

First, we will focus on how the sensory events trigger the sequence of reflexes which produce the motor actions. Figures 7.3 and 7.4 depict hind left limb's hip and knee joint movement, respectively; the motoneurons Ψ, as well as the sequence of activation of the sensory interneurons μ. Initially, the *stance* neuron is active ($\Psi_{\text{stance}} = 1$, dashed orange line in fig. 7.3) due to the existence of ground contact μ_{GC}, producing a constant propulsive motion in the hip. After the hip angle reaches the PEP value ($\mu_{\text{PEP}} = 1$, dashed orange line in fig. 7.4) and the limb load is low enough ($\mu_{\text{Load}} = 0$), the *lift-off* neuron is activated (Ψ_{liftoff}, solid blue line in fig. 7.4), producing a flexion motion of the knee, shortening the leg's length and lifting the foot from the ground. The lack of ground contact ($\mu_{\text{GC}} = 0$) activates the *swing* neuron Ψ_{swing} (solid blue line in fig. 7.3) which produces a flexion motion of the hip, transferring the leg to a rostral position. After reaching the AEP value ($\mu_{\text{AEP}} = 1$, solid blue line in figures 7.3 and 7.4), the *swing* neuron (Ψ_{swing}, solid blue line in fig. 7.3) is deactivated, halting the motion of the hip, and the touchdown neuron ($\Psi_{\text{touchdown}}$, dashed orange line in fig. 7.4) becomes active, producing the extension of the knee and the consequent foot placement. Just as the foot regains contact with the ground ($\mu_{GC} = 1$), the *stance* neuron becomes active ($\Psi_{\text{stance}} = 1$, dashed orange line in fig. 7.3) and produces the propulsive motion of stance. The sequence repeats onwards, producing the stereotyped motions of walking.

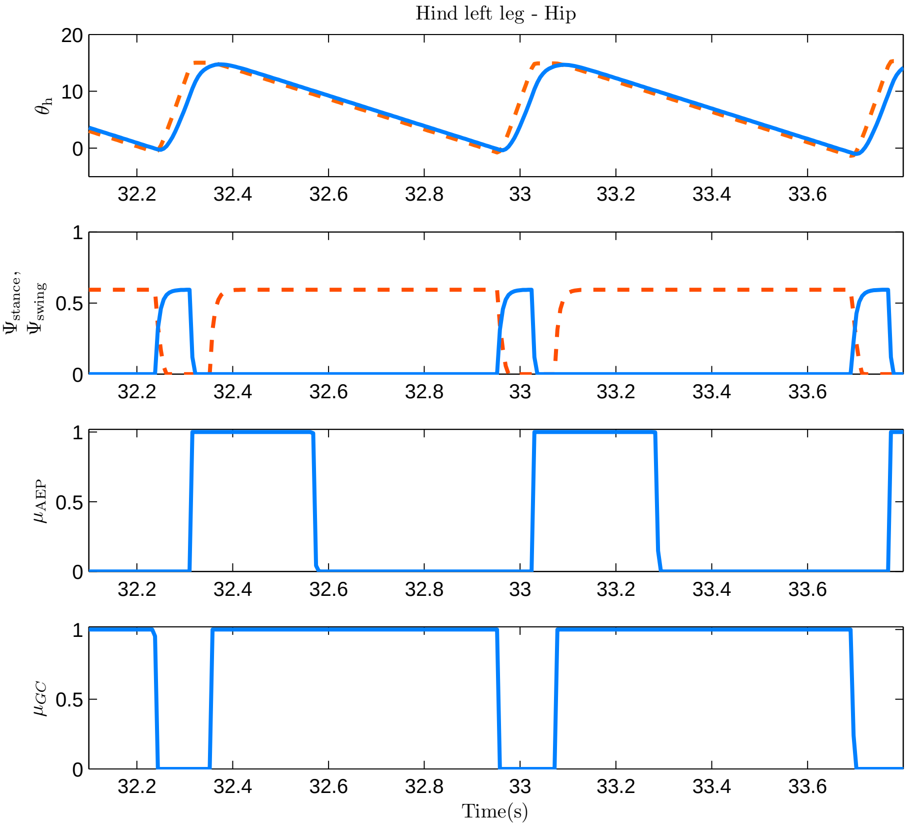

Figure 7.3: Hind left limb's hip joint movement (θ_h), swing and stance motoneurons (Ψ_{swing} and Ψ_{stance}) and sensory interneurons (μ_{AEP} and μ_{GC}). For the hip angle, the dashed orange line represents the reference hip value and the blue solid line the produced joint angle. For the motoneurons (Ψ_{swing} and Ψ_{stance}), the dashed orange line represents the stance motoneuron and the solid blue line the swing motoneuron.

Comparison between the actual reflex network and the reflex network without limb load information

Figure 7.5a presents the obtained stepping sequence for the actual neural network. Observing the figure 7.5a, we can note that the obtained robot's stepping sequence is quite regular, since the stance and swing time for each limb are almost the same during the experiment. This regularity was achieved by the inclusion of the limb load information. Fig. 7.5b presents the stepping sequence when this information was not considered in the network. Note that a much more irregular stepping is verified. Another important aspect to be noticed is that the introduction of the limb load information provided for almost the

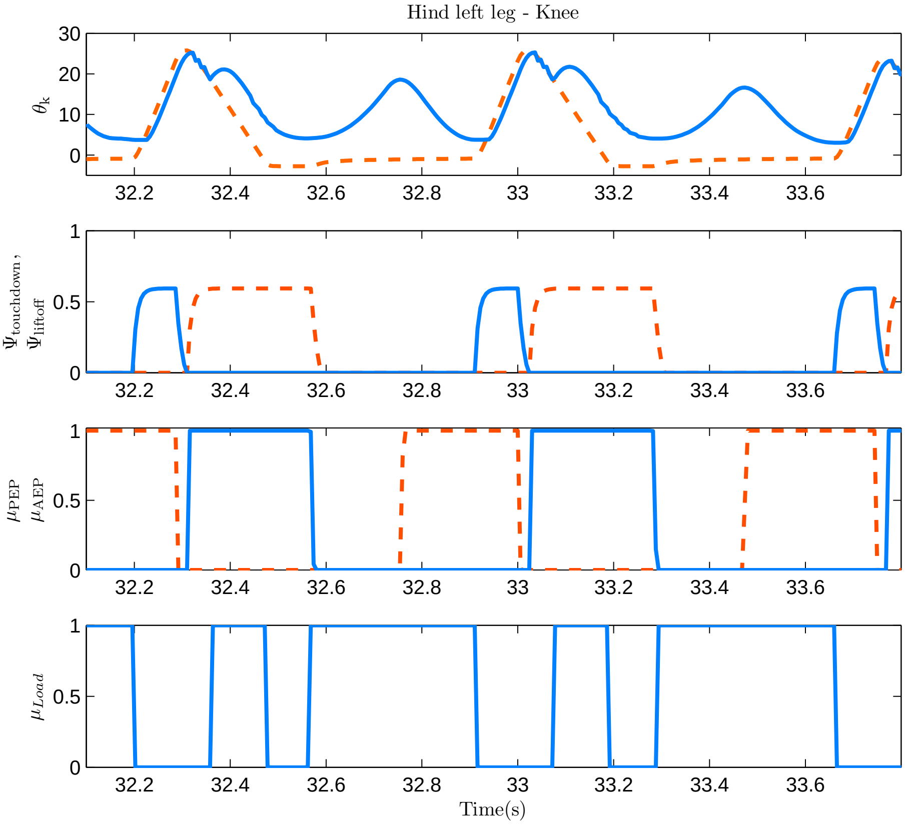

Figure 7.4: Hind left limb's knee joint movement (θ_k), touchdown and liftoff motoneurons ($\Psi_{touchdown}$ and $\Psi_{liftoff}$) and sensory interneurons (μ_{AEP}, μ_{PEP} and μ_{Load}). For the knee angle, the dashed orange line represents the reference knee value and the blue solid line the produced joint angle. For the motoneurons ($\Psi_{touchdown}$ and $\Psi_{liftoff}$), the dashed orange line represents the touchdown neuron and the solid blue line the liftoff neuron.

same duty factor among the girdles, both hind and fore girdles, though more similar in the hind limbs (see table 7.2), since the difference between the duty factors of the hind limbs is equal to 0.002 and between the fore limbs is equal to 0.019. Furthermore, there was an increase in the robot's velocity of 11.7%

The stepping sequence without limb load information (fig. 7.5b) also evidences an asymmetry along the sagittal plane, concerning the fore limbs. In the fore limbs, there is an asymmetry in duty factor, with one limb having a greater support duration, randomly alternating between the right and left fore limbs. In fig. 7.5b, from 5 to 10 seconds and from 15 to 20 seconds it is noticeable this asymmetric pattern (highlighted by red boxes in the figure). Table 7.2 supports the irregularity of the stepping sequence presented in fig. 7.5b. The parameters T_{sw} and T_{st} have higher standard deviations than in experiment A, showing that the stepping pattern of experiment B is more irregular. Furthermore, the velocity in experiment B decreases and the duty factors (β) deteriorate for higher differences (less regular), especially in the fore limbs, since the difference between the duty factors of the fore limbs is equal to 0.126. The gait analysis, in table 7.2, shows us that the reflex network with limb load information (experiment A) has a better frontal displacement, better gait harmony and higher stability, since the three components present higher values than the reflex network without limb load information (experiment B). This analysis allows us to conclude that the reflex network with limb load information has a better performance in terms of quadruped locomotion.

The obtained motor behavior can be said to resemble a trot. From the stepping sequence of figure 7.5a it is possible to ascertain that the robot performs a slow trot (or walking trot) gait (Hildebrand, 1965).

Table 7.2: Locomotion data from the experiments in flat terrain.

		Load				Without load	
Param	Limb	no Noise, no Delay (A)	Noise (D)	Delay (E)	Noise and Delay (F)	no Noise, no Delay (B)	Noise and Delay (C)
$T_{sw}(s)$	FL	0.115 ± 0.068	0.168 ± 0.101	0.285 ± 0.164	0.207 ± 0.145	0.240 ± 0.158	0.105 ± 0.075
	FR	0.128 ± 0.056	0.155 ± 0.099	0.288 ± 0.205	0.259 ± 0.177	0.340 ± 0.159	0.424 ± 0.389
	HL	0.117 ± 0.006	0.120 ± 0.055	0.154 ± 0.097	0.144 ± 0.056	0.148 ± 0.057	0.190 ± 0.018
	HR	0.119 ± 0.006	0.132 ± 0.043	0.176 ± 0.085	0.128 ± 0.065	0.114 ± 0.059	0.366 ± 0.178
$T_{st}(s)$	FL	0.344 ± 0.162	0.420 ± 0.178	0.553 ± 0.280	0.436 ± 0.216	0.547 ± 0.152	0.393 ± 0.345
	FR	0.425 ± 0.163	0.450 ± 0.181	0.503 ± 0.284	0.393 ± 0.232	0.450 ± 0.161	0.462 ± 0.018
	HL	0.597 ± 0.023	0.518 ± 0.189	0.583 ± 0.397	0.612 ± 0.262	0.555 ± 0.195	0.802 ±0.120
	HR	0.596 ± 0.022	0.559 ± 0.154	0.674 ± 0.367	0.480 ± 0.296	0.446 ± 0.229	0.440 ± 0.213
β	FL	0.749	0.714	0.660	0.678	0.695	0.789
	FR	0.768	0.743	0.636	0.603	0.569	0.521
	HL	0.836	0.812	0.791	0.809	0.789	0.809
	HR	0.834	0.809	0.793	0.789	0.796	0.546
disp		0.850	0.760	0.813	0.851	0.770	0.020
harm		0.017	0.025	0.007	0.029	0.013	0.002
stab		0.412	0.386	0.343	0.356	0.360	0.131
v		0.086	0.082	0.083	0.086	0.077	0.043

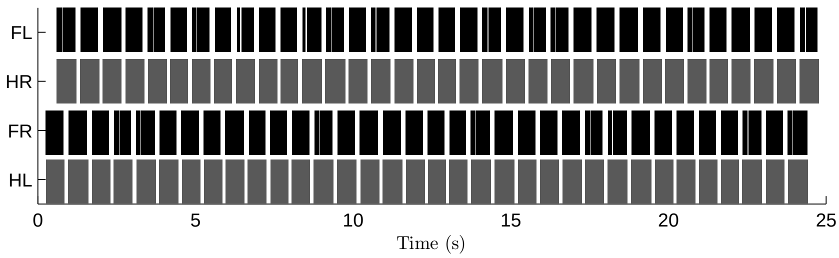

(a) Proposed network with inclusion of limb load information.

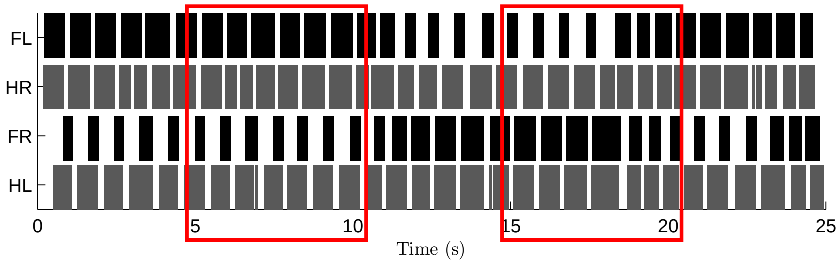

(b) Without inclusion of limb load information.

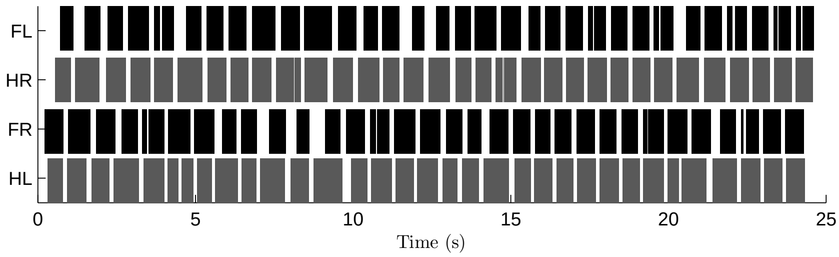

(c) Proposed network with noise of 5%.

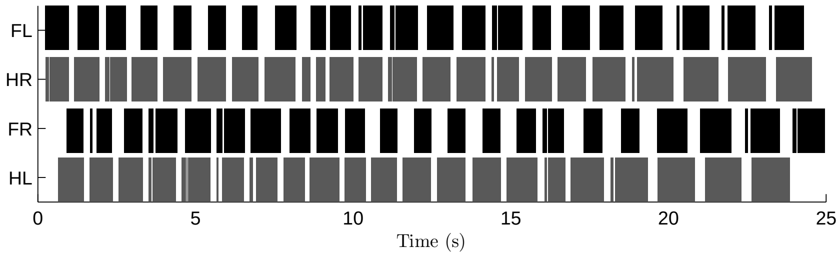

(d) Proposed network when a 12 ms delay is considered.

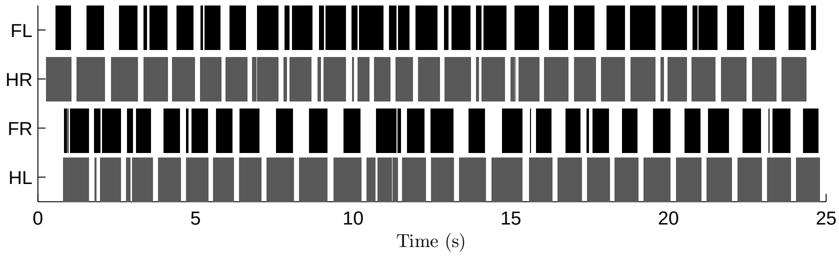

(e) Proposed network when both noise of 5% and a delay of 12 ms are considered.

Figure 7.5: Oncilla stepping sequence in flat terrain.

Actual reflex network with noise

In order to replicate real world behavior in the simulation software, noise magnitude was set at 5% in all of the robot's sensors. On the other hand, white Gaussian noise with an amplitude of 5% was generated and added to the joint positions computed through the proposed controller.

The locomotion generated by the proposed reflex controller is expected to be easily degradable when considering the presence of minimal noise at joint level, leading to a significant lack of robustness in the walking movement. In fact, due to the introduction of noise at joint level, in many trials locomotion can become extremely unstable or proceed in undesirable directions. This is as expected in any pure feedback control system analogous to reflex pathways which is sensitive to imperfect sensors.

Figure 7.5c presents the stepping sequence of the robot in flat terrain with noise. Comparing this stepping sequence with the one obtained without noise inclusion (figure 7.5a), we verify that the stepping pattern is more irregular, as expected. Table 7.2 presents a comparison of the locomotion characteristics for the proposed controller without and with noise inclusion, experiments A and D, respectively. The obtained values support the visual stepping sequence comparison. When we add noise to the system, the standard deviations of T_{sw} and T_{st} are higher, leading to a less regular stepping pattern. With noise, the velocity decreases slightly (less 4.7%) and the gait features (values in table 7.2) show us that the frontal displacement and the stability are worse (less 10.6% and 6.3%, respectively), as expected, but, curiously, the gait harmony is a higher (plus 47%). This comparison shows that noise reduces stability and the achieved frontal displacement. In the overall, results confirm the expectations.

Adding delays to the actual reflex network

Delays are relevant both in biological and physical implementations, therefore, they should be considered. Herein, we add a delay to the proposed controller without noise, by considering a 12 ms delay between sensors and sensory interneurons. This delay means that the sensory input will not affect the output of the sensory interneuron instantaneously, but only after 12 ms. We intend to model the fact that the traveling speed of spikes depends on the nerve fiber properties.

Figure 7.5d shows the robot's stepping pattern resultant from adding this delay (experiment E). Comparing with figure 7.5a, we can see that the stepping sequence is more irregular, which is as expected. Table 7.2, supports our conclusions, resulting from the stepping sequences comparison. When we add the 12 ms delay to the system, the standard deviations of the T_{sw} and T_{st} are higher, leading to a less regular stepping pattern, but still have a good performance in terms of frontal displacement (only less 4.4%). The addition of delays brought more problems in terms of gait harmony and robot's stability, since these components were more affected (less 58.9% of gait harmony and 16.7% of stability).

Adding noise and delays to the actual reflex network

We decided to add, simultaneously, noise and delays to the reflex network to create a model even more similar to the biological counterpart and also a more realistic model. Figure 7.5e shows the robot's stepping sequence resultant from adding noise and delays to the reflex network. This stepping sequence presents a higher degree of visual irregularity compared with the ones of figures 7.5a and 7.5c of experiments A and D, respectively. However, the stepping sequence of experiment E (only with delays) presents a more irregular stepping. Table 7.2 enables a numerical comparison among this controller (experiment F - actual network with noise and delays) and the others (experiment A - actual network without noise and delays, experiment D - actual network with noise and experiment E - actual network with delays). These results corroborate the visual conclusions made earlier. Effectively, the standard deviations of T_{sw} and T_{st} of experiment F are higher than those in experiments A and D, leading to a less regular stepping, and are smaller than in experiment E.

We also compare the gait features of this experiment with those of experiment A, and we conclude that, contrary to what was expected, the frontal displacement and gait harmony of this experiment are higher (0.1% and 70.6%, respectively). As expected, the robot's stability decreases 13.6%.

Adding noise and delays to the reflex network without limb load information

In this experiment, we added both noise and delays to the reflex network without load information - experiment C. Results show that the robot fell. This shows the robustness to noise that the addition of the limb information brought onto the proposed controller. The limb load information is, thus, a crucial element, enabling a locomotion more stable and efficient.

Stumbling reflex

In this section, we test the stumbling reflex which allows the robot to overcome small obstacles with both fore and hind limbs. In this experiment, the robot is expected to overcome an obstacle of 3.5 cm height, while walking. Results show that the robot successfully overcomes the obstacle in the two situations. The robot maintains its locomotion stable while overcomes the obstacle with both fore and hind left limbs (figures 7.6 and 7.7, respectively).

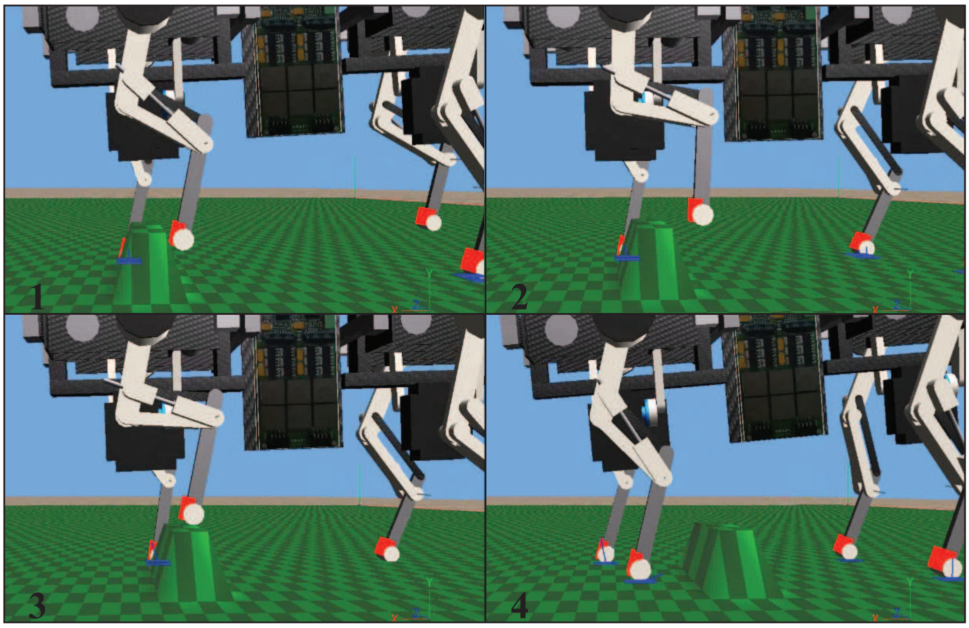

Figure 7.6: Stumbling reflex operation in the fore left leg.

Figure 7.8 shows details of these experiments. The fore left limb interneuron (μ_{DC}) becomes active right after $t \approx 6$ s, and from that moment on, the controller acts directly in the left joints in order to overcome the obstacle (the hip joint was pushed a little back and the knee joint was flexed). The hind left limb found the obstacle around $t \approx 9$ s, and the controller behaved as above, but in this case acting in the hind left limb. After both limbs overcome the obstacle, the robot continued to walk normally.

Figure 7.9 shows the robot's behavior when the stumbling reflex is turned OFF. Note that when the fore left leg touches the obstacle, right after $t \approx 6$ s, the robot gets stuck and ends up falling. These results clearly show the relevance of the stumbling reflex.

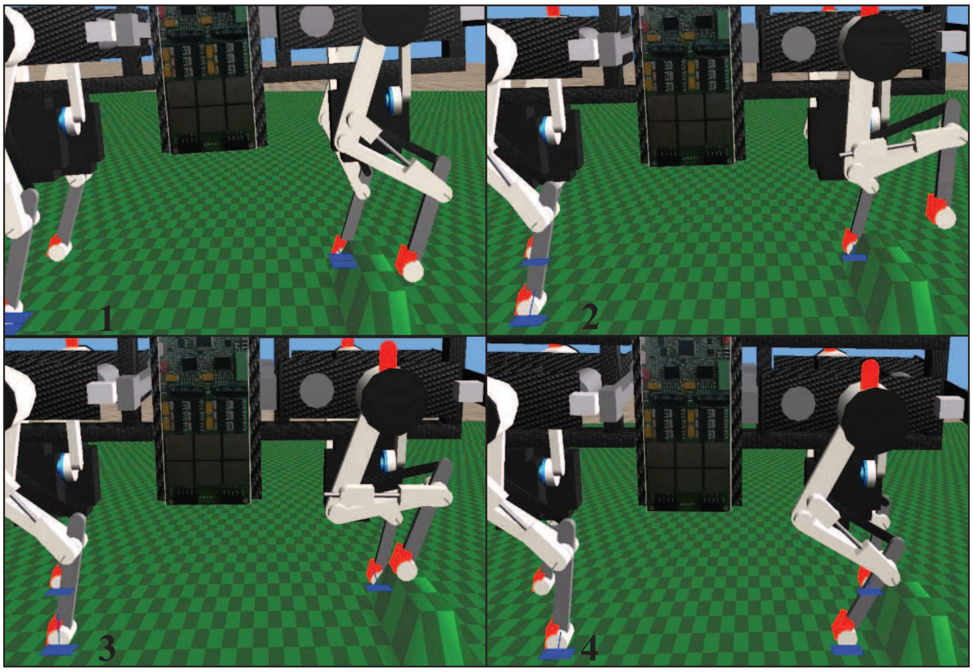

Figure 7.7: Stumbling reflex operation in the hind left leg.

In this experiment, we add noise and a 12 ms delay between sensors and sensory interneurons (fig. 7.10). The stumbling reflex continued to allow the robot to overcome the obstacle with the fore and hind limbs. Right after $t \approx 5$ s, the fore left limb overcomes the obstacle successfully. When the hind limb touched the obstacle, it got stuck because the reflex had been activated when the limb was in touchdown phase. However, after some cycles, the reflex responds and the limb overcomes the obstacle.

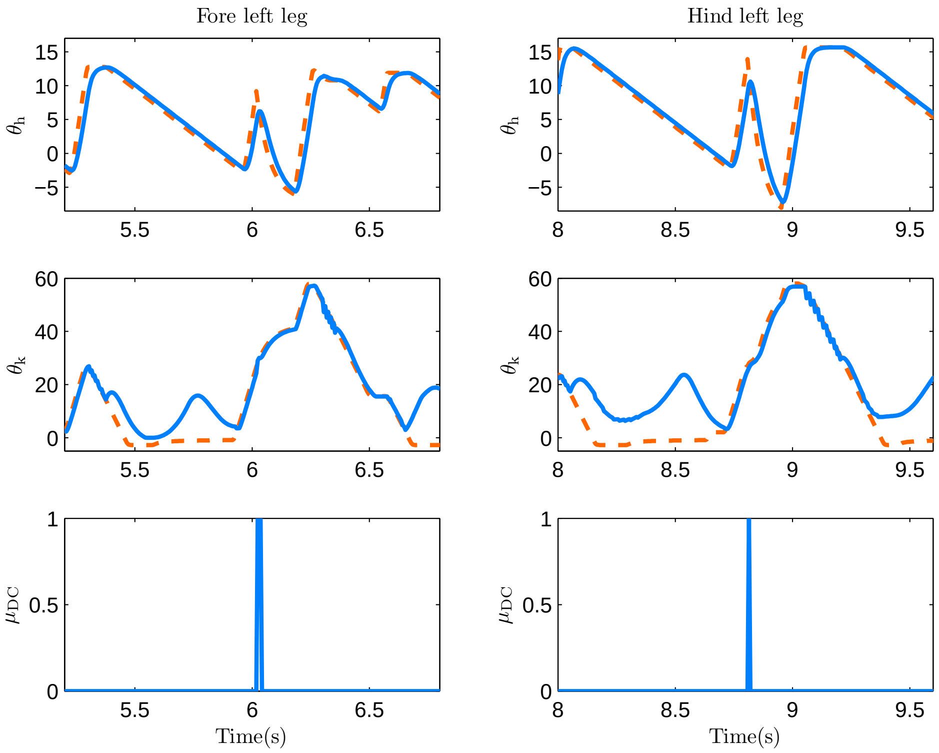

Figure 7.8: Trajectory details of the robot overcoming an obstacle in fore limb followed by an obstacle in hind limb. Left column depicts fore left leg. Right column the hind left leg. Top panels: hip movement (θ_h). Middle panels: knee movement (θ_k). Bottom panels: sensory interneuron (μ_{DC}). For the hip and knee joints movements, the dashed orange lines represent the joints references and the solid blue lines represent the performed joint angle.

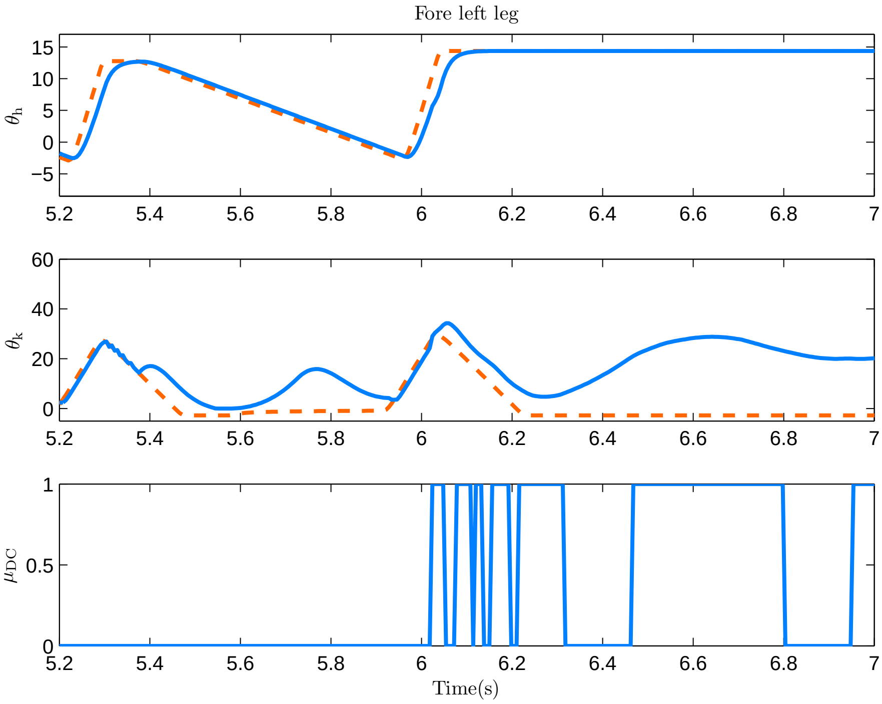

Figure 7.9: Similar legend to Figure 7.8 but when the stumbling reflex is turned OFF.

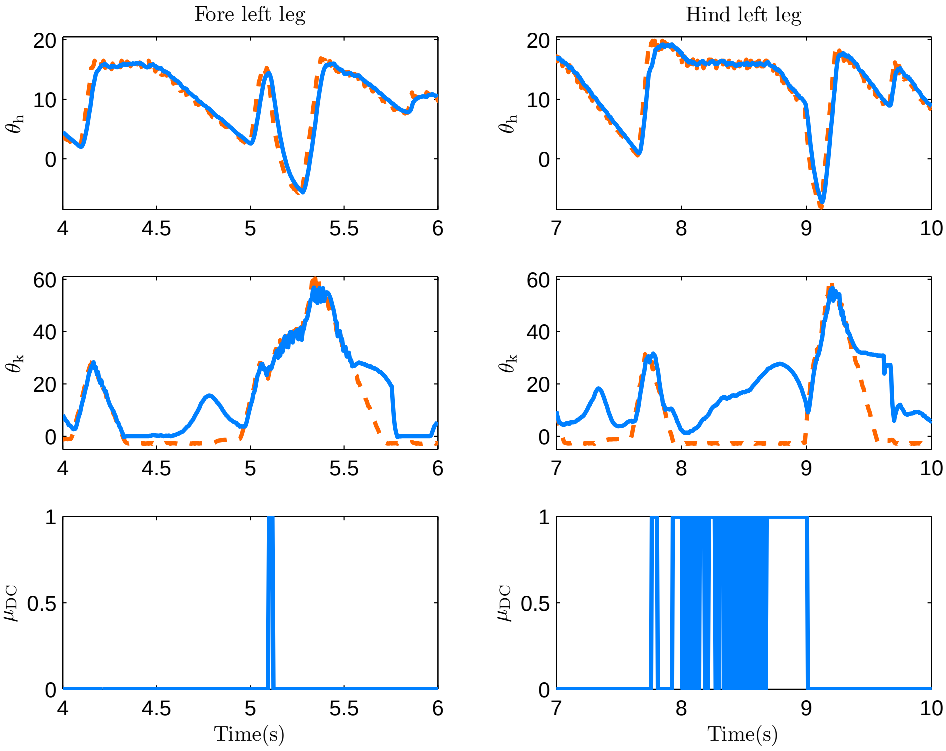

Figure 7.10: Similar legend to Figure 7.8 when the stumbling reflex is turned ON, but both noise and delays were added.

7.1.2 Ramp experiments

In this simulation, the robot climbs up and down a ramp with a maximum inclination of 10%. The role of the vestibulospinal reflex implemented in the neural network is to prevent the center of gravity from being pulled backwards (while climbing up a ramp) or forwards (while going down a ramp). The reflex does this acting on the knees, flexing or extending them, depending on the situation. If the robot is climbing up a ramp, the fore knees should flex and the hind knees should extend. In the opposite case, if the robot is going down a ramp, the fore knees should extend and the hind knees should flex. In both situations, the reflex tries to decrease the body pitch angle to a minimum value that is safer for the robot, trying to maintain the robot stable.

The schematic of the ramp used in these experiments is depicted in figure 7.11. We can divide this ramp and the experiment in three stages: A, B and C. In stage A, the robot climbs up a ramp with a 10% inclination, in stage B the robot stabilizes in a short flat terrain and finally, in stage C, the robot goes down the ramp with the same inclination of stage A. With this scenario, we can evaluate if the reflex has a good performance in both cases, climbing up a ramp, and going down a ramp.

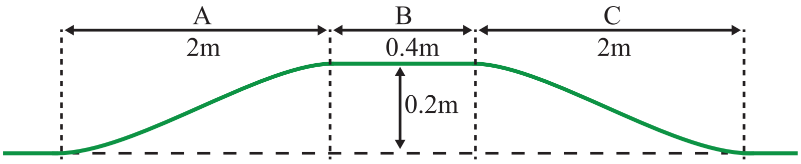

Figure 7.11: Schematic of the ramps used in the experiments.

In order to evaluate the system's robustness to noise, simulations were performed considering and not considering noise inclusion, when the vestibulospinal reflex was turned ON and OFF. Table 7.3 presents the three components of gait analyses and the values of the body roll and pitch angles of the four experiments performed (mean ± SD).

Experiments without noise

Herein, we present results of two experiments made without considering noise in the system, neither at the actuators or sensors level. We compare the robot's performance when the vestibulospinal reflex is turned ON and OFF (fig. 7.12). When the reflex was turned OFF, the robot fell. Initially, the robot climbed up the ramp successfully (stage A

Table 7.3: Locomotion data from the experiments in ramp.

Parameters	No Noise		Noise	
	VR OFF	VR ON	VR OFF	VR ON
disp	0.590	0.735	0.628	0.731
harm	0.002	0.017	0.016	0.013
stab	0.226	0.359	0.178	0.334
$\text{Roll}_{0\to40}$	-1.397 ± 3.337	-1.277 ± 2.358	-1.702 ± 3.405	-1.610 ± 2.135
$\text{Pitch}_{0\to40}$	2.902 ± 4.871	3.984 ± 4.417	3.311 ± 5.130	3.754 ± 4.597
$\text{Roll}_{0\to60}$	2.933 ± 7.948	-1.333 ± 2.440	-12.543 ± 20.168	-2.125 ± 3.522
$\text{Pitch}_{0\to60}$	-49.141 ± 84.641	0.488 ± 6.175	-42.204 ± 77.697	0.036 ± 6.633

of figure 7.11), but the robot fell as soon as it came into stage C, *i.e.*, when it began going down the ramp. This is illustrated in figure 7.12, after $t \approx 40$ s, the body pitch and roll angles (dashed orange lines) began to diverge, and the robot ends up falling.

Initially, when the robot is climbing up the ramp, one can observe that no notorious difference exists in the body picth angle (stage A of the top panel in figure 7.12), even so the standard deviation value of the picth angle is lower, which shows a range of motion more stable. When the robot is going down a ramp, the vestibulospinal reflex has an important role, as we can see during stage C of figure 7.12. The reflex is capable of maintaining the body pitch stable (solid blue line of figure 7.12), helping the robot going down the ramp. On the other hand, we can see that the vestibulospinal reflex improved the roll angle evolution (solid blue line in bottom panel), since the angle amplitude decreased. The body roll standard deviation decreased from 3.3º to 2.4º (less 29.3% - roll from 0 to 40 s) and from 7.9º to 2.4º (less 69.3% - roll from 0 do 60 s). The body roll and pitch values with the reflex turned OFF from 0 to 60 s are inflated by the robot's fall.

Table 7.3 provides more useful information for the evaluation of the effect of the vestibulospinal reflex in the robot's gait. With the reflex turned ON, the frontal displacement had an improvement of 24.6% (from 0.59 to 0.74), the gait harmony had an improvement of 750% (from 0.002 to 0.017) and the robot's stability had an improvement of 58.8% (from 0.23 to 0.36). The vestibulospinal reflex proved to be capable of improving the robot's locomotion in ramp experiments.

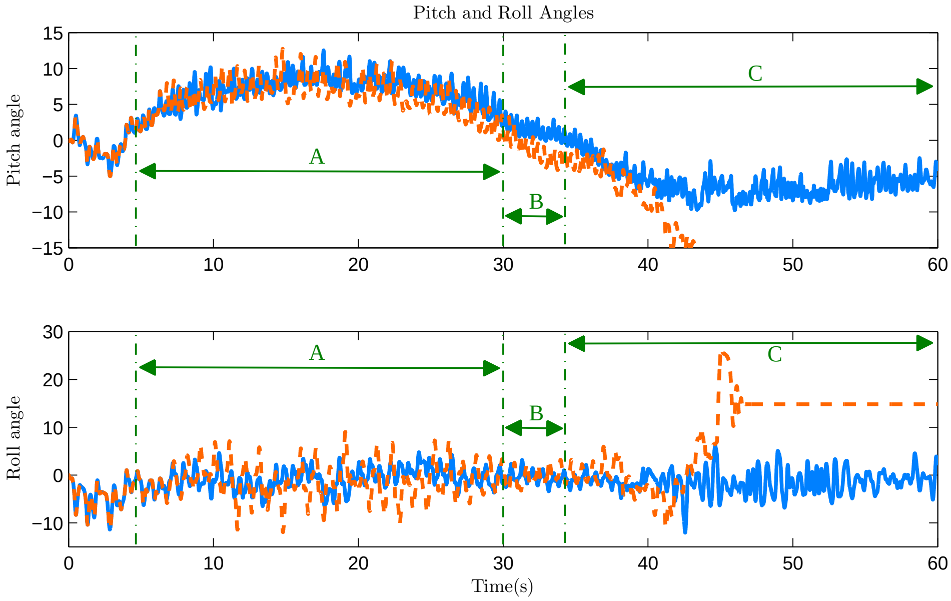

Figure 7.12: Body roll and pitch angles in ramp experiment, when no noise was considered. Top panel: pitch angles. Bottom panel: Roll angles. The blue solid lines represent the variables with the vestibulospinal reflex turned ON, and the dashed orange lines represent the variables with the vestibulospinal reflex turned OFF.

Experiments with noise

The inclusion of the vestibulospinal reflex is expected to provide for improved and more robust robot locomotion. In order to study the robustness of the system to noise, similarly to the experiments in flat terrain, a 5% noise was added to actuators and sensors. In order to evaluate the robustness, two experiments were performed, both including noise, with the vestibulospinal reflex turned OFF and ON. As expected, results show that without the vestibulospinal reflex the robot fell around the same time at when no noise was considered. On the other hand, when the reflex was considered, the robot was able to successfully climb up and down the ramp.

Figure 7.13 illustrates that when the reflex was not considered, the body pitch and roll angles (identified by dashed orange lines in both panels) began to diverge, and the robot ends up falling. On the other hand, these same angles (indicated by solid blue lines in figure 7.13) clearly show the important role that the vestibulospinal reflex performed during the all pathway, helping the robot climbing up and down a ramp.

Additionally, and similarly to the experiments without noise, the reflex improved the frontal displacement (16.4%) and elicited a greater increase in the robot's stability (87.6%).

Curiously, the gait harmony had a slight reduction (18.8%) (check table 7.3 for further details).

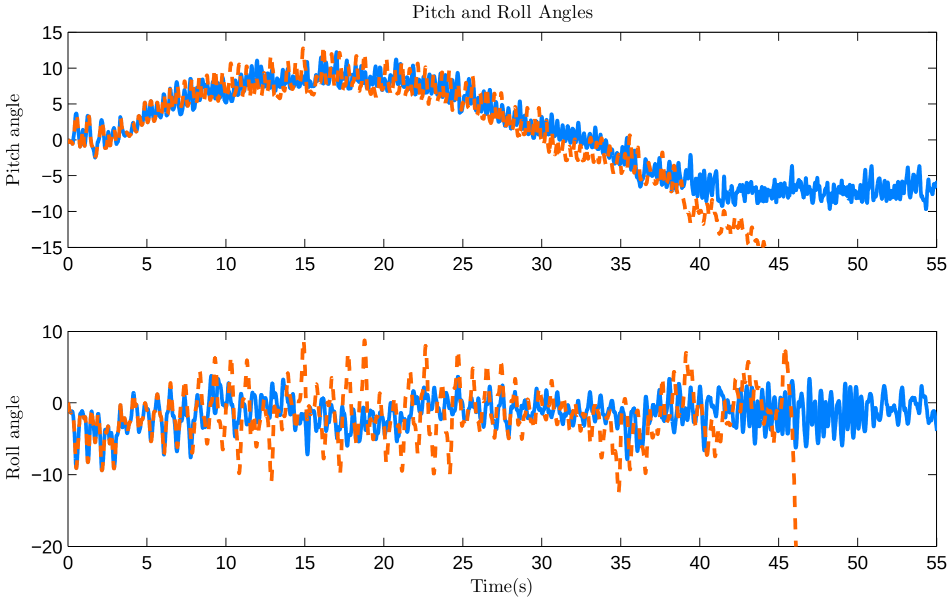

Figure 7.13: Body roll and pitch angles in the ramp experiment, when noise was considered at the sensors and actuators level. Legends were built similarly to the ones of figure 7.12.

7.2 Hybrid controller experiments

The hybrid controller is parameterized empirically based on the authors know-how and on other works (Wadden and Ekeberg, 1998; Maufroy et al., 2008; Ekeberg and Pearson, 2005; Owaki et al., 2012). The controller comprises the feedback control analogous to the reflex pathways implemented in section 7.1. The feedforward parameterization is presented in this section.

The experiments presented below were performed in flat terrain, in which the Oncilla robot should accomplish stable quadruped walking. We start showing the limb CPG parameterization and analyzing its adaptability and coupling with the step cycle. The internal mapping of the four motoneurons in the CPG is presented, as well as the predictor quality of each motoneuron. We verify what percentage is that each CPG can predict in each motoneuron. Furthermore, we study eleven models of hybrid controllers to demonstrate the effect of reflex and CPG combinations. This study allowed to choose models that exhibit the most interesting properties in terms of velocity, displacement, stability, harmony, and stepping sequence. The best models are compared with the reflex controller of section 7.1, expecting to improve the robot's walk in flat terrain. We verify the proposed network robustness by adding noise to sensors and actuators, and adding delays to create a more biologically relevant model. It is expected that the hybrid controller improves the Oncilla's walking, by increasing its stability, harmony, velocity and making the stepping sequence even more regular, mainly in the situations with noise and delays.

As previously, as far as startup conditions are concerned, the joint positions are established such that the contralateral limbs are at the AEP and PEP positions, and initial neuron activities are set to the respective step phase. The CPG activity of each limb is initiated when the robot's walk stabilizes, *i.e.*, when it starts to perform regular stepping patterns. This start-up period lasts an average of 6 seconds. Table 7.4 shows the set of parameters used for these experiments; the sensory thresholds necessary for the sensory interneurons; the hip and knee joint positions for the attractors; the CPG parameters and the joint output parameters.

Simulations show that the hybrid controller improves the robot's locomotion, correcting the shortcomings of the reflex controller, *i.e.*, reducing the negative effects of the presence of noise and delays on the reflex controller. The CPG should filtrate the noise (Kuo,

Table 7.4: Sensory thresholds, attractors values, joint output parameters and CPG parameters.

Parameters	Limbs	
	Fore	Hind
Θ_{AEP}	8	10
Θ_{PEP}	5	5
$F_{\text{threshold}}$	1	1
$F_{\text{threshold}_{\text{DC}}}$	10	10
$F_{\text{threshold}_{\text{Load}}}$	8	8
Θ_{StH}	-7	-10
Θ_{StK}	42	40
α_h	45	45
γ_h	400	400
α_k	300	300
γ_k	500	500
ω	3.04π	2.86π
σ	0.35	0.35

2002) and predict the motor actions to compensate the internal delays (More et al., 2010) implemented in the Oncilla robot.

7.2.1 Synchronization and adaptability of CPGs

The CPGs should be synchronized with the robot's step cycle, in order to correctly predict the motoneurons' activity of the reflex component. In order to ensure that CPGs stay synchronized with the gait phases which they are predicting, the coupling has to be correctly specified and tuned. As a first step, four CPGs, one for each limb, coupled to the corresponding load information of each limb, were used. No output from these CPGs is used in the generation of locomotion and for now on this will be called the passive mode.

Figure 7.14 shows that the CPG is constantly adapting its phase (solid blue line), in order to synchronize with the reflex network's step cycle, defined by the sensory interneuron of ground contact (dashed orange line). When a transition from one to zero occurs in the GC sensory interneuron, μ_{GC}, the step cycle initiates, and finalizes when this event occurs again. Since the period of the reflex network's step cycle is not constant, due to the gait's irregularity, the CPGs need to adapt its phase evolution on an online fashion. Thereby, the local sensory feedback (f) from the force sensor in each foot plays an important role in the synchronization of the CPG with the gait phases, accelerating or decelerating the evolution of the CPG phase (ϕ). The limb oscillator should accelerate when the limb is not supporting load (GRF = 0) and should decelerate when the limb is supporting load (GRF > 0), *i.e.*, the CPGs accelerate when the $\mu_{\text{GC}} = 0$ and decelerate when the $\mu_{\text{GC}} = 1$. Comparatively to other state of the art works such as Dzeladini et al. (2014), this is one of the main differences and advantages of our work. There is no phase reset and the oscillator tries to adapt in an online fashion. Besides, the proposed CPG will act at the motor level instead of acting at the sensory feedback level.

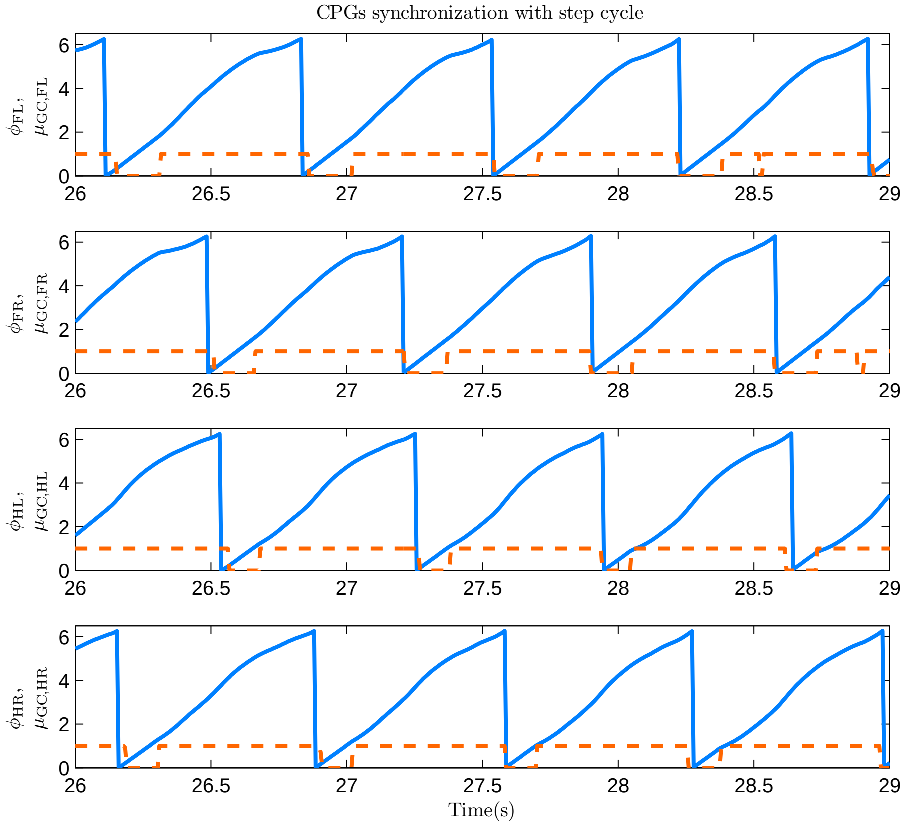

Figure 7.14: CPG activity (solid blue line) and sensory interneuron of ground contact (GC) (dashed orange line), for each limb. The step cycle is defined by the sensory interneuron of GC (μ_{GC}).

This adaptability of the CPG is supported by table 7.5, which shows that the period of the CPG step cycle ($T_{\text{step cycle,CPG}}$) varies, proving that each CPG is trying to adapt to the variations of the reflex network's step cycle. It is interesting to notice that due to the type of the gait, walking trot, the fore left (right) and hind right (left) limbs present a similar CPG period.

The reflex step cycle period of the fore limbs ($T_{\text{step cycle,RC}}$) present higher standard deviations. This is related with some shortcomings of the fore limbs' step cycle that can be seen in the first and second panels of figure 7.14, where sensory interneurons GC, μ_{GC}, show non expected transitions, right around 28.5 s (first panel) and immediately before the 29 s (second panel).

Table 7.5: Step cycle period of the reflex controller ($T_{\text{step cycle,RC}}$) and the CPG ($T_{\text{step cycle,CPG}}$).

Period	Limb			
	Fore Left	Fore Right	Hind Left	Hind Right
$T_{\text{step cycle,RC}}$	0.483±0.170	0.510±0.175	0.713±0.024	0.714±0.025
$T_{\text{step cycle,CPG}}$	0.699±0.099	0.713±0.015	0.713±0.013	0.698±0.104

7.2.2 Internal mapping of the four motoneurons in the CPG

Based on our hypothesis that CPGs can be viewed as motoneurons predictors, we first build an internal mapping of the motor actions that should reproduce the typical shape of the motoneurons generated by the reflex network.

The typical shape of the motoneurons is obtained by observation of the motoneurons activity when the proposed reflex controller generates locomotion. The internal mapping from the motoneurons' to CPGs phases during one step cycle period is depicted in figure 7.15. In each panel, the orange area represents a specific predicted motoneuron, and the gray area represents the remaining predicted motoneurons. Large part of the step cycle period is used for the stance and touchdown phases, being the swing phase the shortest.

7.2.3 Predictor quality

In order to verify the predictor quality of the proposed mapping, we compare the outputs of the motoneurons of the proposed reflex controller with the ones from the predicted motoneurons according to the CPGs phases. Note that this experiment is performed without any link between the CPGs and the motoneurons. Table 7.6, presents the correlations between the predicted motoneurons (Ψ_{CPG}) and the motoneurons of the reflex controller (Ψ_{RC}). The maximum value of correlation is 0,816 for touchdown motoneurons. The low values of this correlation are justifiable considering that during the locomotion there is no mechanism responsible for the reset of the CPGs. Remember that in the proposed hybrid

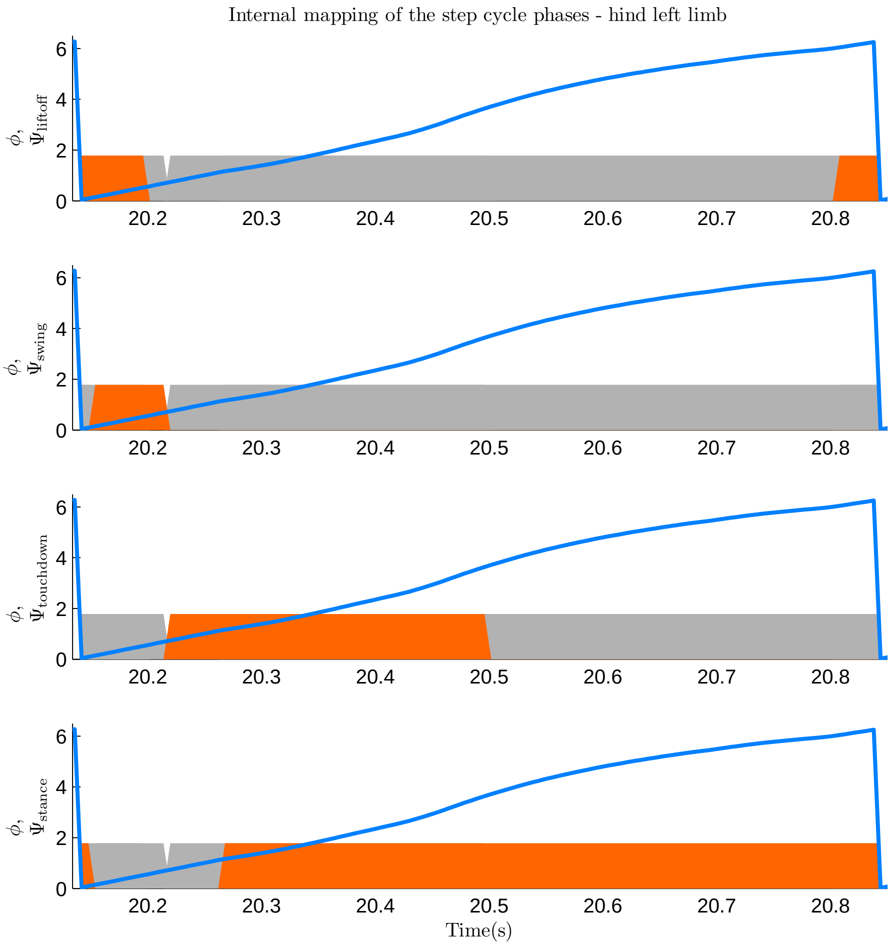

Figure 7.15: Internal mapping of motoneuron activity to the CPG phase. The blue line represents the CPG phase. In each panel, the orange area shows the activity of the corresponding motoneuron, and the gray area represents the remaining predicted motoneurons.

controller, the CPG must adapt automatically to the robot's step cycle over time, through the feedback mechanism that entrains CPGs, enabling an automatic synchronization of the robot with the environment. Therefore, since the produced gaits are a bit irregular, the achieved correlation values are low and this is as expected.

7.2.4 Motoneurons replacement

In order to study the replacement of the motoneurons by their CPG predictors, we ran a systematic search in which we increase $\upsilon = 1 - \varphi$ (*i.e.*, the relative importance of the CPGs in eq. 5.14) from 0 to 1.0, in steps of 0.1. This experiment is done for each motoneuron, maintaining the relative importance of the CPGs for the remaining motoneurons equal to

Table 7.6: Correlations between predicted motoneurons (Ψ_{CPG}) and reflex motoneurons (Ψ_{RC}).

Correlation	Limb			
	Fore Left	Fore Right	Hind Left	Hind Right
$\Psi_{\mathrm{stance,RC}}$ *vs* $\Psi_{\mathrm{stance,CPG}}$	0.737	0.729	0.751	0.721
$\Psi_{\mathrm{swing,RC}}$ *vs* $\Psi_{\mathrm{swing,CPG}}$	0.619	0.638	0.676	0.663
$\Psi_{\mathrm{touchdown,RC}}$ *vs* $\Psi_{\mathrm{touchdown,CPG}}$	0.793	0.809	0.816	0.756
$\Psi_{\mathrm{liftoff,RC}}$ *vs* $\Psi_{\mathrm{liftoff,CPG}}$	0.618	0.646	0.667	0.669

zero.

In our approach, none of the motoneurons can be fully predicted.

Figure 7.16, shows the maximum CPG prediction for each motoneuron. The maximum value corresponds to the situation in which the locomotion starts to be affected negatively by the predictor and becomes unstable, eventually falling. In summary, the percentage of CPG activity can be increased to 50% for the touchdown motoneuron ($\overline{\Psi}_{\mathrm{touchdown}}$), 90% for the liftoff motoneuron ($\overline{\Psi}_{\mathrm{liftoff}}$), 40% for the swing motoneuron ($\overline{\Psi}_{\mathrm{swing}}$) and 60% for the stance motoneuron ($\overline{\Psi}_{\mathrm{stance}}$). The liftoff motoneuron ($\overline{\Psi}_{\mathrm{liftoff}}$) activity can almost be set only by the CPG-feedforward component, and the swing motoneuron ($\overline{\Psi}_{\mathrm{swing}}$) is more dependent on the reflex system. This highlights the importance of swing motoneuron ($\overline{\Psi}_{\mathrm{swing}}$) for the gait's stability.

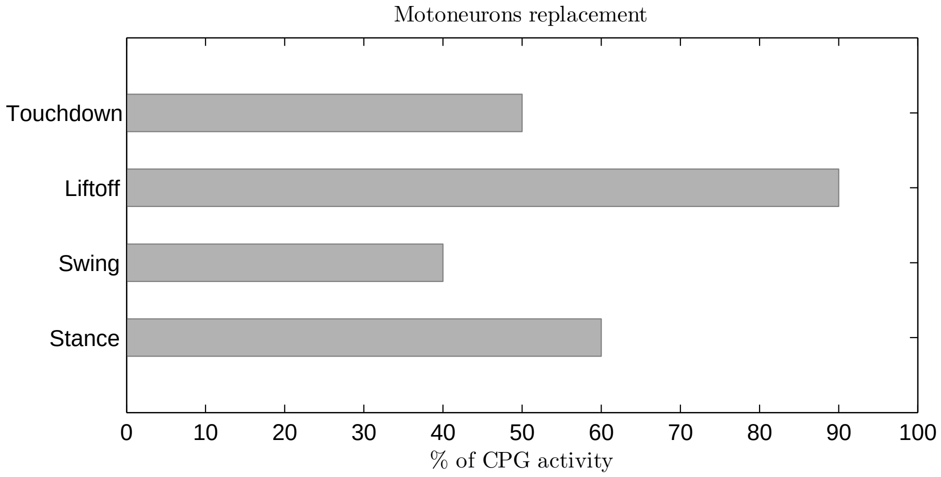

Figure 7.16: Maximum CPG prediction for each motoneuron.

7.2.5 Hybrid models: combining feedback and feedforward models

In this section, we are interested in studying more complex combinations of motoneurons and CPGs, other that one motoneuron at a time, when using CPG predictors. Thus, we proposed eleven different models that enable the demonstration of the hybrid controller effects in locomotion.

These models differ in the feedback-feedforward combination, *i.e.*, in each model we present a different combination of the predicted motoneurons for each limb. Table 7.7, shows the different combinations used, in which we can have two, three or four predicted motoneurons turned ON (CPG contribution different from zero), although all with the same percentage of activation.

Table 7.7: Eleven hybrid models.

Models	Predicted motoneurons			
	$\Psi_{\text{stance,CPG}}$	$\Psi_{\text{swing,CPG}}$	$\Psi_{\text{touchdown,CPG}}$	$\Psi_{\text{liftoff,CPG}}$
Model 1	OFF	OFF	ON	ON
Model 2	OFF	ON	OFF	ON
Model 3	OFF	ON	ON	OFF
Model 4	OFF	ON	ON	ON
Model 5	ON	OFF	OFF	ON
Model 6	ON	OFF	ON	OFF
Model 7	ON	OFF	ON	ON
Model 8	ON	ON	OFF	OFF
Model 9	ON	ON	OFF	ON
Model 10	ON	ON	ON	OFF
Model 11	ON	ON	ON	ON

The figure 7.17 shows the experiments made with the eleven models.

Each model was tested in six situations. In the first five situations, we ran a systematic experiment in which we increase the relative importance of the CPGs from 20% to 100%, in steps of 20%. In all these situations, all the predicted motoneurons that are ON have the same importance. In the last situation, the relative importance of the CPG activity is defined based on the maximum CPG prediction for each motoneuron previously determined and is set as follows: $\upsilon_{\text{stance}} = 60\%$, $\upsilon_{\text{swing}} = 30\%$, $\upsilon_{\text{touchdown}} = 40\%$ and $\upsilon_{\text{lifftoff}} = 80\%$.

These situations are evaluated according to the components of the gait analysis previously suggested (chapter 6): *harm*, *disp* and *stab* components. The obtained results are depicted in figure 7.17, for the six situations of the eleven models, in which each model has three stacked bars, corresponding to the performed evaluations. The blue bars represent the harmony (*harm*) component, the orange bars represent the stability component (*stab*) and the gray bars represent the displacement (*disp*) component. The green lines in each bar represent the final reward for the hybrid controller resultant from the combination of the three gait evaluation components, and the ticked-dotted gray line represents the reward of the reflex controller. This enables a comparison among these controllers.

Analyzing the data recorded and figure 7.17, we can get some relevant conclusions. Model 7 tends to increase the robot's harmony and maintain the displacement, while model 9 tends to increase the robot's displacement and decrease stability. Models 3, 8 and 10 are the weakest, jeopardizing the robot's behavior in almost all situations. When we increase the CPGs contribution to 80% and 100%, the robot, in several models, presents a bad performance and, in some cases, ends up falling. For CPG contributions of 80% and 100%, almost every model presents a reward with a lower value, comparing with the reward of the reflex controller. For the special situation, the models present less variations of displacement, stability and harmony, since we can observe in figure 7.17 that ten models present the same stability and the displacement and harmony are very similar, when compared with the other situations, where we can see that we have much more models that have greater variations. Furthermore, we can see in figure 7.17 that, in the special case, we have only one model in which the reward value is lower than the reward of the reflex controller, while in the other five situations we have always more models that present reward values lower than the reflex controller reward, showing that the models with the special case calibration present less variations.

Making an overall data analysis, we conclude that the best models are 2, 4, 7, 9 and 11 models. In these five models, only model 2 has just two predicted motoneurons turned ON, which shows the importance of having the largest possible number of predicted motoneurons turned ON.

Table 7.8 presents four models, in which the first three models are the best according to this evaluation. The last model was included in this group due to its good performance in situations where noise and delays are considered. Furthermore, this model is among the top 10 experiments in this evaluation, in a total of 66. The first three models have a CPG

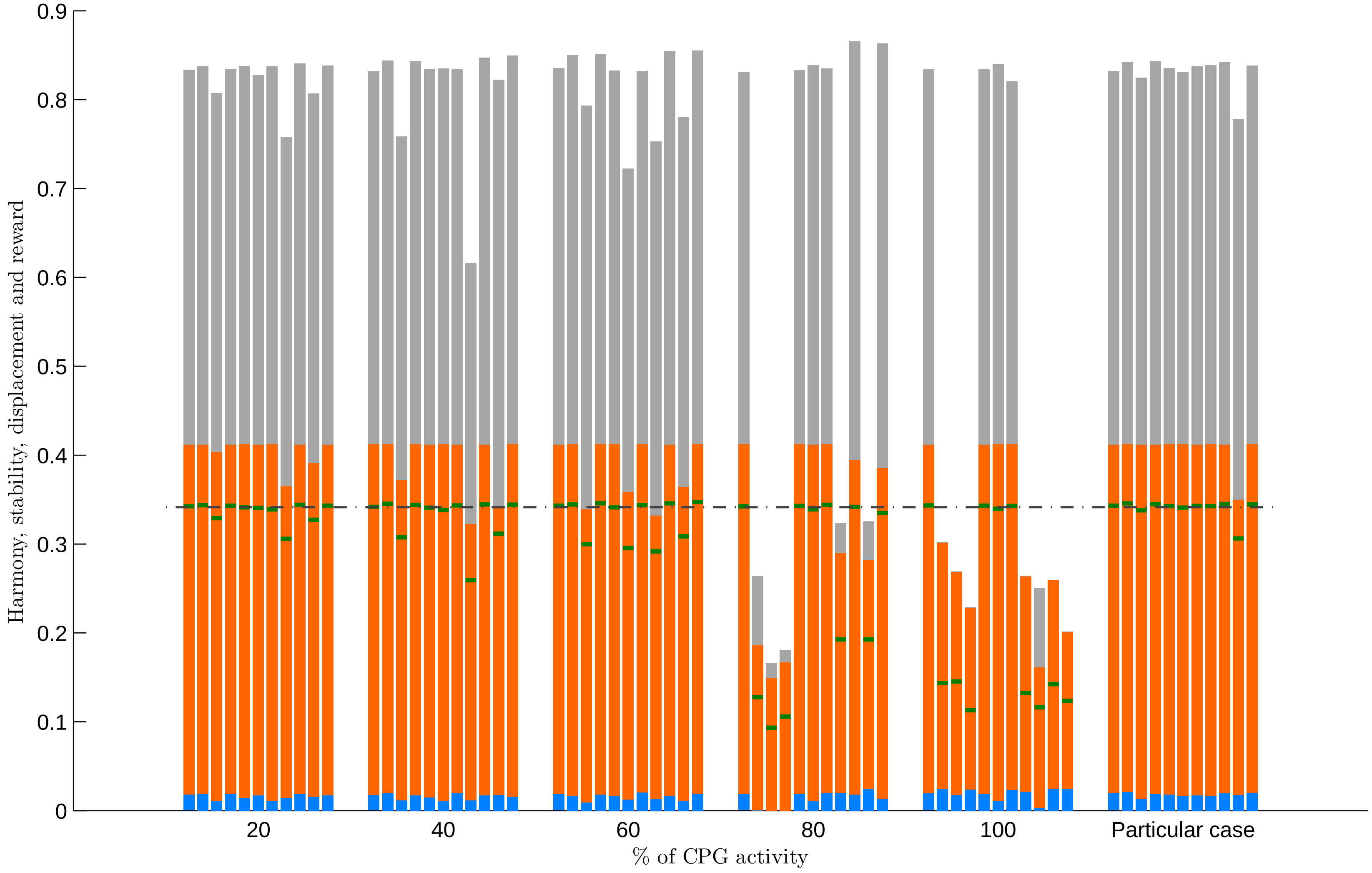

Figure 7.17: Gait analysis of the eleven models, tested in six different situations. The blue, orange and gray bars represent the *harm*, *stab* and *disp* components, respectively. The green and gray lines represent the rewards of the models and reflex controller, respectively.

contribution of 60% and the last model has a CPG contribution of 40%. The best model (model 11A) and the last model have all the predicted motoneurons turned ON.

Table 7.8: Three best hybrid models and the corresponding rewards.

Models	CPG contribution (%)	Reward
Model 11A	60	0.3473
Model 4	60	0.3460
Model 9	60	0.3458
Model 11B	40	0.3443

7.2.6 Comparison between the reflex controller and the hybrid controller

Hereinafter, we compare the reflex controller of section 5.1 with four hybrid controllers, considering the displacement, harmony, stability, velocity and stepping sequence regularity of the generated walking gait. We use the four hybrid models presented on table 7.8.

In these experiments, we have addressed locomotion in flat terrain when no noise and delays are considered, when only noise is considered, with only delays and with both noise and delays. Tables 7.9, 7.10, 7.11 and 7.12, summarize the collected information. These tables display the locomotion features such as the swing time (T_{sw}), the stance time (T_{st}), the duty factor (β), the robot's velocity (v), the three components of gait analysis (*disp*, *harm* and *stab*) and the final reward (*reward*).

Figure 7.18 depicts the hind left limb's hip and knee joint movement (θ_{h}, θ_{k}) and the final motoneurons $\overline{\Psi}$ of the model 11A along with the corresponding curves of the reflex controller. Although the waveform of the final motoneurons ($\overline{\Psi}$, solid blue line) is slightly different compared with the reflex controller (dashed orange line), the joint trajectories of the model (solid blue lines of the first and fourth panels) are not affected, with the limb performing a similar joint movement to the one performed by the reflex controller (dashed orange lines of the first and fourth panels).

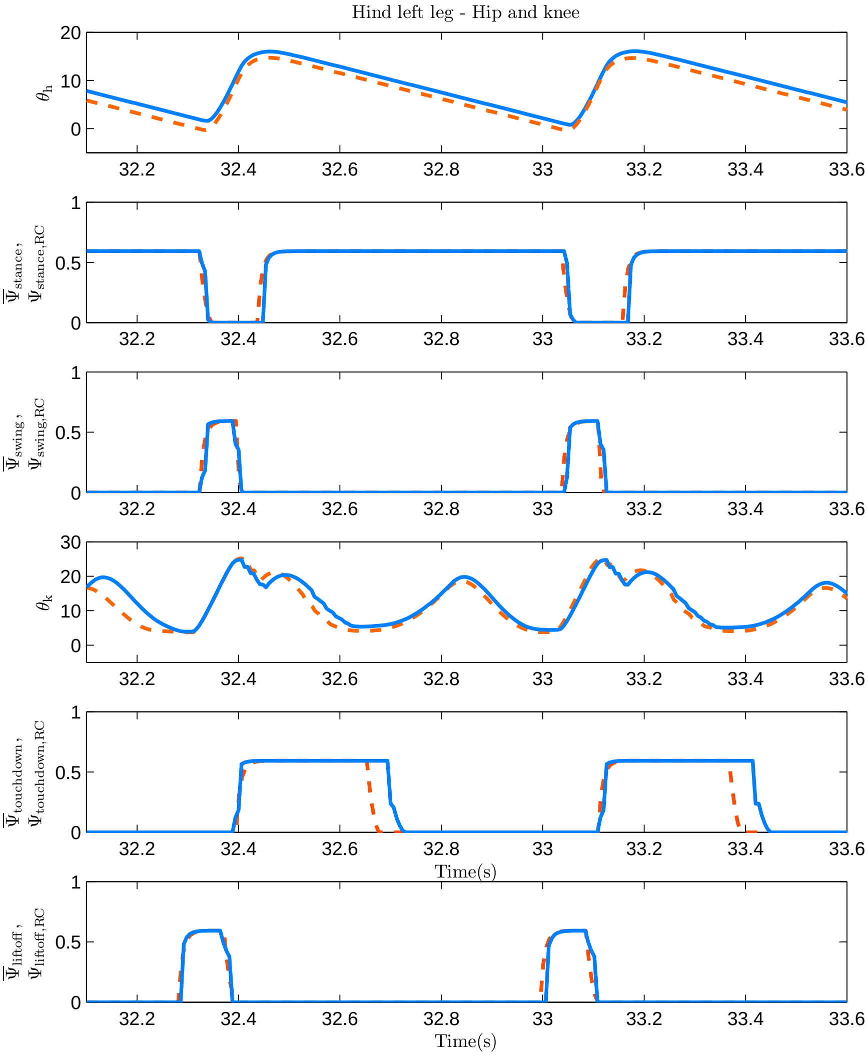

Figure 7.18: Hind left limb's hip and knee joint movement (θ_h and θ_k, respectively), final motoneuron activity ($\overline{\Psi}$) and reflex network motoneurons (Ψ) of swing, stance, touchdown and liftoff. For the hip and knee angles (θ_h and θ_k, respectively), the dashed orange lines represent the hip and knee signals of the reflex controller and the solid blue lines the produced joints angle of the hybrid controller. The final motoneurons ($\overline{\Psi}$) are represented with solid blue lines and the reflex network motoneurons (Ψ) with dashed orange lines.

Controllers without noise and delays

Figure 7.19 presents the stepping sequences for the reflex controller and the four hybrid models, when no noise and delays were considered. By visual inspection we can verify they are all fairly regular. A more rigorous analysis is provided through table 7.9, that enable some important conclusions. The standard deviations of the T_{st} for all limbs in the four hybrid models are lower, leading to a more regular stance period. The hybrid models provide for almost the same average stance and swing times (T_{st} and T_{sw}) among the girdles, mainly in the fore girdles, since the hind girdles had already the same stance and swing time ((T_{st}) and (T_{sw})). Another relevant aspects are that, for all the hybrid models, the velocity and the displacement increased, and the stability remained equal to the one of the reflex controller. Model 4 and 11A increased the harmony value.

Table 7.9: Locomotion data from the experiments in flat terrain without noise and delays.

Param	Limb	Reflex controller	Hybrid controller			
			Model 4	Model 9	Model 11A	Model 11B
$T_{sw}(s)$	FL	0.115 ± 0.068	0.106±0.069	0.107±0.076	0.102±0.075	0.112±0.072
	FR	0.128 ± 0.056	0.109±0.067	0.115±0.075	0.104±0.076	0.107±0.072
	HL	0.117 ± 0.006	0.123±0.005	0.121±0.005	0.122±0.004	0.118±0.003
	HR	0.119 ± 0.006	0.123±0.006	0.118±0.005	0.120±0.004	0.121±0.004
$T_{st}(s)$	FL	0.344 ± 0.162	0.265±0.136	0.300±0.148	0.280±0.135	0.289±0.157
	FR	0.425 ± 0.163	0.254±0.134	0.301±0.158	0.280±0.140	0.322±0.153
	HL	0.597 ± 0.023	0.596±0.008	0.593±0.006	0.594±0.006	0.593±0.008
	HR	0.596 ± 0.022	0.597±0.007	0.597±0.008	0.596±0.008	0.590±0.008
β	FL	0.749	0.715	0.738	0.733	0.721
	FR	0.768	0.698	0.724	0.730	0.751
	HL	0.836	0.829	0.831	0.830	0.834
	HR	0.834	0.830	0.835	0.832	0.830
$disp$		0.850	0.869	0.872	0.874	0.865
$harm$		0.017	0.018	0.017	0.019	0.016
$stab$		0.412	0.412	0.412	0.412	0.412
$reward$		0.341	0.346	0.346	0.347	0.344
v		0.086	0.088	0.089	0.089	0.088

The best hybrid model in this situation, without noise and delays, is the model 11A (figure 7.19d), since it presents the higher values of displacement and harmony, and therefore, a higher reward value. The displacement increased 2.8%, the harmony increased 11.8% and velocity increased 3.5%.

Controllers with noise

The locomotion generated by the reflex controller is easily degradable when considering the presence of minimal noise at joint level, leading to a significant lack of robustness in the walking movement. Due to the introduction of noise at joint level, in many trials locomotion can become extremely unstable or proceed in undesirable directions.

Based on Kuo (2002) work, we hypothesized that the hybrid controller must be capable of increasing the walking stability, providing a more robust and efficient locomotion.

In order to replicate real world behavior in the simulation software, noise magnitude was set at 5% in all robot sensors. On the other hand, white Gaussian noise with an amplitude of 5% was generated and added to the joint positions computed through the proposed controller.

In figure 7.20, we present the robot stepping sequences in flat terrain when noise was included in the reflex controller and in the considered four hybrid models. We can visually verify that the hybrid models 9, 11A and 11B are much more regular that the reflex controller. Table 7.10 supports our visual conclusions, since the hybrid models improved several locomotion parameters. Almost all of the T_{st} and T_{sw} standard deviations are lower, leading to a more regular stepping. Furthermore, all the hybrid models provide almost the same stance and swing time (T_{st} and T_{sw}) among the girdles, both hind and fore girdles. Another important aspects to be noticed is that the velocity and the displacement increased in all the hybrid models and the stability increased in the models 9 and 11B. Curiously, the gait harmony decreased in all the models, with the model 9 closer to the reflex controller harmony.

Table 7.10: Locomotion data from the experiments in flat terrain with noise.

Param	Limb	Reflex controller (Noise)	Hybrid controller (Noise)			
			Model 4	Model 9	Model 11A	Model 11B
$T_{sw}(s)$	FL	0.168 ± 0.101	0.159±0.087	0.121±0.072	0.122±0.082	0.120±0.079
	FR	0.155 ± 0.099	0.167±0.102	0.124±0.079	0.128±0.072	0.127±0.080
	HL	0.120 ± 0.055	0.116±0.021	0.116±0.020	0.116±0.020	0.117±0.022
	HR	0.132 ± 0.043	0.118±0.008	0.119±0.006	0.112±0.028	0.115±0.020
$T_{st}(s)$	FL	0.420 ± 0.178	0.288±0.161	0.276±0.160	0.262±0.152	0.304±0.154
	FR	0.450 ± 0.181	0.292±0.153	0.288±0.154	0.292±0.159	0.321±0.165
	HL	0.518 ± 0.189	0.575±0.081	0.570±0.078	0.571±0.076	0.569±0.080
	HR	0.559 ± 0.154	0.594±0.014	0.587±0.009	0.554±0.105	0.570±0.079
β	FL	0.714	0.644	0.695	0.681	0.718
	FR	0.743	0.637	0.670	0.696	0.716
	HL	0.812	0.832	0.831	0.831	0.830
	HR	0.809	0.835	0.832	0.832	0.832
disp		0.760	0.885	0.876	0.870	0.874
harm		0.025	0.021	0.024	0.020	0.016
stab		0.386	0.380	0.395	0.380	0.405
reward		0.316	0.337	0.343	0.334	0.343
v		0.082	0.092	0.091	0.090	0.089

All hybrid models have improved locomotion in the Oncilla robot when noise was considered. Although the models 9 and 11B present the same reward value, we consider that the model which features better performance is model 11B, due to some factors: the stability is increased to a value close to the experiment without noise (0.405) and this model provided for almost the same duty factor among the girdles, mainly in the fore girdle, since the difference between the duty factors (β) of the fore girdle in the reflex controller is equal to 0.029 and in the model 11B is equal to 0.002. In summary, with model 11B, the displacement increased 15%, the robot stability increased 4.9% and the velocity increased 8.5%.

The hybrid models proved to be capable of improving the walking behavior of the Oncilla robot comparatively to the reflex controller when a noise of 5% is added to the system.

Controllers with delays

The next step is to verify the system robustness when a 12 ms delay between sensors and sensory interneurons is considered in the reflex controller and in the four hybrid controllers. Note that no noise is included. This delay means that the sensory input will not affect the output of the sensory interneurons instantaneously, but only after 12 ms. We intend to model the fact that the traveling speed of spikes depends on the nerve fiber properties and also the possible delay in electronic and mechanic transmissions.

An important study of More et al. (2010) shows that the CNS should have an internal model capable of predicting the best future motor actions, compensating the internal delays existing in animals. We based our hypothesis in this study, in which the feedforward component of the hybrid controller should predict the motoneurons activity, improving the robot walking behavior.

In these experiments, we do not consider hybrid model 4, since the robot falls when delay is considered. Figure 7.21 shows the robot stepping patterns resultant from adding the 12ms delay to the controllers. Models 9 (figure 7.21b), 11A (figure 7.21c) and 11B (figure 7.21d) present a stepping pattern significantly more regular, but model 9 is the most regular. Table 7.11 supports the visual stepping sequence comparisons. All the T_{st} and T_{sw} standard deviations are clearly lower, leading to an evident more regular stepping. All hybrid models provide almost the same swing time (T_{sw}) among both hind and fore girdles and the same stance time (T_{st}) among the hind limbs. Model 9 is the only one that provide the same stance time (T_{st}) among the fore limbs. Furthermore, all the hybrid models improved the displacement, gait's harmony, robot's velocity and models 11A and

11B decreased the stability.

Table 7.11: Locomotion data from the experiments in flat terrain with delays.

Param	Limb	Reflex controller (Delays)	Hybrid controller (Delays)		
			Model 9	Model 11A	Model 11B
$T_{sw}(s)$	FL	0.285 ± 0.164	0.106 ± 0.079	0.121 ± 0.067	0.108 ± 0.069
	FR	0.288 ± 0.205	0.110 ± 0.080	0.112 ± 0.074	0.113 ± 0.067
	HL	0.154 ± 0.097	0.130 ± 0.005	0.124 ± 0.004	0.128 ± 0.005
	HR	0.176 ± 0.085	0.129 ± 0.005	0.127 ± 0.004	0.126 ± 0.005
$T_{st}(s)$	FL	0.553 ± 0.280	0.257 ± 0.123	0.246 ± 0.145	0.273 ± 0.142
	FR	0.503 ± 0.284	0.266 ± 0.136	0.283 ± 0.148	0.251 ± 0.135
	HL	0.583 ± 0.397	0.588 ± 0.008	0.595 ± 0.009	0.601 ± 0.009
	HR	0.674 ± 0.367	0.589 ± 0.008	0.592 ± 0.007	0.603 ± 0.008
β	FL	0.660	0.709	0.669	0.717
	FR	0.636	0.708	0.716	0.690
	HL	0.791	0.819	0.828	0.824
	HR	0.793	0.820	0.823	0.828
disp		0.813	0.832	0.818	0.855
harm		0.007	0.022	0.019	0.019
stab		0.343	0.343	0.341	0.316
reward		0.303	0.313	0.308	0.316
v		0.083	0.090	0.091	0.089

We consider that model 9 is the best in these experiments with delays, since it is the only one that was capable of maintaining the stability while providing for almost the same duty factor (β) among the fore and hind girdles. With this model, the robot displacement increased 2.3%, the gait harmony increased 214.3% the velocity increased 8.4% and the robot stability was maintained.

The three hybrid models present a better performance compared with the reflex controller, which shows the relevance of the feedforward signals that predict the motor processes.

Controllers with noise and delays

In order to achieve more realistic and more similar models with their biological counterparts, both noise and delays were considered in the reflex network and hybrid models implementation.

Figure 7.22 shows the robot stepping patterns resultant from this experiment. Models 4 (figure 7.22b), 9 (figure 7.22c), 11A (figure 7.22d) and 11B (figure 7.22e) present a stepping pattern significantly more regular, when compared with the stepping sequence of the reflex controller (figure 7.22a). Table 7.12 allows us to conclude that the hybrid models improve the robot walking behavior. All the T_{st} and T_{sw} standard deviations are lower, leading to an evident more regular stepping. The four hybrid models improve the robot displacement and velocity, however, only the models 9 and 11B are capable of increasing the robot stability. Regarding the gait harmony, none of the hybrid models were capable of improving it.

Table 7.12: Locomotion data from the experiments in flat terrain with noise and delays.

Param	Limb	Reflex controller (Noise and Delays)	Hybrid controller (Noise and Delays)			
			Model 4	Model 9	Model 11 (A)	Model 11 (B)
$T_{sw}(s)$	FL	0.207 ± 0.145	0.158 ± 0.090	0.133 ± 0.091	0.145 ± 0.079	0.128 ± 0.077
	FR	0.259 ± 0.177	0.162 ± 0.087	0.125 ± 0.085	0.143 ± 0.091	0.127 ± 0.082
	HL	0.144 ± 0.056	0.122 ± 0.008	0.122 ± 0.021	0.108 ± 0.032	0.115 ± 0.032
	HR	0.128 ± 0.065	0.121 ± 0.021	0.125 ± 0.007	0.124 ± 0.008	0.116 ± 0.033
$T_{st}(s)$	FL	0.436 ± 0.216	0.277 ± 0.161	0.265 ± 0.146	0.266 ± 0.168	0.256 ± 0.158
	FR	0.393 ± 0.232	0.289 ± 0.156	0.263 ± 0.145	0.260 ± 0.151	0.275 ± 0.164
	HL	0.612 ± 0.262	0.599 ± 0.012	0.569 ± 0.079	0.545 ± 0.128	0.543 ± 0.128
	HR	0.480 ± 0.296	0.580 ± 0.081	0.586 ± 0.010	0.588 ± 0.009	0.542 ± 0.128
β	FL	0.678	0.636	0.665	0.648	0.666
	FR	0.603	0.641	0.678	0.645	0.685
	HL	0.809	0.831	0.824	0.835	0.825
	HR	0.789	0.828	0.825	0.826	0.824
$disp$		0.851	0.883	0.897	0.898	0.866
$harm$		0.029	0.015	0.011	0.012	0.021
$stab$		0.356	0.340	0.387	0.349	0.397
$reward$		0.324	0.319	0.339	0.324	0.340
v		0.086	0.091	0.091	0.092	0.092

The models 9 and 11B increase the robot performance, since the reward values are higher than the ones of the reflex controller. Model 11B shows best results, since it increases the robot displacement in 1.76%, the robot stability in 11.5% and the velocity in 7%.

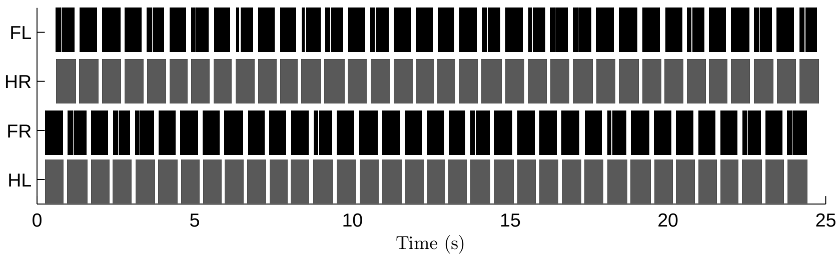

(a) Reflex controller.

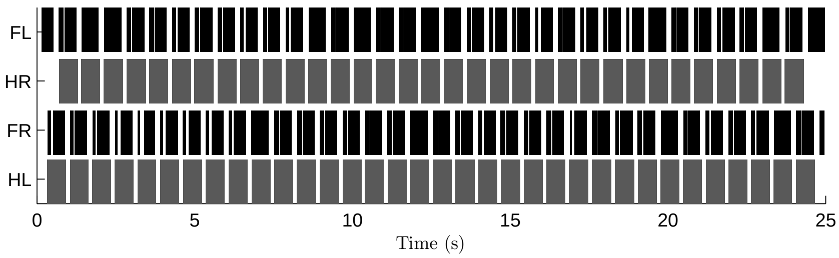

(b) Hybrid controller - model 4.

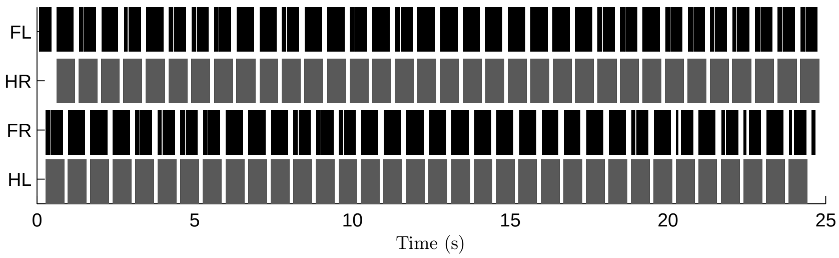

(c) Hybrid controller - model 9.

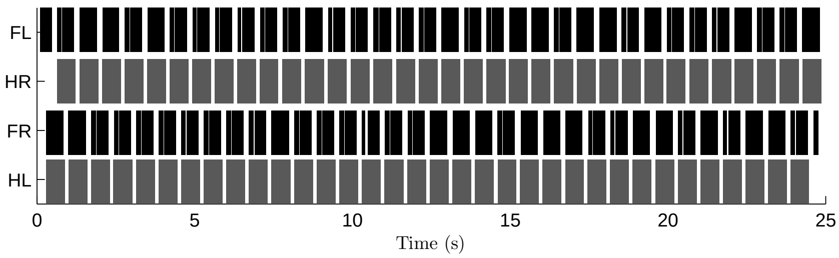

(d) Hybrid controller - model 11A.

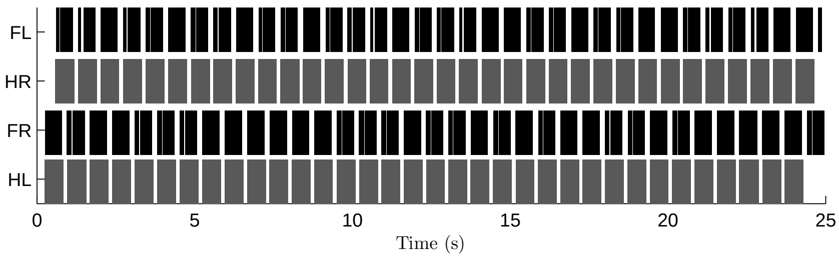

(e) Hybrid controller - model 11B.

Figure 7.19: Oncilla stepping sequences in flat terrain without noise and delays.

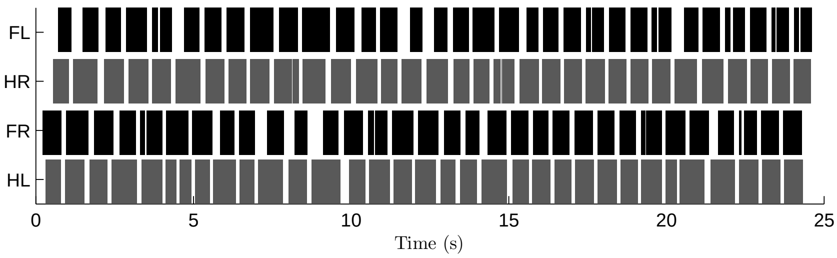

(a) Reflex controller.

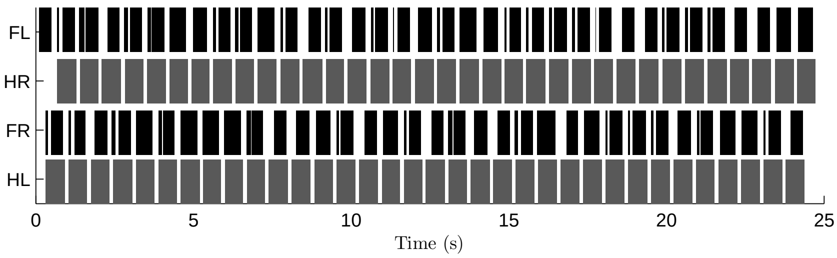

(b) Hybrid controller - model 4.

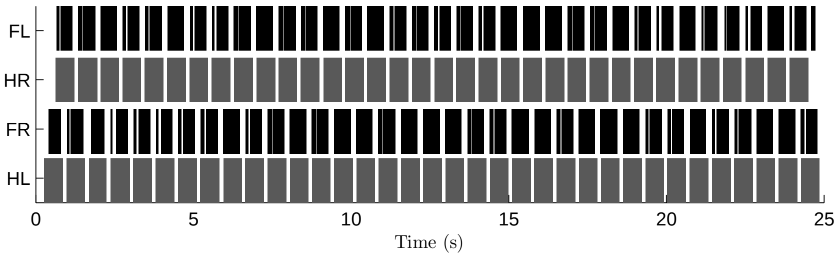

(c) Hybrid controller - model 9.

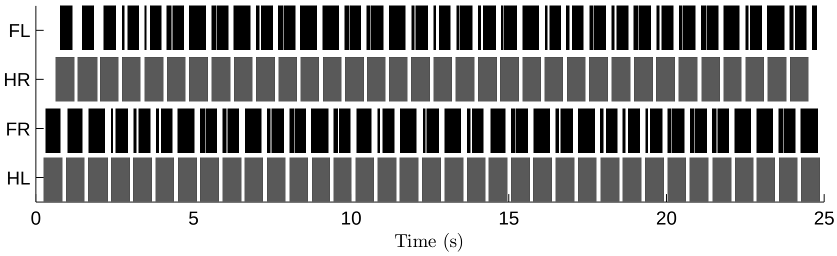

(d) Hybrid controller - model 11A.

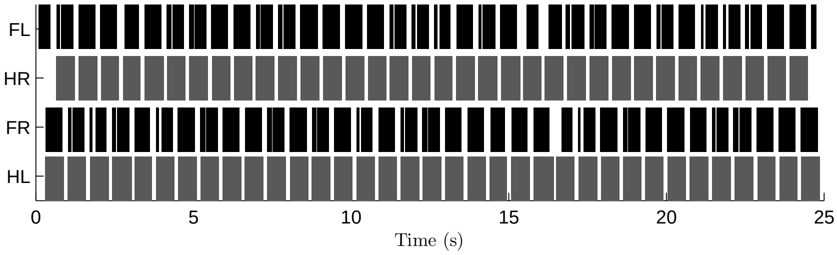

(e) Hybrid controller - model 11B.

Figure 7.20: Oncilla stepping sequences in flat terrain with noise of 5%.

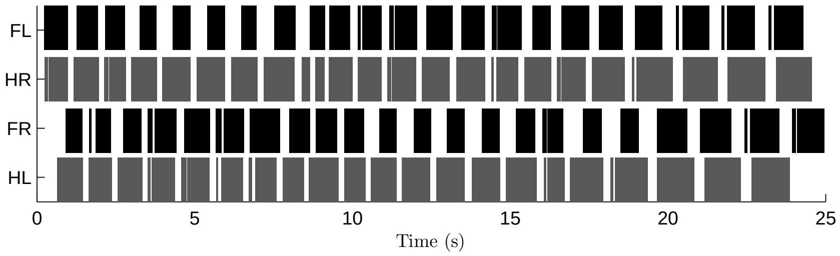

(a) Reflex controller.

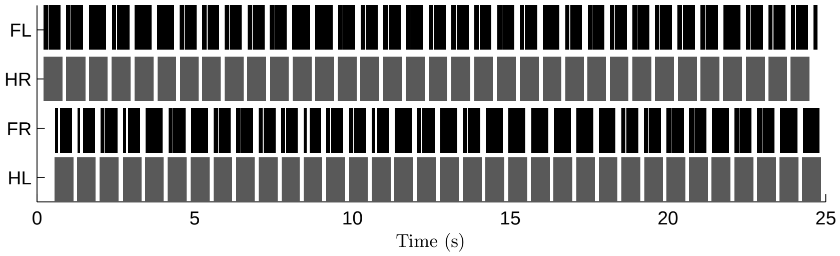

(b) Hybrid controller - model 9.

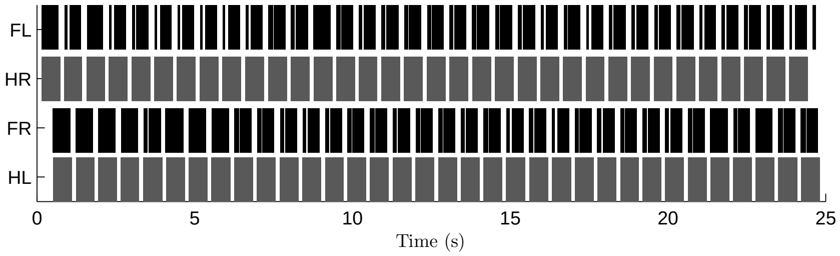

(c) Hybrid controller - model 11A.

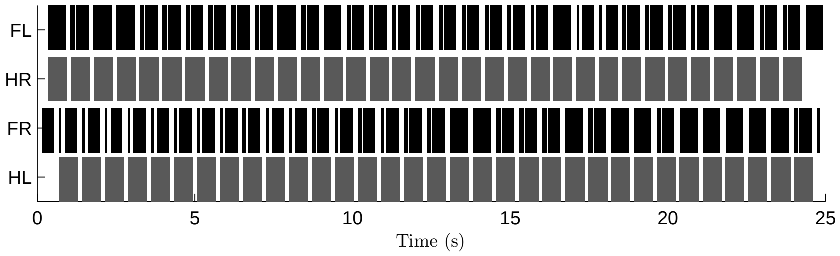

(d) Hybrid controller - model 11B.

Figure 7.21: Oncilla stepping sequences in flat terrain when a 12 ms delay is considered.

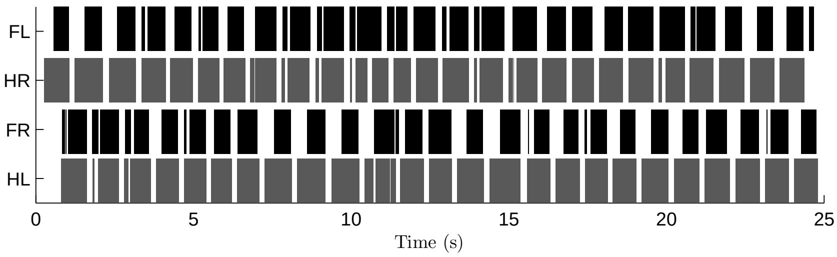

(a) Reflex controller.

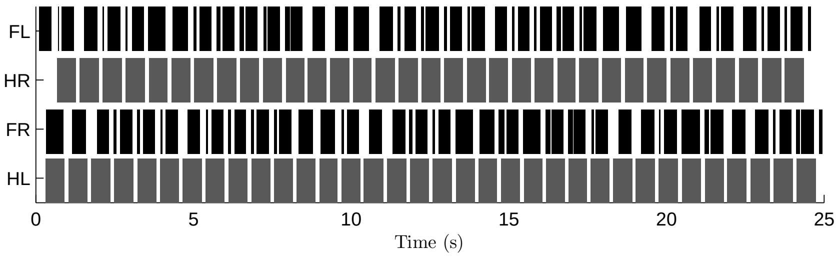

(b) Hybrid controller - model 4.

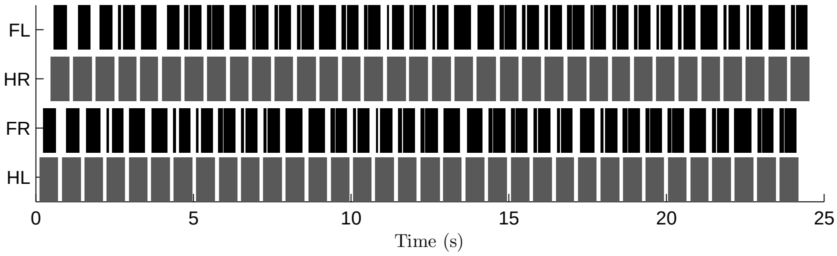

(c) Hybrid controller - model 9.

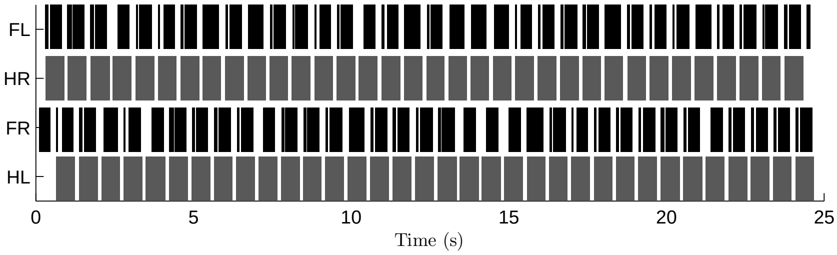

(d) Hybrid controller - model 11A.

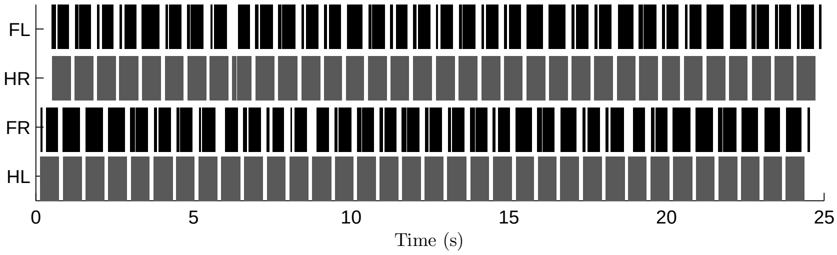

(e) Hybrid controller - model 11B.

Figure 7.22: Oncilla stepping sequences in flat terrain when both noise of 5% and a delay of 12 ms are considered.

Chapter 8

Conclusions

The work carried out during this past year is the first step in the development of bio-inspired controllers that combine concepts of Central Pattern Generators and reflexes. Such an approach is duly justified with biological evidences, which show that, despite engineering evidence favoring feedback approaches, the combination of both these approaches seems to be required in order to achieve robotic controllers capable of flexibly dealing with several situations of the real world. The development of bio-inspired controllers serve as basis for the future development of controllers for robotic prostheses, specifically cybernetic prostheses.

This research's main contribution to knowledge is related with the hybrid controller, which presents an innovative approach. The CPGs have a different function when compared to the actual state of the art of bio-inspired controllers that combine CPGs and reflexes, since they work as motor actions' predictors, improving the Oncilla's walking behavior.

This work included an extensive summary of the most important works related with bio-inspired controllers developed for legged robots. This review allowed to understand and realize what is already done in the robotic locomotion field and, furthermore, to identify which aspects have to be developed to improve the robustness and adaptability of bio-inspired controllers.

In order to correctly design controllers biologically inspired, a detailed literature review on the biological mechanisms responsible for the generation of locomotion is presented, enabling a deep knowledge regarding the animals' locomotor system.

This research presented a sensory-driven controller that resorts to the minimum number of reflexes to generate a stable walking behavior, resilient to external perturbations. This was the first controller developed during the past year, and it is totally dependent on the robot's interactions with the environment.

We also designed a hybrid controller that introduces CPGs, modeled by nonlinear oscillators, as gait modulators on top of a reflex-based model. This controller combined the advantages of CPGs and reflexes, and tried to minimize the disadvantages of each one of the controllers.

In order to evaluate the performance of the generated locomotion, we implemented a reward function that includes three different components, thus evaluating the frontal displacement of the robot, the robot's stability and its gait's harmony.

The work herein presented enables to answer the research questions (RQ) outlined in the introduction section.

RQ: "What are the most important reflexes in a quadruped robot that may enhance the generated locomotion in terms of regular gait?". Results showed that the implemented reflex controller had the necessary reflexes to generate stable and robust quadruped locomotion. The sensory information of ground contact (GC), anterior extreme position (AEP), posterior extreme position (PEP) and limb loading are crucial to the generation of locomotion in straight flat terrains. The vestibulospinal and stumbling reflex are important to make the controller capable of dealing with external perturbations, like slopes and small obstacles, respectively.

RQ: "Is it possible to design a reflex network capable of generating stable, regular and robust quadruped locomotion?". The developed work shows that the reflex controller is capable of producing the required limb's movements for quadruped locomotion and presents a regular stepping pattern. Furthermore, it proved to be capable of dealing with slopes without changing the parameters, and it was able to deal with small obstacles, overcoming them successfully.

RQ: "How can we measure the performance of a quadruped gait?". In order to evaluate the performance of the generated locomotion by the controllers, we implemented a reward function that includes three different components, thus evaluating the frontal displacement of the robot, the robot's stability and its gait harmony. Furthermore, we evaluated the gait by observing the resultant stepping sequence of the experiments and analyzing the locomotion characteristics usually considered in gait analysis, namely, the swing time

(T_{sw}), the stance time (T_{st}), the duty factor (β) and the robot's velocity (v).

RQ: "Since we address a real problem that includes delays and noise, how can we achieve a system that is robust to such disturbances?". The addition of noise and delays to the reflex network degraded the robot's locomotion, mainly by reducing the robot's stability. Thereby, a way to make the robot's controller robust to delays and noise is the addition of a feedforward component, capable of predicting the robot's motor actions. We proposed a hybrid controller that combines a feedforward and a feedback component. The predictor showed to be important, since the controller was capable of improving the shortcomings of the reflex controller, mainly, to increase the robot's robustness when noise and delays were considered in the system. According to the simulation results of the hybrid controller with noise and delays, it increases the robot's stability, the gait's harmony and the displacement of the robot. Furthermore, using the feedforward signals, the robot's velocity increases in all experiments. Our approach proved that CPGs can be regarded instead as a regulator of the sensorimotor processes, filtrating the system's noise and anticipating the delays in the generation of motor actions.

RQ: "In order to add a feedforward component to the system, how can we predict the robot's motor actions?". The hybrid controller designed in this thesis generates stable and harmonious locomotor patterns. The controller is based on the hypothesis that CPGs can serve as predictors of the robot's motor actions. We implemented the predictor based on the observation of the motor actions generated by the reflex controller. The prediction of the limb's state was used to build a motoneuron map. The feedforward component improved the robot's behavior by increasing its stability, harmony and displacement, in almost all of the experiments. Furthermore, the stepping patterns become more regular due to the inclusion of the feedforward component in the system, filtrating the noise and anticipating the robot's motor actions.

8.1 Future work

The main goal of the research team is the development of bio-inspired controllers capable of walking and running on unpredictable terrains. These controllers should be applied in real robots, testing their interaction skills with real world and making them capable of adapting to dynamical environments.

The controllers designed in this thesis denote a significant advance in the development of bio-inspired systems, since we presented an innovative controller that combines two biological concepts in a different way. However, things can still be improved. Regarding to the reflex component, the addition of more reflexes can be relevant, in order to further improve the capabilities of the robot. For example, a corrective stepping reflex and a tonic reflex can be important to improve the robot behavior in holes and roll ramps, respectively.

The system that predicts the motor actions should be improved, being capable of generating the shape of the motor actions' signals automatically. The reflex controller presents some limitations, mainly related to the fact that the controller does not allow the speed modulation and gait specification. Thereby, one function of the CPGs to be implemented is to be capable of modulating the robot's velocity, enabling a previous definition of the desired robot's velocity, chosen by descending inputs from the brain. Another relevant function to be implemented is the possibility of choosing the gait type, being, perhaps, necessary to make an online modification of the reflex network's weights by the CPGs. Another future task is the improvement of the hybrid models through the implementation of an optimization system capable of obtaining the best values that define the relative importance of CPGs in each experiment.

Bibliography

Alexander, R. M. (1984). The gaits of bipedal and quadrupedal animals. *The International Journal of Robotics Research*, 3(2):49–59.

Alexander, R. M., Bordeux, C., Boulic, R., Thalmann, D., Boulic, R., Magnenat-Thalmann, N., Thalmann, D., Boulic, R., Thalmann, D., Bradski, G. R., et al. (1976). Mechanics of bipedal locomotion. *International journal of sports medicine*, 18:177–190.

Andre, J., Costa, L., and Santos, C. (2014). Skill memory in biped locomotion.

Bässler, U. (1986). On the definition of central pattern generator and its sensory control. *Biological Cybernetics*, 54(1):65–69.

Brown, T. G. (1911). The intrinsic factors in the act of progression in the mammal. *Proceedings of the Royal Society of London. Series B, containing papers of a biological character*, pages 308–319.

Brustein, E. and Rossignol, S. (1998). Recovery of locomotion after ventral and ventrolateral spinal lesions in the cat. i. deficits and adaptive mechanisms. *Journal of neurophysiology*, 80(3):1245–1267.

Burke, R. E. (2007). Sir charles sherrington's the integrative action of the nervous system: a centenary appreciation. *Brain*, 130(4):887–894.

Cartmill, M., Lemelin, P., and Schmitt, D. (2002). Support polygons and symmetricalgaits in mammals. *Zoological Journal of the Linnean Society*, 136(3):401–420.

Cavagna, G. A., Heglund, N. C., and Taylor, C. R. (1977). Mechanical work in terrestrial locomotion: two basic mechanisms for minimizing energy expenditure. *Am. J. Physiol*, 233(5):243–261.

Cavagna, G. A., Thys, H., and Zamboni, A. (1976). The sources of external work in level walking and running. *The Journal of physiology*, 262(3):639–657.

Cohen, A. H. (1992). The role of heterarchical control in the evolution of central pattern generators. *Brain, Behavior and Evolution*, 40(2-3):112–124.

Cohen, A. H. and Boothe, D. L. (1999). Sensorimotor interactions during locomotion: principles derived from biological systems. *Autonomous Robots*, 7(3):239–245.

Cruse, H., Kindermann, T., Schumm, M., Dean, J., and Schmitz, J. (1998). Walknet—a biologically inspired network to control six-legged walking. *Neural networks*, 11(7):1435–1447.

Daun-Gruhn, S. and Büschges, A. (2011). From neuron to behavior: dynamic equation-based prediction of biological processes in motor control. *Biological cybernetics*, 105(1):71–88.

Duysens, J. and Pearson, K. (1976). The role of cutaneous afferents from the distal hindlimb in the regulation of the step cycle of thalamic cats. *Experimental brain research*, 24(3):245–255.

Duysens, J. and Van de Crommert, H. W. (1998). Neural control of locomotion; part 1: The central pattern generator from cats to humans. *Gait & posture*, 7(2):131–141.

Dzeladini, F., van den Kieboom, J., and Ijspeert, A. (2014). The contribution of a central pattern generator in a reflex-based neuromuscular model. *Frontiers in Neuroscience*, 1.

Ekeberg, Ö. and Pearson, K. (2005). Computer simulation of stepping in the hind legs of the cat: an examination of mechanisms regulating the stance-to-swing transition. *Journal of Neurophysiology*, 94(6):4256–4268.

Ferreira, C., Matos, V., Peixoto dos Santos, C., and Ijspeert, A. (2014a). Sensory-driven purely reflex controller for quadruped locomotion. *Dynamic Walking 2014*.

Ferreira, C., Matos, V., Santos, C. P., and Ijspeert, A. J. (2014b). Quadrupedal locomotion based in a purely reflex controller. In *ICINCO 2014 - Proceedings of the 11th International Conference on Informatics in Control, Automation and Robotics, Volume 1, Vienna, Austria, 1 - 3 September, 2014*, pages 324–331.

Forssberg, H. (1979). Stumbling corrective reaction: a phase-dependent compensatory reaction during locomotion. *J Neurophysiol*, 42(4):936–953.

Forssberg, H., Grillner, S., and Rossignol, S. (1977). Phasic gain control of reflexes from the dorsum of the paw during spinal locomotion. *Brain research*, 132(1):121–139.

Fukuoka, Y., Kimura, H., and Cohen, A. H. (2003). Adaptive dynamic walking of a quadruped robot on irregular terrain based on biological concepts. *The International Journal of Robotics Research*, 22(3-4):187–202.

Geyer, H. and Herr, H. (2010). A muscle-reflex model that encodes principles of legged mechanics produces human walking dynamics and muscle activities. *Neural Systems and Rehabilitation Engineering, IEEE Transactions on*, 18(3):263–273.

Gorassini, M. A., Prochazka, A., Hiebert, G. W., and Gauthier, M. J. (1994). Corrective responses to loss of ground support during walking. i. intact cats. *Journal of Neurophysiology*, 71:603–603.

Gossard, J.-P., Dubuc, R., and Kolta, A. (2011). A hierarchical perspective on rhythm generation for locomotor control. *Breathe, Walk and Chew; The Neural Challenge: Part II*, page 151.

Grillner, S., McClellan, A., and Perret, C. (1981). Entrainment of the spinal pattern generators for swimming by mechano-sensitive elements in the lamprey spinal cord in vitro. *Brain research*, 217(2):380–386.

Grillner, S. and Rossignol, S. (1978). On the initiation of the swing phase of locomotion in chronic spinal cats. *Brain research*, 146(2):269–277.

Grillner, S. and Wallen, P. (1985). Central pattern generators for locomotion, with special reference to vertebrates. *Annual review of neuroscience*, 8(1):233–261.

Grillner, S. and Zangger, P. (1979). On the central generation of locomotion in the low spinal cat. *Experimental Brain Research*, 34(2):241–261.

Hiebert, G. W., Gorassini, M. A., Jiang, W., Prochazka, A., and Pearson, K. G. (1994). Corrective responses to loss of ground support during walking. ii. comparison of intact and chronic spinal cats. *Journal of Neurophysiology*, 71:611–611.

Hiebert, G. W., WHELAN, P. J., PROCHAZKA, A., and PEARSON, K. G. (1995). Suppression of the corrective response to loss of ground support by stimulation of extensor group i afferents.

Hildebrand, M. (1965). Symmetrical gaits of horses. *Science*, 150(3697):701–708.

Hildebrand, M. (1977). Analysis of asymmetrical gaits. *Journal of Mammalogy*, pages 131–156.

Ijspeert, A. J. (2008). Central pattern generators for locomotion control in animals and robots: a review. *Neural Networks*, 21(4):642–653.

Iosa, M., Marro, T., Paolucci, S., and Morelli, D. (2012). Stability and harmony of gait in children with cerebral palsy. *Research in developmental disabilities*, 33(1):129–135.

Iosa, M., Morone, G., Fusco, A., Pratesi, L., Bragoni, M., Coiro, P., Multari, M., Venturiero, V., De Angelis, D., and Paolucci, S. (2011). Effects of walking endurance reduction on gait stability in patients with stroke. *Stroke research and treatment*, 2012.

Kaushik, R., Marcinkiewicz, M., Xiao, J., Parsons, S., and Raphan, T. (2007). Implementation of bio-inspired vestibulo-ocular reflex in a quadrupedal robot. In *Robotics and Automation, 2007 IEEE International Conference on*, pages 4861–4866. IEEE.

Kiehn, O. (2006). Locomotor circuits in the mammalian spinal cord. *Annu. Rev. Neurosci.*, 29:279–306.

Kimura, H., Fukuoka, Y., and Cohen, A. H. (2007). Adaptive dynamic walking of a quadruped robot on natural ground based on biological concepts. *The International Journal of Robotics Research*, 26(5):475–490.

Kimura, H., Fukuoka, Y., and Nakamura, H. (2000). Biologically inspired adaptive dynamic walking of the quadruped on irregular terrain. In *ROBOTICS RESEARCH-INTERNATIONAL SYMPOSIUM-*, volume 9, pages 329–336.

Klein, T. J. and Lewis, M. A. (2012). A physical model of sensorimotor interactions during locomotion. *Journal of neural engineering*, 9(4):046011.

Kuo, A. D. (2002). The relative roles of feedforward and feedback in the control of rhythmic movements. *MOTOR CONTROL-CHAMPAIGN-*, 6(2):129–145.

Laboratory, B. (2014). Oncilla robot @ONLINE [accessed on may 12, 2014]. URL `http://biorob.epfl.ch/amarsi`.

Marder, E., Bucher, D., Schulz, D. J., and Taylor, A. L. (2005). Invertebrate central pattern generation moves along. *Current Biology*, 15(17):R685–R699.

Maufroy, C., Kimura, H., and Takase, K. (2008). Towards a general neural controller for quadrupedal locomotion. *Neural Networks*, 21(4):667–681.

McCrea, D. A. (2001). Spinal circuitry of sensorimotor control of locomotion. *The Journal of physiology*, 533(1):41–50.

McVea, D. A., Donelan, J. M., Tachibana, A., and Pearson, K. G. (2005). A role for hip position in initiating the swing-to-stance transition in walking cats. *Journal of neurophysiology*, 94(5):3497–3508.

Michel, O. (2004). Webots: Professional mobile robot simulation. *Journal of Advanced Robotics Systems*, 1(1):39–42.

More, H. L., Hutchinson, J. R., Collins, D. F., Weber, D. J., Aung, S. K., and Donelan, J. M. (2010). Scaling of sensorimotor control in terrestrial mammals. *Proceedings of the Royal Society B: Biological Sciences*, page rspb20100898.

Orlovsky, G., Deliagina, T., and Grillner, S. (1999). *Neuronal Control of Locomotion: From Mollusc to Man*. Oxford Neuroscience S. Oxford University Press.

Owaki, D., Morikawa, L., and Ishiguro, A. (2012). Listen to body's message: Quadruped robot that fully exploits physical interaction between legs. In *Intelligent Robots and Systems (IROS), 2012 IEEE/RSJ International Conference on*, pages 1950–1955. IEEE.

Pearson, K. (2008). Role of sensory feedback in the control of stance duration in walking cats. *Brain research reviews*, 57(1):222–227.

Pearson, K., Ekeberg, O., and Buschges, A. (2006). Assessing sensory function in locomotor systems using neuro-mechanical simulations. *Trends in neurosciences*, 29(11):625–631.

Pearson, K. G. (1995). Proprioceptive regulation of locomotion. *Current opinion in neurobiology*, 5(6):786–791.

Pearson, K. G. (2004). Generating the walking gait: role of sensory feedback. *Progress in brain research*, 143:123–129.

Pfeifer, R., Lungarella, M., and Iida, F. (2007). Self-organization, embodiment, and biologically inspired robotics. *science*, 318(5853):1088–1093.

Prochazka, A., Sontag, K.-H., and Wand, P. (1978). Motor reactions to perturbations of gait: proprioceptive and somesthetic involvement. *Neuroscience letters*, 7(1):35–39.

Quevedo, J., Stecina, K., Gosgnach, S., and McCrea, D. A. (2005). Stumbling corrective reaction during fictive locomotion in the cat. *Journal of Neurophysiology*, 94(3):2045–2052.

Raibert, M. H. et al. (1986). *Legged robots that balance*, volume 3. MIT press Cambridge, MA.

Rossignol, S., Dubuc, R., and Gossard, J.-P. (2006). Dynamic sensorimotor interactions in locomotion. *Physiological reviews*, 86(1):89–154.

Rybak, I. A., Shevtsova, N. A., Lafreniere-Roula, M., and McCrea, D. A. (2006). Modelling spinal circuitry involved in locomotor pattern generation: insights from deletions during fictive locomotion. *The Journal of physiology*, 577(2):617–639.

Sousa, J., Matos, V., and Peixoto dos Santos, C. (2010). A bio-inspired postural control for a quadruped robot: an attractor-based dynamics. In *Intelligent Robots and Systems (IROS), 2010 IEEE/RSJ International Conference on*, pages 5329–5334. IEEE.

Teixeira, C., Costa, L., and Santos, C. (2014). Biped locomotion-improvement and adaptation. In *Autonomous Robot Systems and Competitions (ICARSC), 2014 IEEE International Conference on*, pages 110–115. IEEE.

Verdaasdonk, B., Koopman, H., and Van der Helm, F. C. (2007). Resonance tuning in a neuro-musculo-skeletal model of the forearm. *Biological Cybernetics*, 96(2):165–180.

Wadden, T. and Ekeberg, Ö. (1998). A neuro-mechanical model of legged locomotion: single leg control. *Biological cybernetics*, 79(2):161–173.

Yakovenko, S., Gritsenko, V., and Prochazka, A. (2004). Contribution of stretch reflexes to locomotor control: a modeling study. *Biological cybernetics*, 90(2):146–155.